Simulation of Manoeuvring Safety of Ships in Adverse Weather Conditions when Subject to Limited Power Imposed by EEDI Improvement by Engine Derating.

by

Emmanuel IRIMAGHA

This Dissertation Submitted for the degree of Doctor of Philosophy

Marine, Offshore and Subsea Technology

School of Engineering

Faculty of Science, Agriculture and Engineering

Newcastle University

Newcastle upon Tyne

August 2019

School of Engineering

Armstrong Building

Newcastle University

NE1 7RU

United Kingdom

Dedication

To Jesus Christ my Lord and Saviour, my brother, Mr. Peter Irimagha, and in memory of my Parents, Late, Wariopusenibo Rogers Enenimibo-ofori IRIMAGHA and Mrs. Eunice Rogers Irimagha

Abstract

Motions of a ship in adverse weather conditions results in increased effects on roll, pitch and heave motions to non-negligible values that would increase the speed drop to a disproportionate level, likelihood of contact with seabed in shallow waters, propeller emergence, passenger discomfort. Predicting the influence of adverse weather on the safety of a ship if the engine is derated for the purpose of improving the Energy Efficiency Design Index (EEDI) has been a hot topic since its recommendation by the Marine Environment Protection Committee (MEPC) of the International Maritime Organisation (IMO). A lot of research is being done towards developing an acceptable method of predicting the impact of derating a ship's engine. Presently, most researches are based on predicting the power loss and speed drop.

This research proposes a method for determining power level to which a ship's engine can be derated such that safe operations is sustained at defined environmental conditions. Normally, the tests to predict the manoeuvring capabilities of a ship at the design stage are usually achieved through detailed captive, free running physical model tests in the laboratory (or designated basin) or by the use of Computational Fluid Dynamics techniques. Thus to predict the suggested dynamic characteristics at different levels of power in adverse weather condition will require numerous modelling attempts, which is a very expensive and time consuming process.

Developing Eshipman is an attempt to demonstrate that it is possible to practically minimise the time and financial demands of carrying out these predictions with minimal error but acceptable accuracy. In order to test the idea, the physical dimensions of a specimen ship and non-dimensional hydrodynamic derivatives of the ship's hull, rudder and propeller, from the experimental results from published article (see section Chapter 9 – Appendix A for the data) were used to simulate the motion of the ship in calm weather and the results were compared with the experimental plots. The program that simulates the environmental conditions were merged with the calm water code, thereby creating in a program that simulates the motion of a ship in adverse weather condition. EShipman was used to simulate the motion of the ship in calm weather; the results of the turning circle trajectories with its associated roll

effects in calm waters, and zigzag motion simulation were compared with the experimental results. This thesis also shows a zigzag motion plot which was labelled to show how the logic for writing the algorithm was produced.

In the present state of manoeuvring studies, the windage area of the ship was given (even by the class societies and researchers alike) as a constant value or some formula that does not take the effect of roll motion on the windage area into account. A formula for obtaining the approximate lateral windage area was modified to obtain a new formula which incorporates the effect of instantaneous roll angle so as to obtain a more indicative result. The simulation of the vessel with low metacentric height in ballast to perform a turning circle motion with the rudder at 35 degree angle, showed a stable roll angle of 10 degrees which implies a 53% increase in windage area on one side of the ship. If this happens to be the windward area, it will result in an overturning moment which may lead to a capsize in a combined wind and wave effect. Applying this correction to the windage area formula for modelling the motion of a ship in a wind only (initially 270 degrees) condition shows an increased roll angle and some drift motion in the form of reduced tactical diameter. Details is in section 5.1.

A turning circle motions simulation using a subject ship showed an unacceptable drop in speed (i.e. below 4 knots being minimum navigational speed provided, IMO (2017) due to reduced rudder inflow velocity which disproportionately reduces the rudder performance) when power was reduced to 65% (a region of maximum efficiency). It also shows how the roll angle does reduce with a reduction in ship power and additional simulations were done to show the speed drop for different sea states (Beaufort number) under the influence of wind and wave. This was compared with the semi-empirical work of Kwon (2008) and the empirical work of Kim *et al.* (2017). It also demonstrates how the heave and pitch response increases with reducing power and then starts dropping from 65% power. These motions, indicates that reducing the maximum continuous rating by 35% or more in order to improve the efficiency, will make the ship unsafe when faced with the defined environmental condition or higher.

Also, the modular principle proposed by the Mathematical Modelling Group of Japan (MMG), was tested and it was derived that with a 9% increase in rudder area, the

65% MCR simulated turning circle tactical diameter in calm water was reduced to the calm water 100% MCR turning circle tactical diameter. It was demonstrated that increasing the rudder area improved the ship's dynamic performance in adverse weather condition.

EEDI calculations were done for 100%MCR and 80%MCR to demonstrate that the efficiency actually improves with reduced power. Furthermore, some explanation highlighted the fact that just reducing the power alone will not always improve the efficiency due to the specific fuel oil consumption characteristics which has a minimum point at 70% MCR. Equations were formulated which fits the specific fuel oil consumption curve to make for ease of application.

On the overall outlook, this research does propose a methodology that can be easily used to evaluate how derating the engine of a ship (for the purpose of improving its EEDI) will influence its manoeuvring safety in adverse weather condition.

Acknowledgements

The efforts of several persons have had a substantial influence towards the success of this research.

I would firstly like to thank my supervisors, Professor. Zhiqiang Hu and Professor Richard Birmingham of the School of Engineering and Associate Professor Michael Woodward, of the University of Tasmania for giving me their professional support and invaluable insight to this study. Also Professor Grant Burgess, and Dr. David Trodden who have been providing strategic and academic support and some helpful encouragement and who have taken out from their personal time to attend to my work. Mr. Frans Quadvlieg, Senior Project Manager at MARIN, (Nijmegen Area, Netherlands), who took some interest in my work during my presentation at the A.Yücel ODABAŞI Colloquium Series 2nd International Conference, November 2016, in Istanbul, and introduced me to some useful references including SHOPERA (an European Union (EU) funded research project.

My wife, Mrs. Rosemary Ibifiri Irimagha, whose persistent encouragement enabled me to continue in spite of all odds, and to my Children (Samuel, Favour, Hephzibah and Bezaleel) who surprisingly showed an unusual sense of maturity by keeping it calm and not insisting on my purchasing the latest gadgets during my times of studies at home and had consistently prayed for my success.

A big thanks to Mr. and Mrs. Robert and Elsie Page of South Shields, who have for many years, been a friend of our family and have backed us up when we had some tough challenges. Also to Mr. Charles Orji, who encouraged and assisted with certain computations and development of some formulations of my work, Mr. John Gairside who assisted with the proof-reading of the texts; Mr. Xutian Xue, Mrs. Kawthar Al Balushi, Mr. Alla Balkees, Mr. Ayman Badawy, Dr. I. Emovon, Dr. Serena Lim and Miss Lynna Rosli who each have been a great source of encouragement and have given useful advise that kept me going.

Most of All, I give all thanks to God who Empowered my wisdom, health and that of my family, and made channels of financial resources that enabled me to go this far in life in spite of many circumstances naturally pointing to me giving up.

Table of Contents

Nomenclature

Table 1-1 Parameters description

symbol	*description*	*unit*
L, L_{pp}	*length between perpendiculars (LBP)*	m
Loa	*Length overall*	m
B	*Breadth moulded*	m
m	*Mass of ship*	kg
D	*Depth Moulded*	m
T	*Mean Draught*	m
Δ	*Mass Displacement of Ship*	kg
∇	*Volume Displacement of ship*	m^3
$S(x)$	*Sectional wetted area*	m^2
$S_y(x)$	*Sectional added mass in sway*	kg
$S_y(x)l_n$	*Section added moment of inertia in roll*	kgm^2
A_w	*Surface area of water plane, in (m2), at the design draught,*	m^2
A_{33}	*added hydrodynamic mass of ship in heaving*	kg
A_{44}	*moment of inertia for the hydrodynamic added mass in pitching*	
k_{yy}	*Longitudinal radius of gyration (0.236 L)*	m
K_M	*Distance from Keel to Metacentre*	m
K_G	*Keel to Centre of Gravity*	m
C_B	*Block coefficient (0.572)*	-
C_m	*Midship coefficient*	-
GM_L	*GML is the longitudinal metacentric height*	m
GM_T	*GMT is the initial transverse metacentric height*	m
$Gz(\phi)$	*Righting moment as a function of roll angle*	m
I_X, I_Y, I_Z	*Moments of inertia about the body axis system*	$Kg.m^2$
I_{XZ}, I_{YZ}, I_{XY}	*Products of inertia about the body axis system*	$Kg.m^2$
K, M, N	*Hydrodynamic moment components along body axes*	*Nm*
p, q, r	*Rotational velocity components of ship relative to inertial reference system along body axes in roll, pitch and yaw, respectively*	*Rad/s*
u, v, w	*Translational velocity components of ship relative to fluid along body axes*	m/s
$\dot{u}, \dot{v}, \dot{w}$	*Surge, Sway, linear accelerations*	m/s^2
$\dot{p}, \dot{q}, \dot{r}$	*Roll and Yaw angular accelerations*	rad/s^2
Vs	*The resultant velocity at mid-ship*	m/s
V	*Initial velocity of ship*	m/s
x, y, z	*Distance along the principal axes*	m
x_G, y_G, z_G	*Coordinates of the centre of gravity in the body axis system*	m

symbol	*description*	*unit*
$xpos, ypos$	*Component of the resultant position of the origin, O, of the ship along a fixed set of earth axes,* x_0 *and* y_0.	m
h	*Time step*	s
X, Y, Z	*Hydrodynamic force components along body axes*	N
x_G, y_G, z_G	*Coordinates of the centre of gravity in the body axis system*	m
Δ	*Displacement weight of ship*	kg
θ	*pitch angle: bow up positive*	rad
ρ	*Mass density of sea water*	Kg/m^3
φ	*roll angle: starboard down positive*	rad
ψ	*yaw angle: bow to starboard positive*	rad
u_c	*surge velocity relative to current, in the ship's coordinate system*	m/s
v_c	*sway velocity relative to current, in the ship's coordinate system*	m/s
$V_{current}$	*Velocity of current*	m/s
V_{wind}	*Velocity of wind*	m/s
L_w, λ	*Wavelength*	m
ω_w	*Wave frequency*	rad/s
ζ_w	*Wave amplitude*	m
k	*Wave number*	$1/m$
ξ_G	*Longitudinal position of centre of ship gravity from a wave trough*	m
$\xi_G{}'$	ξ_G/wavelength	-
v_{mw}	*Mean velocity*	m/s
$\overline{u}$	*Gust speed*	m/s
$Y'_{\dot{v}}$	*Non-dimensional Added mass due to sway acceleration*	-
Y'_v	*Non-dimensional sway force due to velocity*	-
$N'_{\dot{v}}$	*Non-dimensional Yaw moment due to sway acceleration*	-
N'_v	*Non-dimensional Yaw moment due to sway velocity*	-
$\dot{N}_{\dot{r}}$	*Non-dimensional Added mass due to yaw*	-
$\dot{N}_r$	*Non-dimensional Yaw restoring moment*	-
χ	*Heading angle from wave direction*	rad
ξ_G	*Longitudinal position of centre of ship gravity from a wave trough*	m
$\xi_G{}'$	ξ_G/wavelength	-
h_R	*Rudder span length*	m
h_H	*vertical distance between calm water surface and point upon which lateral force,* Y_G *acts.*	m
A_R	*Rudder area*	m^2
δ	*Rudder angle*	rad
c_{pv}, c_{pr}	*Propeller flow rectification coefficients*	-
$c_{\delta r}, c_{\delta rrr}, c_{\delta rrv}$	*Rudder wake coefficients in equation for* v_R	-

symbol	*description*	*unit*
D_p	*Propeller diameter*	*m*
γ	*Rudder Flow rectification coefficient*	*-*
F_N	*Normal force action on the rudder*	*N*
J	*Advance coefficient*	*-*
SMCR	*Specified Maximum Continuous Rating*	*KW*
κ	*Experimental Constant for determining* u_R	*-*
K_T	*Thrust coefficient*	*-*
T_p	*Propeller thrust*	*N*
T_p'	*Non-dimensional propeller thrust*	*-*
χ	*heading angle from wave direction*	*rad*
χ_{wind}	*Wind angle of attack*	*rad*
n	*Number of propeller revolutions*	*Revs/sec*
u_P	*Effective propeller inflow velocity*	*m/s*
u_R, v_R	*Components of rudder effective inflow velocity*	*m/s*
V_R	*Effective rudder inflow velocity*	*m/s*
w_p	*Effective propeller wake fraction*	*-*
x_H	*x coordinate of point on which normal force* F_N *acts*	*m*
x_P	*x coordinate of propeller position in equation for* u_P	*m*
x_R	*x coordinate of point on which rudder force* Y_δ *acts*	*m*
z_R	*z coordinate of point on which rudder force* Y_δ *acts*	*m*
z_H	*Vertical coordinate of the acting point of the hull lateral force*	
Λ	*Rudder aspect ratio*	*-*
α_R	*Effective rudder inflow angle*	*rad*
a_H	*Rudder – hull interaction coefficient*	*-*
δ_E	*Command rudder angle*	*rad*
K_p	*Proportional action factor*	*-*
τ	*Constant in the Equation for* u_P	*-*
ε	*Constant in the Equation for* u_R	*-*
EEOI	*Energy Efficiency Operational Indicator*	
WHRS	*waste heat recovery system*	*-*
Y_W^{Diff}, K_W^{Diff}, N_W^{Diff}	*Diffraction components of wave loading in sway, roll and yaw.*	*N*
X_{FK},Y_{FK}	*Froude-Krylov forces in surge and sway respectively*	*N*
K_{FK}, N_{FK}	*Froude-Krylov moments in roll and yaw respectively*	*Nm*

Chapter 1 Introduction

In the past, the design and production of ships was driven by operational costs, owner requirements, reliability and overall efficiency while ensuring that environmental regulations were being followed. Today, the need for environmental protection is fast dominating all other factors. Researchers have been investigating methods of reducing emissions through design for improved efficiency, optimal operational practices, etc. For instance, Schröder *et al.* (2017), presented a study of the environmental impact of exhaust emissions caused by shipping in the Artic areas with special focus on ice scenarios. This study does show the sensitivity of vessel performance and amount of exhaust emissions that optimize arctic traffic with respect to efficiency, safety and environmental impact. At its 62nd Session, held from 11th to 15th July 2011, the International Maritime Organisation adopted mandatory measures towards reducing Greenhouse Gas (GHG) emissions from International Shipping. In this respect, there was an amendment which added a new Chapter 4 to MARPOL Annex VI (Regulation for the Prevention of Air Pollution from Ships) Regulation on Energy Efficiency, and for Ships to make mandatory the Energy Efficiency Design Index (EEDI) for new Ships and, the provision of a Ship's Energy Efficiency Management Plan (SEEMP) for all ships.

EEDI is a measure on the amount of carbon-dioxide (CO_2) that is emitted by a ship for one unit of cargo carried. In other words, the EEDI requires a minimum energy efficiency target (e.g. tonne mile) for different ship types and sizes. The attained EEDI is the actual calculated and verified EEDI value for an individual ship based on the data in the EEDI technical file. The required EEDI is the maximum allowable EEDI for a given type of ship. EEDI provides a specific target figure for an individual ship design, expressed in grams of carbon dioxide (CO_2) per ship's capacity-mile and it is calculated by a formula based on a given set of ship's design parameters – smaller Energy Efficiency Design Index, thus implies a more energy efficient ship design. In respect of the above, there was some progress on an agreed Work Plan in which the Marine Environmental Protection Committee (MEPC) was tasked with further improving:

a) Guidelines on the method of calculation of the EEDI for new ships,

b) Guidelines for the development of a SEEMP for all ships,

c) Guidelines on Survey and Certification of the EEDI, and

d) Interim Guidelines for determining the minimum propulsion power and speed to enable safe manoeuvring in adverse weather conditions or sea states.

The EEDI formula does estimate the carbon dioxide (CO_2) output per tonne-mile: Its numerator represents the CO_2 emissions after accounting for any "innovative" machinery and electrical energy efficiency technologies that are incorporated into the design. The denominator is a function of the speed, cargo capacity, and ship specific factors. A simplified equation is:

$$EEDI = \frac{CO_2\ emissions\ per\ unit\ time\ of (main\ engines + aux\ engines - WHRS - innovations)}{cargo\ capacity \times ship's\ speed} \qquad 1\text{-}1$$

Included in the plans assigned to the Marine Environmental Protection Committee (MEPC) was the need to improve on the "*draft interim Guidelines for determining minimum propulsion power and speed to enable safe manoeuvring in adverse weather conditions or sea state*".

With the aim to clarify this last point, it is imperative to note that most ships were in the past, built with very high power output to increase the factor of safety; this adjustment in priorities which calls the need to install the minimum necessary propulsive power for sailing is clearly very useful in reducing environmental pollution however this might end up creating other problem(s). For example:

a) Vessel may not be able to meet with the need to freely manoeuvre in certain possible adverse weather conditions that are normally encountered in service.

b) It might be reasonable for a customer to determine their minimum propulsive and operational power requirement considering a certain route that the vessel is expected to operate over at the time of build. However, most ships get eventually become sold or have to be used for operations in sea areas with different environmental conditions at some point in their service life.

c) Reduction in scheduled speed in a bid to improving efficiency say by a redesign to take more cargo or derating the engine (i.e. accepting longer voyage times) may mean that more ship(s) may be needed to carry cargo as

the extra cargo gain may be unfavourably proportionate to the speed loss for maximum efficiency. An extra ship in the fleet may thus create more emissions.

d) With age, engine power output may reduce, vessel route may change to areas with more adverse weather, and hull conditions may not be in as-built condition, vessels may not continue to be commercially viable as more time may have to be spent at sea in normal passage with same amount of cargo and the ship operator will have to pay a disproportionately higher amount in staff salaries for delivering the cargo.

e) Reduced speed increases the risk of hull fouling, which leads to increased emissions for given distance.

f) The rudder effectiveness may reduce substantially in adverse weather condition if not properly matched, especially for retrofitted ships, this could result in collision or grounding.

g) Significant energy saving provision may be incapacitated, for instance, auxiliary boilers may be required to run continuously to service the heating systems. This may generally increase the EEDI.

Hence, the need to study the dynamic behaviour of the ship in certain defined adverse weather condition with a view to determining possible practical solutions at the design stage especially when there is a decision to reduce the engine's power to a minimum safe level; both for a new design and for the evaluation of an existing ship. A fast-time program of the type being used to prove this methodology would enable a prospective ship buyer or a regulatory authority to readily mathematically model a ship in the adverse environmental cases that may be encountered on a planned or a future new route, so that a decision can professionally be reached on whether or not its installed power is enough for the vessel to sustain safe motions.

A vast amount of theoretical studies on manoeuvring are available. Most of them have been validated with data obtained from experiments of manoeuvring in calm water and also data that has been obtained from assessment of seakeeping performance in wave condition separately and generally not with experimental data including that which applies to both simultaneously as in Letki and Hudson (2005),

where experiments were conducted and used to validate a unified mathematical model that was proposed by Bailey (1997). The limited number of available experiments is generally due to the large number of parameters that are involved, such as the ship's speed, water depth (for studies that involve shallow water effects), frequency and amplitude of the experienced waves, as well as the ship's rigid body responses, which may be either linear or non-linear e.g. large pitch and heave motions that could induce bottom touching in shallow water, and there is risk of damage if such experiments are carried out in reality. This program was developed to help make a relatively inexpensive and quick decision to be reached and as well as to narrow down the number of probable experimental runs.

To determine the minimum power some criteria needed to be used to make some judgement. For this work, since it is known that an undesirable reduction in speed could will occur when manoeuvring in an adverse weather condition, the criteria chosen is to conduct some set of turning circle motion and reduce the power each time, until the power is reduced to such a level that the speed loss during the turning circle motion is such that reduces the manoeuvring speed to below 4knots at any point in time. This is because, in IMO (2017) and Shigunov (2012b), it was stated that a vessel whose manoeuvring speed reduces to less than 4 knots substantially reduces its ability to respond to rudder control. Also, during a turning circle motion, the vessel is more likely to face all directions and at some point be subject to the greatest effects contributed by wind and current in addition to the waves in a defined environmental condition, thus reasonable judgement can be made. The result from the trial of this methodology showed that at 65% MCR, the ship speed at some point reduces to a value just below 4knots, thus it is said to have just crossed to an unsafe margin at 65% MCR power and as such the engine cannot be derated to an MCR power level below 70% of its present maximum MCR.

Also, a coupled heave and pitch response was analysed as this will give an indication of the level of power where this responses can be very high and cause such effects as propeller emergence which will lead to propeller racing and loss of efficiency, bow immersion, Thus an engine will not be derated to run with such power as its maximum continuous rating when such a defined weather condition is to be encountered. The simulation result from testing this method showed that at the defined adverse weather condition, the heave and pitch motion increased while the

engine maximum continuous rating (MCR) was reduced until about 65% MCR after which the values started reducing.

1.1 Aims and Objectives

This study is aimed at developing a method of predicting the dynamic characteristics of a ship at different levels of power in calm weather and in defined weather conditions so as to enable a stakeholder to know the magnitude of the acceptable minimum level of installed power that will allow the ship, in its in-service condition, to meet certain safe performance criteria. This study, when fully developed, will create a tool that can easily be used for the preliminary prediction of vessel's manoeuvring performance using the basic initial design parameters, which will reduce the number of trials when going into an otherwise time-consuming and expensive CFD modelling and analysis process (for instance, Duman and Bal (2017) that used unsteady Reynolds-averaged Navier-Stokes – URANS, and Dubbioso *et al.* (2013) that used an cnavis solver applying Dynamic Overset Grids) for predicting the turning and zigzag manoeuvring performance of a surface ship) thus reducing both cost and elapsed time. Shenoi *et al.* (2016), mentioned that the application of CFD in the field of ship manoeuvring has been significant in the past two decades and cited many authors that have used various CFD methods in the field of ship manoeuvring studies which are time consuming.

The objectives are thus to:

a. Propose a wholesome method for assessing the effect of environmental loading on a ship when its engine is derated for the purpose of improving EEDI and testing this method will involve:

b. Indicate acceptable criteria for manoeuvring performance of a ship in calm water conditions and defining criteria that will be considered unsafe in adverse weather conditions,

c. Establishing a definition for adverse environmental condition, including wind, current and waves.

d. Developing a cheap fast-time and efficient simulation tools that can model the manoeuvring performance of a given ship when attempting the defined criteria manoeuvres (b) in the identified environmental conditions (c).

e. Derive an algorithm for running repeated scenarios using the derived simulation tool (d), subject to irregular inputs (c) and capable of outputting a pass-or-fail decision, based on the identified criteria (a), and

f. Perform trial runs of program based on (e) for different defined scenarios evaluate the results.

In Chapter 2 the background of this research was given and a review of the work of other researchers, organisations and individuals that have made useful contributions in the field of ship motion studies and simulations, EEDI related studies and environmental effects simulations. Chapter 3 outlines the formulations used to develop the algorithms for the ship motion code and the method applied for simulating the environmental states, presents the necessary assumptions made to simplify the application of the formulae. Chapter 4 further illustrates the modelling of the ship, giving details of the dynamic motion analyses, Hull, propeller and rudder forces and moments and how they were configured to establish the manoeuvring motion in the program. Chapter 5 demonstrates the modelling of the various components of the environmental forces and moments acting on the ship and how they were implemented in the code. Chapter 6 analyses the output of the program and discusses relevant results, and Chapter 7 gives the concluding remarks.

Chapter 2 Background and Literature Review

As noted earlier, the IMO adopted a new chapter to its MARPOL Annex VI in July 2011, in which the Energy Efficiency Design Index (EEDI) was made mandatory for new ships and a Ship Energy Efficiency Management Plan (SEEMP) was required for all ships. These include a package of mandatory technical and operational measures to be implemented in order to effectively reduce Green House Gas (GHG) emissions from international shipping activities. This was said to be the first legally binding climate change treaty to be adopted since the Kyoto Protocol (IMO (2011), Copela (2013)). The context of concern in that chapter (Inclusion of regulations on energy efficiency for ships in MARPOL Annex VI) is the need to improve the energy efficiency of new ships through improved design and propulsion technologies, and for all ships, old and new through improved operational techniques. The Marine Environment Protection Committee IMO (2016) made a revision of the guidelines through technical and practical considerations and introduced an evaluation for determining the minimum installed propulsion power in order to maintain the manoeuvrability of ships in adverse weather conditions. This research work is guided by adopting some of these provisions.

2.1 Energy Efficiency Design Index

In the process of conducting this research one took into consideration, the guidance of the Marine Environmental Protection Committee, and other scholars that in one way or the other made contributions regarding the minimum safe power requirement of the Energy Efficiency Design Index, this section cites related works.

In order to assist with the implementation of the mandatory regulation on the Energy Efficiency for Ships, the Marine Environment Protection Committee (MEPC) has amongst other developments, adopted/approved or amended the following important guidelines:

a. MEPC (2017), does contain guidelines in order to assist ship owners, ship builders, manufacturers and other concerned parties on the methods of the calculation of the attained Energy Efficiency Design Index (EEDI) for new ships and which should be taken into consideration when developing and

enacting national laws which gives force to and the implementation of provisions set in regulation 20 of MARPOL Annex VI, as amended.

b. *MEPC (2013) are Guidelines for calculation of reference lines for use with the Energy Efficiency Design Index (EEDI)* which apply to the following ships types: bulk carrier, gas carrier, tanker, container ship, general cargo ship, refrigerated cargo carrier, combination carrier, ro-ro cargo ship, ro-ro cargo ship (vehicle), ro-ro passenger ship and LNG carrier.

c. IMO (2017) which is practically meant to assist administrations and recognized organizations in verifying that ships complying with the EEDI requirements set out in regulations on energy efficiency for ships do have sufficient installed propulsion power to maintain the manoeuvrability in adverse conditions, as specified in regulation chapter 4 of MARPOL Annex VI.

d. MEPC (2012). These guidelines mainly contain some correction factors for ship specific design elements and other factors such as, availability factor of innovative energy efficiency technology (f_{eff}), weather factor, cubic capacity correction factor (fc) and capacity factors Strasser *et al.*) were indicated and of the methods of arriving at them being given for various types of ships. Earlier in its sixty-fourth session (1 to 5 October 2012) The Marine Environment Protection Committee, circulated a developed guidelines for calculating the coefficient f_w (Weather Factor) for the decrease in ship speed in a representative sea condition for trial use MEPC (2012) , as contained in the 2012 Guidelines on the method of calculation of the attained Energy Efficiency Design Index for new ships MEPC (2017).

In a study jointly sponsored by the American Bureau of Shipping (ABS) and Herbert Engineering Corp. (HEC), Ozaki *et al.* (2011) noted that the EEDI baseline falls short due to the fact that the proposed EEDI baseline curve calculations utilised simplifying assumptions because they were based on existing ships data bases and which do not contain all of the data required for the EEDI calculation. They discussed their findings after developing “standard” ship designs for tankers, container ships, and LNG carriers over a range of ship sizes on the assumption of highly efficient hull performance and having modern power plants. By evaluating the baselines for tankers, LNG carriers, and containerships utilising the “standard” ships, the study

proposed the attained EEDI that can be achieved with well-designed new-buildings prior to the application of any innovative technologies. As such, they suggested their work as being an effective metric for validating the proposed EEDI baselines. Greece submitted a proposal to the International Maritime organisation as can be seen in IMO (2010), in accordance with MSC-MEPC.1/Circ.2, guidelines on the organization and method of work and makes some additional observations on the EEDI formula. The main reason for the document was to highlight possible misapplications of the EEDI formula if the ship is underpowered, and thus proposed that:

- Until full development of a reliable weather factor (fw) is completed, apply 15% sea margin to the speed to account for the transition from sea trial confirmation to actual sea conditions and, thus, to truly select an engine MCR and its related SFOC for 75% MCR operation in actual sea conditions.

- It is required explicitly, in case an engine is derated, to use the derated MCR in the EEDI formula.

These are amongst key proposals being considered by the classifications societies.

Borkowski *et al.* (2012), presented a calculation for the EEDI for a container ship based on the characteristics of the ship at build, incorporating parameters such as ship capacity, engine power and fuel consumption. The intended application of their work was to stimulate innovation and the technical development of all elements influencing the energy efficiency of a ship starting from its design phase. However, they pointed out that, regarding the EEDI for ships of types not covered in their paper, some suitable formulae will need to be developed. Ančić *et al.* (2013), proposed a method of calculation for the attained EEDI for passenger and Ro-Ro passenger ships, considering their specific operational requirements and power system configurations. Their method was based on the performed EEDI calculation for a ferry with both conventional and integrated power system. In their work, they discussed certain inconsistencies in the existing guidelines and also highlighted their opinion that the current approach is quite rigid and unable to adapt to the newer configurations of ship's power systems. Thus they proposed a new and simplified approach in the ship's power system evaluation process which includes a new scheme that more clearly represents marine power systems.

In SHOPERA (an European Union (EU) funded research project which was set up in order to address the safety concerns of ships if the EEDI requirements were to be achieved by simply reducing the installed engine power), Papanikolaou *et al.* (2016) discussed the background of the research of SHOPERA, and presents some early results of the project that elaborates on the criteria for ship's manoeuvrability and safety under adverse operational conditions. Shigunov (2012a) and Shigunov (2012b) formulated the criteria for ship propulsion and steering abilities which included that the ship should be able to keep course in waves and wind from any direction and secondly, keep advance speed of at least 4.0 knots in waves and wind from any direction. The corresponding weather conditions were not made severe, because ship masters do not stay near the coast in an increasing storm and either search for a shelter or leave to the open sea and take a position with enough room for drifting. The recommended environmental conditions to be applied in a scenario where escape is impossible were also proposed. Cariou (2011) studied the effect of slow steaming strategies being implemented by many shipping lines have significantly reduced carbon-dioxide emissions from international shipping, especially in container shipping. However, this was with a view to investigating the sustainability of the speed reduction due to increasing fuel price and proposed that such reductions can only be sustained around bunker price of at least $350–$400 for the main container trades. With the drive towards environmental protection, the sustainability assessment now needs to principally consider the reduced carbon-dioxide (CO_2) emissions in to the assessment and not just cost fuel cost alone.

A study which investigated the impact of EEDI on very large crude carrier (VLCC) with regards to their design and CO2 emissions was carried out by Devanney (2011), of the Centre for Tankship Excellence, (CTX). This report contained detailed calculations supporting the organisation's position, which amongst other contents of the conclusion, is the point that, under more realistic assumptions, EEDI actually increases the VLCC carbon-dioxide emissions slightly. Badea *et al.* (2015) highlighted some of the shortcomings of EEDI, explaining that they appear mainly due the fact that this index covers only a couple of energy systems comprising of transport (in the form of the prime mover which may be a diesel engine) and, the processes or services, for example, heating and other auxiliary services (boilers, etc.), that are far too different in their method of assessment. They proposed a method of assessment and regulation of the ship energy performance, which

considers the main purpose of an increase in the level of performance by selecting the most effective measures of performance improvement from the available measures.

Attah and Bucknall (2015) presented some analyses of future powering options for LNG carriers when considering the Energy Efficiency Design Index (EEDI). They discovered in their study that the current EEDI reference baseline is not sufficient to stimulate improvements in the design of future LNG carriers because the current Dual Fuel Diesel Electric (DFDE) propulsion systems proposed to be installed on majority of future LNG Carriers orders already achieves EEDI values that are compliant with the EEDI baseline. They also suggested in their paper that the corresponding greenhouse gas emission index value could potentially rise by up to more than double, implying that the EEDI is limited in its value to reduce global warming, due to the unburnt methane emissions (methane slip) of the DFDE, and proposed the inclusion of methane slip emissions into the existing EEDI calculations.

Trodden (2014), proposed a propeller selection method that is most suited to ships which are susceptible to relatively large drift angles and/or relatively high installed power requirements. He suggested that the EEDI in its present implementation discourages design for in-service conditions. The value for the EEDI that the ship attains is verified from sea trials (in calm water). A ship that is optimised for service conditions may not be optimal when run in trial conditions, and thus may even fail the EEDI requirement, however in real working conditions the design may surpass the EEDI requirement. Hasan (2011), investigated the impact of EEDI on ship design and on the hull hydrodynamics. In order to find the impact on ship design and hydrodynamics, parametric analyses of ship is accomplished for different ship types such as bulk carrier, tanker, container vessel etc. He used the Holtrop and Mennen (1982) method to predict the Ship's resistance from which the main engine power was calculated. Then finally calculated the Energy Efficiency Design Index with the then current IMO formulation.

In a recent publication, Vladimir *et al.* (2017) gave a detailed explanation of the effect of ship size on the EEDI requirements for large container ships with more emphasis being placed on the formulation of the ship size and sailing speed to be included in the EEDI formula, using the IMO documents as a framework for their analysis. They

also proposed the need for updating of existing baseline formulation allow for the new ultra large container ship data available in the IHS Fairplay (The World's Register of Ships) database; by extending the EEDI reference line into the EEDI reference surface for container ships as a function of ship capacity and speed; and by establishing a relationship between the deadweight used in the EEDI calculations and the real ship capacity as measured in terms of TEU (twenty-feet Equivalent Unit) which enables for more practical data handling in overall container ship design procedures. Ma *et al.* (2017) considered that the inclusion of waste heat recovery systems (WHRS) could improve the overall ship efficiency and as well reduce emissions simultaneously and as such, they proposed three types of WHRS for recovering waste heat from a 10,000 TEU conceptual large container ship driven by a modern low speed marine diesel engine. Two software packages were developed by them for calculating the EEDI and the EEOI (energy efficiency operational index) of the subject container ship, and their results indicated that the large container ship itself can reach the IMO requirements of EEDI at the first stage with a reduction factor 10% under the reference line value. It was also claimed that the proposed waste heat recovery systems can improve the ship EEDI reduction factor by up to 20% under the reference line value.

Calleya *et al.* (2014) highlighted possible effects of EEDI on operating profitability and on CO_2 emissions, and investigated the potential implications of designing for EEDI and designing for profit maximisation, with both considered as incentives to reduce CO_2 emissions. Longva *et al.* (2010) presents an approach where a required index level can be determined through a cost-effectiveness assessment of the available reduction measures. For illustration purposes, eleven emission reduction measures were analysed for implementation on a representative ship, and the required index (IR) was reached after applying the measures fulfilling the decision criterion. They further proposed that other regulatory requirements such as a cap on emissions from shipping, e.g. for use in a shipping emissions trading scheme, could be developed by using the same principles, and suggested that using a cost-effectiveness approach in setting a required index or determining a cap will avoid the need for more prescriptive regulations detailing specific measures to be implemented, and the costs imposed by new requirements may be justified on the basis of the achievable emission reductions and cross-sector potential for achieving a global reduction target.

The wind power technology is an alternative means of complimentary source and may serve to meet the ship's energy requirement at sea and substantially reduce carbon-dioxide emissions. The Flettner rotors, a unique type of powered sail has attracted greater attention in recent times due to its improved potential to reduce fuel consumption on ships and thus make for a better Energy Efficiency Design Index. Pearson (2014) described the approach that was applied to create a software model for the use of auxiliary wind propulsion on common ship types of the UK fleet, giving preliminary indications of the benefits achievable, using the Flettner rotor as its subject model. It is worthy to point out a reservation on the use of the modern wind power technology being that their reliability has not been robustly proven, and if used as a substantial proportion of the energy source and a major failure occurs to it, then the ship may be incapacitated in an adverse weather condition; the methodology being proposed in this research can be applied in predicting safe operation of the ship in this condition. Some researchers have investigated how the implementation of EEDI would affect their individual countries when considering the global view.

Zheng *et al.* (2013) attempted to illustrate how the shipbuilding industry in China would be influenced by the implementation of the International Maritime Organization's (IMO's) Energy Efficiency Design Index (EEDI). They identified the characteristics of energy consumption in shipping and the stakeholders who involved in the EEDI application process, made analyses of the relationships among stakeholders in the shipbuilding industry in China, and pointed out the drivers and barriers in the implementation. They also discussed the impacts of EEDI on the Chinese shipbuilding industry, and explored future scenarios including the possible income and of China's position in the global shipbuilding industry using two cases typical of the Chinese shipbuilding firms. Some policy recommendations were provided to the shipbuilders and the government in order to promote the objective of the GHG reduction as well as the development of the Chinese shipbuilding industry itself. Finally, they concluded that the implementation of EEDI has profound impacts not only for China but also for all shipbuilding countries around the world, and that it may even trigger another migration of the shipbuilding industry in the future.

Rahman (2017) made some assessment and developed the EEDI for inland vessels of Bangladesh. Some assessment of the present situation of inland class vessels in terms of EEDI were made and a database developed and used for establishing the

EEDI references lines for different types of inland vessels of Bangladesh. The derived reference lines were validated and compared with the EEDI requirements of some other countries. Also, the impact of design parameters on EEDI for different types of inland vessels of Bangladesh were evaluated and the present status of existing inland vessels in terms of EEDI investigated, then sensitivity analysis of inland vessels of Bangladesh were performed in terms of EEDI considering socio-economic and technical factors in Bangladesh. Some recommendations were proposed for assessment of the energy efficiency of different types of ship at the design stage so that it can be helpful for regulatory authority to introduce some tools for EEDI for the inland shipping in Bangladesh in near future. These are amongst the numerous studies that have been carried out regarding the energy efficiency design index implementation showing how it is fast gaining attention globally. While the implementation of the EEDI is geared towards reduction of greenhouse gas emission, there is need to pay appropriate attention to other side effects of following the option of reduced speed such as the risk of collision, etc., which could create other forms of environmental pollution (e.g. cargo spill due to collision, etc.). Policies should be mostly aimed at newer ships with a view to combining the modifications of ship forms, addition of energy saving provisions to speed modifications for improved efficiency so that the dynamic performance can be improved with reduced installed power (speed) rather than just reducing speed.

It can be seen that substantial investigation have been carried out in identifying gaps the method of determining the EEDI and remediation proposals made. In a submission by the International Association of Classification Societies, IACS (Shigunov (2012a)), data from different types of ships within the EEDI framework were used to statistically derive a safe minimum manoeuvring speed of a ship for adequate turning and course-keeping ability in an environment with wind and wave effects. This information is particularly useful for this research as the ability of the ship to manoeuvre safely in defined adverse weather condition considered a reduction in speed below the safe minimum manoeuvring speed as failure criteria in the simulation studies.

2.2 Ship Manoeuvring and Associated Formulations

Several researchers have undertaken a substantial amount of work in the field of ship manoeuvring, however, the achievements thus far are still in an evolutionary state. There is still a lot to be accomplished for research into manoeuvring of ships to evolve to a definitive level such as:

- Empirical derivation of hydrodynamic derivatives using ships physical dimensions. Present level of research outcomes though is being applied in some studies, still do have significant deviations from experimental data;
- Studies on effects such as bank and shallow water, and associated formulations;
- Standardisation of formulations in the area of studies on the effects of environmental loads while manoeuvring especially in coastal waters.

Clarke *et al.* (1983) proposed some equations for analytically determining the approximate values for the hydrodynamic derivatives for a vessel at its design stage using the known scantlings on the assumption that the hydrodynamic added mass can be reliably approximated by the use of empirical formulas. They proposed some criteria for comparing the manoeuvrability of ships using mathematical expressions developed from linear theory and also proposed some empirical methods for deducing the linear acceleration and velocity derivatives from a basis of the external hull geometry. The dependence of the suggested criteria on hull geometry was discussed and the results of the linear treatment were compared with full-scale trials results. However, these formulations are still in their evolutionary stage and shows substantial errors for certain types of ships more research is needed in this area.

McCreight (1991), presented mathematical model for a time domain simulation of a surface ship manoeuvring in calm water. The presented six degree of freedom mathematical model was said to be applicable to conventional mono-hulls or SWTAHs and included calm water hydrodynamic forces, hydrostatic forces, unsteady wind forces, slowly-varying wave drift forces, and forces due to a towed body. The model depends upon data derived from model experiments. It was claimed that the model represents an improvement over previous models in several respects, such as, the speed loss prediction which improved due to the changes in the modelling of

the combined resistance due to calm water surge hydrodynamic forces, and propeller-rudder interaction.

A model was proposed by the Manoeuvring Modelling Group (MMG), which is a research group in Japanese Towing Tank Conference (JTTC), and which adopted a modular approach by presenting the hydrodynamic forces and moment's and the interaction effect between them in three parts as: acting on the ship hull, propeller and the rudder in all the forces and moments components. This relatively simple model as can be seen from Ogawa and Kasai (1978) , is currently popularly used manoeuvring mathematical model as many researchers see the result from this method as being much closer to real life conditions and does have closer agreement with model experimental results, in addition to its convenience of application.

Kijima and Tanaka (1993) later proposed some approximate formulae for determining the hydrodynamic forces on a ship with closed stern, popularly known as the MMG formulae. These formulae were obtained semi-empirically by the results of model tests and from numerical calculations by the use of the lifting surface theory, Kijima's method. Kijima's method was considered efficient in predicting the ship's manoeuvrability at the initial design stage and is even able to assess the effects of changes in stern design. Whereas because the Kijima's formulae are limited for a ship with closed stern, these could not be adopted for the manoeuvring prediction for a ship with a stern bulb, thus Lee and Shin (1998) carried out some studies aimed at improving Kijima's model used to predict ship's manoeuvrability at the initial design stage in consideration of ships having a stern bulb. The mathematical model was adopted as in Kijima's model and regression analyses were carried out for hydrodynamic derivatives and hull-propeller-rudder interaction coefficients. They simulated a ship's manoeuvrability, in order to validate the present MMG model and then compared these with results of Planar Motion Mechanism (PMM) tests and proposed a method to revise the earlier approximate formulas for hydrodynamic derivatives of full ships. According to their paper, they confirmed the effectiveness of their work using the practical prediction methods proposed by Kijima's method.

In the field of ship motion studies, Lewis (1989), gave an in-depth explanation of ship motions mathematical modelling equations and controllability; expressions that define the forces, moments and accelerations, and the criterion for stability and the practical

conditions that will affect the said criteria were derived and methods of application explained.

Fossen and Paulsen (1992), proposed a design approach on the application of feedback linearisation to lead to the automated steering of ships, which is flexible in its procedure such that it allows for the autopilot to be optimised for both course-keeping and course changing manoeuvres. Direct adaptive versions of both the course-keeping and the turning controllers were derived. The proposed work considered that its optimal course-keeping autopilot will be superior to conventional autopilots with respect to fuel economy. The global stability of both adaptive controllers was proven by applying nonlinear stability theory, with a level of performance that was illustrated in a simulation study, however, this method was not applied in this research as the researcher applied a simple but functional PD control system that makes for speedy computation.

Manoeuvring motions were normally simulated in 3 degrees of freedom (surge, sway and yaw) on the assumption that roll, pitch and heave are negligible on a ship's ability to manoeuvre. However, Son and Nomoto (1981), demonstrated the fact that in practice, roll motions can be observed during sharp turning in calm water because of the rudder and centrifugal forces and proposed a 4 degree of freedom equation which has been used in this work. These dynamic equations based on Newton's law of motion are as follows:

$$X = (m - X_{\dot{u}})\dot{u} - (m - Y_{\dot{v}})vr \qquad 2\text{-}1$$

$$Y = (m - Y_{\dot{v}})\dot{v} + (m - X_{\dot{u}})ur - Y_{\dot{r}} \qquad 2\text{-}2$$

$$K = \left(I_x - K_{\dot{p}}\right)\dot{p} + WGM_T\phi \qquad 2\text{-}3$$

$$N = (I_z - N_{\dot{r}})\dot{r} + N_{\dot{v}} \qquad 2\text{-}4$$

Where X and Y are surge and sway forces, K and N roll and sway moments, $\dot{u}$ and $\dot{v}$ are surge and sway linear accelerations, $\dot{p}$ and $\dot{r}$ ar the roll and yaw angular accelerations, u and v are surge and sway velocities, r is the yaw velocity, ϕ is the roll angle, and W the weight of the vessel. They also, pointed out that the manoeuvring coefficient variations due to wave are one of the important factors for course keeping stability in wave, which is critical for broaching prediction. This model have been

used by many authors and known as the conventional 4-degrees of freedom manoeuvring model and recently, Dong *et al.* (2015), conducted a 4 DOF manoeuvring experiment in order to estimate the manoeuvring characteristics of a ship at large heel angles greater than 10 degrees. The results from the experiments were analysed and a modified 4-DOF manoeuvring model was proposed which gives better level of accuracy at roll angles higher than 10 degrees.

Cepowski (2017), proposed some mathematical relationships for estimating the installed required main engine power for new container ships, based on data from vessels built during 2005-2015, using both simple linear regression and multivariate linear regression analyses. The said relationships estimate the engine power as a function of the length between perpendiculars and the number of containers (TEU) that the ship is being designed to carry. The paper claims that the given equations do have practical application for the estimation of the container ship engine power that is needed at the preliminary parametric design of the ship, and as well concluding that the use of multiple linear regression to predict the required main engine power of a container ship has a better accuracy than does the simple linear regression.

Based on the drive towards improving Ship's efficiency through the reduction of in the installed power to a minimum safe level, Shigunov (2015) discussed possible criteria for sufficient manoeuvrability in adverse weather conditions and proposed practical assessment procedures and examples of its application. The paper further outlined some necessary developments that could be pursued to improve the assessments outcomes. Molland (2011), contains useful information relating to Ship design and powering. It was the source of some basic equations, MAN (2011) gave extensive information that has to do with powering of ships also. Holtrop and Mennen (1982), developed a method based on statistical regression analysis of random model experiments and full-scale data, available at the Netherlands ship model basin, that is used for estimating the resistance of displacement ships in calm water condition. Because the accuracy of the method was reported to be insufficient when unconventional combinations of main parameters were used, an attempt was made by the authors to extend the method by adjusting the original numerical prediction model to test data obtained in some specific cases and this adaptation of the method resulted in a set of prediction formulae with a wider range of application. However the accuracy of this method is limited to ships whose hull forms resembles the average

ship described by the main dimensions and form coefficients that are identified, low design and operating speeds and thus low Froude numbers. For extreme shapes, the accuracy of the estimates is not good. The method was used as a guide to selecting a suitable engine rating that was utilised in this research and the resistance vs ship velocity characteristics does very closely compare with the model of the engine manufacturer chose.

2.3 Manoeuvring with Environmental Loads

The motion of ships in an adverse weather condition leads to additional loading on the vessel which further increases the effects of roll, pitch and heave motions to a level that is no longer negligible. These motions are oscillatory motions in addition with their associated effects and consequences, (e.g., inertial effects), generally known as dynamic effects caused by relative motion of ships depending on the ship's characteristics and environmental conditions. These effects can be divided into 'vertical effects' comes from heaving and pitching motions, and 'rolling effects' which comes from the Rolling motions (Bhattacharyya (1978)) and includes:

a. Loss of forward speed in a seaway,

b. Free racing of engine due to propeller emergence (which is assumed to occur when one-third of the propeller is out of the water),

c. The shipping of green water over the bow (is said to occur when the relative amplitude exceeds the freeboard at a particular location),

d. Slamming (bottom slamming and bow flare impact), particularly in the forward bottom part (which takes place when the ship's bow re-enters the water with a relative vertical velocity between the ship and the waves exceeding certain threshold value), and

Acceleration effects, especially, vertical accelerations at critical areas such as accommodation, bridge deck and machinery space, and vertical and lateral accelerations which may result from rolling and pitching.

Here the work of authors that have included environmental loads in their manoeuvring studies and some seakeeping studies are identified. Most works have associated manoeuvring with emphasis on the performance in calm water predictions which assumes that hull forces are independent of the frequency of motion and are usually based on body-fixed axes, while seakeeping predictions are usually based on translating earth reference axes and considers the influence of motion frequency with the vessel as it operates in wave and windy environments. However, Bailey (1997) proposed a unified mathematical model that describes the manoeuvring of ship in a seaway but it was not validated. Letki and Hudson (2005) in their work, presented a summary of the principle of a unified mathematical model for the manoeuvring of a vessel travelling in seaway. They carried out some validations of the Unified Mathematical model proposed earlier by Bailey (1997) using a British Bombardier tanker for defined manoeuvres and gave the results of their study of the effects of waves on the ship's manoeuvring characteristics for both following and for head seas. Martins and Lobo (2007) predicted trajectories in earth fixed reference frame through a proposed method of applying feed-forward neural networks for predicting manoeuvring behaviour at the design phase or following changes on a new design. The feed-forward neural network was trained using sea manoeuvring trials data of similar vessels. They verified their proposal by applying it to a set of 47 manoeuvring from two different vessels.

Sandaruwan *et al.* (2009), developed a ship simulation system for simulating ship motions in six degrees of freedom, (surge, sway, pitch, heave, roll, and yaw) in a virtual environment with respect to environment disturbances such as sea wave, wind and sea currents. It was claimed that the system is simple and responds in real-time to interactions and it is based on a mathematical ship model derived from the non-linear speed equations, Newton's laws of motion, fluid dynamics and other basic physics. They used multivariable functions to model the ocean surface with superposition of sinusoid functions. The paper stated that the model simulator requires fewer amounts of ship data and that the chosen mathematical ship model can be used with different types of ships and thus can be used in real time virtual reality applications.

Khattab and Pourzanjani (1997), developed a ship motions modelling software package, and undertook a comprehensive study, applying a four-quadrant

mathematical model for simulating ship handling behaviour in both open seas and in confined waters. In their work, the human handling technique was modelled following a routine sequence of operational procedures, with an emphasis on the ship handling behaviour rather than on the human operator. They gave some examples of certain scenarios, such as normal handling performance and engine failure and partial tug failure modes were given. In their mathematical modelling of the external forces and moments, they included docking effects (such as tug, fender forces, mooring ropes and anchors, etc.) with emphasis on the effects of the tug bollard pull. However, this effect will not be considered in this current work. Yasukawa and Nakayama (2009), proposed a practical method for simulating ship manoeuvring and wave induced motions, using a numerical method based on the strip theory, for calculating the hydrodynamic forces and wave induced motions on a container ship (S-175), a sister ship of the subject ship whose hydrodynamic experimental data was used for this simulation.

Ayaz *et al.* (2006) proposed a 'horizontal body axis system' in the development of a coupled non-linear 6-DOF model with frequency dependent coefficients, which incorporate memory effects and random waves, and which allows for a straightforward combination of seakeeping and manoeuvring models while describing extreme motions. In page 29 of his PhD thesis, Ayaz (2003) acknowledged that the 6 degrees of freedom non-linear mathematical models are proving to be robust tools for simulating the manoeuvring behaviour of vessels in waves. However, to overcome the complex non-linear problems and to simplify the equations of motion, he pointed out that if a ship advances at relatively high speed, the encounter frequency becomes much smaller than the natural frequency in heave and pitch, and which makes it possible for these motions to be calculated by simply tracing their static equilibrium and as such the mathematical model can be reduced to 4 degrees of freedom, excluding the heave and pitch motion. In this research, a coupled four degrees of freedom (surge, sway, roll and yaw) experimentally derived non-linear hydrodynamic derivatives and equation were applied as this improves the results of the non-linear effects such as the Froude-Krylov forces and moments, and agreement when large rudder angle non-dimensional hydrodynamic coefficients are properly estimated. Additionally, coupled heave and pitch response in waves was considered.

Generally, the effect of environmental loading on the motion of ship has been considered in various aspects, such as speed loss, power loss, motion response and concepts such as broaching etc. Also, the effect of derating an engine have been studied with a view to ascertaining its benefits in terms of fuel savings, being an option adopted when prices of fuel are high as was studied in the work of Notteboom and Vernimmen (2009). The perspective of studying the safety implications for reducing speed in an attempt to improve EEDI is topical issue that is currently being investigated IMO (2010), and this research proposes a method of assessing the overall dynamic effects due to environmental loading on the derated ship and develops an easily affordable tool that can quickly model these effects at various levels of installed power with a view to ascertaining the least power for safe and efficient operation.

2.3.1 Wind Load Parameter

This section discusses the contribution that have been made by several authors in the area of analysis and prediction of wind loading. Normally, wind flow over the ocean surface from any direction forms a natural boundary layer which implies that the wind velocity has a profile that is such that its magnitude at the surface is zero and increases with higher altitude. The local wind field caused by the motion of a ship does not have such a boundary layer and is homogenous. Thus the resultant wind field encountered by the above-water surface section of the ship is a combination of the wind field with the boundary layer and the ship motion generated wind field due to its forward speed. Wind loading is normally experimentally evaluated with the aid of wind tunnels, however, this combined wind field is difficult to create in any wind tunnel but several researchers have made some attempt towards predicting wind loading by making some reasonable assumptions and constraints of their results to specific circumstances.

Wind loading on a ship is an important parameter to be considered, though the mean static forces and the moments created by it does result to only a fraction of the resultant loading on the ship. There are instances when the effects of these forces and moments become critical resulting in cracks occurring in booms due to dynamic wind loading especially in event of resonance flows Oppen and Kvitrud (1995). Proper estimation of wind loads plays important roles in the modelling of ship loading as wind loading does affect the efficient operation of a ship's propulsion plant and

consequently on her manoeuvrability. Also, wind loads do pose significant influence on operations such as the towing of ships, dynamic positioning and mooring of ships and offshore structures.

Empirical formulations for deriving Wind Forces and moments and associated parameters have been proposed by several scholars. Isherwood (1973) utilised the results of an analysis of wind resistance experiments carried out at several different test establishments on a number of hull models and superstructure models covering a wide range of merchant ships in order to generate equations of linear multiple regression models for wind coefficients in terms of eight parameters, namely: the transverse wind current projected area, lateral wind current projected area, lateral projected area of the superstructure, beam of the hull, distance from bow of centroid of lateral projected area, length overall, number of distinct groups of masts or kingposts seen in projection, length of perimeter of the lateral projection of vessel excluding the hull below waterline and slender bodies such as masts and ventilators. This work has been appreciated by many researchers as having a high level of accuracy and versatility, however, the prominent observation on this is that it is limited to these three degrees of freedom and new ship forms, e.g. cruise ships are not included in the database and it has not been updated for more than 40 years.

Blendermann (1995), carried out a parametrical study of the wind loading on ships based on both wind tunnel tests and on semi-empirical loading functions and provides coefficients of lateral and longitudinal resistance, the cross-force and the rolling moment. Case studies of a car carrier and a floating dock were presented. Results were given using statistical terms. Yang Xingyan (2013) proposed a method for calculating ship’s windage area based on Ship forms and tonnages. This method has good practical application for ship in it design stage and useful for the purpose of computerised programming of such prediction. Fujiwara *et al.* (1998), proposed a linear multiple regression model for estimating the wind forces and moments acting on a ship. They developed a model which can be used for new ship types such as large pure car carriers (PCCs), Liquefied Natural Gas (LNG) carriers, container ships, VLCCs, and passenger ships. The model have been widely used by various researchers. It provides results for change of wind direction between 0 and 180 degrees.

Fujiwara et al. (2006) presented a model based on the hydrodynamic physical components of ship responses. Included in the formulations are contributions from the hull, rudder, and propeller, and of the above waterline structure in conjunction with the wind and sea state dynamics. Part of the model includes the calculations of wind induced forces and moments on a vessel. The model was based on both wind tunnel and towing tank tests. Actual ship parameters were used in order to calculate the overall forces and moments. Wind angles were shown from 0 degrees at the stern (i.e. a following wind) to 180 degrees on the bow (a head wind) on the 'sign Convention'. The coefficients that are given are only valid for vessels with superstructures at the stern i.e. conventional tankers and bulk carriers. The coefficient 'C_{xw}', and area 'A_T' refer to the as-viewed head-on projected area of the above waterline portion of the vessel. Because any changes in the freeboard have the most significant impact on the wind coefficient, certainly soon the projected cross-sectional area, they developed separate curves for the fully loaded and ballasted conditions. Variations in bow shape configuration also produce a substantial difference in the longitudinal force coefficient for a ballasted tanker. The wind-drag coefficients in their study assumed zero trim in the fully loaded condition and, for tankers, 0.8 degrees trim in the ballast condition.

Ueno *et al.* (2012) Proposed a simple method for estimating the wind load coefficients of ships using ship type and ship length. The Selected ship types and conditions are full loaded oil tankers, oil tanker in ballast condition, bulk carrier full loaded, bulk carrier in ballast, LNG carrier in full load, LNG carrier in ballast, containerships in full loaded condition, passenger ships, and others. The simple method employs a procedure to estimate wind load coefficients using these estimated eight parameters. The validation was carried out making comparison with of data of 76 ships wind load coefficients estimated by the simple method with wind tunnel test data and those by some precise method and their proposed approach showed allowable precision and usefulness, especially recommended for situations where there is limited information or time constraints. Żelazny (2014) proposed an approximate method of calculating wind forces and moments acting on for bulk carriers, in a form useful for preliminary ship design, when only basic ship dimensions are known. The coefficients were approximated by a polynomial that only depends on the relative wind direction based on the measured aerodynamic tunnel model test results of Brix (1987), and the longitudinal and lateral projected areas were

calculated for 33 for bulk carriers, and then applying the linear regression method, an appropriate polynomial including only basic ship parameters (bulk carrier) was developed.

Andersen (2013) carried out some investigation of the influence of the container configuration on the deck of a 9000+ TEU containership on wind forces through a series of wind tunnel tests carried out in a naturally existing boundary layer of the wind tunnel, using a 1:450 scale model. The longitudinal and transverse forces and the yaw moment were measured and the measurements were corrected for the effects of boundary layer and blockage in the wind tunnel. The results were presented as two different types of non-dimensional coefficients. The paper suggested how the wind resistance can be reduced by adjusting the configuration of the containers.

The Oil Companies International Marine Forum (OCIMF) had published guidelines on wind load data in ‘Mooring Equipment Guidelines’ (MEG3), OCIMF (2008) which includes a method for estimating the wind loads based on the results from wind tunnel model tests using four models representing similar tankers of 155000, 280000, 400000 and 500000 tonnes deadweight, and involves the use of non-dimensional coefficients which were transferred into curves relating the wind angle relative to the ship to coefficient magnitude OCIMF (2010). Knowledge of the true wind speed, direction and the above water projected cross-sectional area of the vessel allows a wind induced force to be estimated. Additionally, model test data on more modern tanker forms carried out recently had confirmed that the same coefficients are, in most cases, still sufficiently accurate when applied to smaller ships and that they therefore may be used for a range of oil tankers down to approximately 16,000 tonnes dwt.

These works have contributed immensely to the prediction of wind load on ships, however, there is need for more research as a lot of those formulations in common use are old and will not meet the requirement of modern ships or for one-of-a-kind ships. New research is mostly hindered by financial constraints as most related researches are done using expensive and time consuming wind tunnel facility.

The work of Blendermann (1995) was used for this programming due to the availability of data. It is worthy to note that a ship is a susceptible to roll motions while

in service and wind effect does affect its magnitude, most of the authors have given formulations as a function of wind direction ship dimensions etc., and their application have mostly been directed towards determining the resultant effect on forward speed and fuel consumption,. Since this research is about suggesting a wholesome approach to predicting the environmental effect, there is the need to also include the additional effect that the wind does create during roll motion which Blendermann's method does account for, as when combined with the other effects may create a significant outcome.

2.3.2 Wave Load and Related Parameters Derivations

The work of some scholars that gave extensive formulations relating to wave loading are discussed here. An earlier attempt to analytically determine the wave making resistance of a ship in motion was from the work of Mitchell (1898), who presented a general solution of the problem of the waves produced by a ship of given form, moving with a uniform velocity in an inviscid liquid, and proposed a method for determining the resulting wave–resistance to the motion of the ship. Its main assumption is that the hull is thin (the beam is small in relation to other characteristics lengths (the slender body assumption), and depending on the model may have some appreciable level of accuracy. Havelock (1937), proposed a method that determined the mean value of the longitudinal component of the pressure forces integrated over the wetted part of the oscillating ship's hull. In his treatment of the problem the water pressure was taken as the undisturbed pressure of the incident wave, which implies the use of the Froude-Krylov hypothesis. This was done to avoid the difficult problem of the evaluation of the complicated diffracted waves which originate from the oscillating ship in the incident waves. Hence, Havelock recommended that the proposed solution be considered as a first approximation. Gerritsma and Beukelman (1972) derived their formula for added resistance in waves using the radiated energy considerations, the method equates the work of the added resistance to the energy contained on the damping waves radiated away of the ship.

Boese (1970) proposed a method of determining added resistance of a ship by directly integrating pressure forces over the wetted surface of the ship. However, Boese's method was only derived for head sea waves, and neglected the quadratic velocity term in the Bernoulli's equation and one term arising from using pressure on the instantaneous position of the wetted surface of the ship instead of using pressure

on the average position of the ship. Faltinsen *et al.* (1980) in a bid to improve the accuracy included the terms missing from Boese's work in their prediction of the involuntary reduction in speed due to added resistance in waves. They proposed a procedure for calculating the transverse drift force and mean yaw moment on a ship in regular waves of any wave direction. They also presented a derivation of an asymptotic formula for small wave lengths and explained the influence of wave induced motions on the wake using the direct pressure integration approach. The pressure integration method is a near-field method which computes the added resistance from hydrodynamic pressure integration on the body surface using Bernoulli's equation, and a Taylor expansion of the pressure about the mean position of the ship. The said procedure proposed by these authors was assumed to be valid for small Froude numbers (i.e. Fn ≤ 0.2), however, the deficiency of the method being limited to regular waves was made up by proposing a simplified way of applying the results from a regular wave to short waves as was further illustrated in Faltinsen (1993).

Bhattacharyya (1978) presented many examples on wave load computations in ship motion and provides an expression that relates the wave encounter frequency to the wave frequency (ω_e) for a regular wave as:

$$\omega_e = \omega_w(1 - \frac{\omega_w V}{g} cos\psi) \qquad 2\text{-}5$$

$$\omega_w = gk + k^3 T_{ss}/\rho \qquad 2\text{-}6$$

where ω_w is the wave frequency and ψ is the Ship's heading angle with respect to average wave direction, V, is the Ship's velocity, g is gravitational acceleration, k is the wave number. The resultant resistance of a ship in waves does include the effects of wave reflection to added resistance due to ship motion while Tsujimoto *et al.* (2008), recognised that modern conventional formula for the added resistance due to wave reflection was derived for blunt ships and as such has poor agreement with that for fine form ships such as a container ship. They then proposed a practical correction method for estimating the added resistance (i.e. over and above the still, calm water condition), head seas in waves for fine form, low block coefficient ships, and this method includes correction of the effects of draft and frequency. A typical large container ship was used for their evaluation. The correction was made using a

towing tank test in the estimation of added resistance due to wave reflection. The tests were conducted with different ship speeds in short head seas waves of a single value of wave length. Their correction method and a comparison with the experimental values were presented, and thereafter, the influence of a decrease in ship speed in actual seas for a large container ship and found that the ship speed without their proposed correction was estimated to be 0.3 knots smaller than that with their correction in head wind and waves, which is quite relevant when evaluating carbon-dioxide emissions.

Most of the researchers that have been mentioned so far either carried out research that is directed towards predicting of wave loading or motion dynamics. However Hroshi Isshiki (2015), considered the IMO initiative on improving EEDI and the set target of cutting CO2 emissions by 30% in 2025, and discusses the use of wave energy to improve the propulsive efficiency and seakeeping performances of a ship in rough weather. He suggested that by fixing a relatively small hydrofoil to the ship's bow, ship's motion can be reduced and enough thrust generated to counter the speed drop that could have endangered the ship due to its engine power being reduced to improve EEDI. He also pointed out that the foil will increase resistance in calm waters and thus fuel consumption, thereby suggesting a detachable foil which poses practical challenges. Also, rough weather in most areas are seasonal and in this day of improved weather forecast and information technology, most Masters tend to take to routes that helps to avoid the adverse weather as much as practicable, thus the proposal will only work well for some ships that are projected to virtually always pass through some routes so such decision ned to be properly assessed.

Wave loading is a single most influential external loading on a ship in motion. The speed reduction associated with wave load is highly significant and does have great influence on the energy efficiency design index, thus its factor needs to be reasonably determined. This research considered the wave loading as a combination of Fraud-Krylov and the diffraction wave effects applying the well-known strip theory approach the ship divided in to equally spaced sections and the centre of gravity assumed to be at the geometric centre of the ship and other assumptions stated in the relevant sections later in this thesis.

Chapter 3 The Methodology

This chapter gives details of the content of the program (EShipman) developed to test the methodology, explains manoeuvring motion theory and the motion types considered in this research, describes the formulations used in deriving the algorithms used for developing the methodology and how the parameters used were obtained, including those derived from approximate relationships given by other researchers.

3.1 Description of the Program Developed for Proving the Method

The program developed in this research is basically ship manoeuvring capability estimation program that can be used to estimate a minimum and efficient power requirement for safe manoeuvring of a ship, such that can easily be adapted to predict how the application of the EEDI minimum safe power requirement might affect the ship with respect to safe manoeuvring. A subject ship was used to demonstrate the functionality of this program. To achieve this, the physical dimensions, power (maximum continuous rating) and hydrodynamic (forces and moments) parameters of the ship's hull, rudder and propeller, from the experimental results from published article (Son and Nomoto (1981)), were obtained. Known manoeuvring formulations based on principles of dynamic motions derived from first principles with assumptions that simplifies their applications with minimal and acceptable loss of accuracy were used.

The dynamic equations were used to compute the accelerations, velocities, positions (linear and angular), forces and moments acting on the ship in calm water condition with the influence of its propulsion and control devices, applying input of codes that makes it run and output results in time domain. On successful writing of that aspect of the code, another code was built to simulate the environmental condition (wave wind and current) using realistic environmental parameters such as wave height, wind speed, ocean current speed, etc.). This code was now merged with the calm water code following the superposition principles (the modular principle), thereby resulting in a code that could compute the motion of a ship in adverse weather condition. It is then possible to adjust the power of the ship prior to starting a run of the code and monitor the point where the ship is not able to manoeuvre safely.

These formulations and the method of putting them together including the assumptions made are explained. Also, the overall structure of the methodology is shown in Figure 3-1.

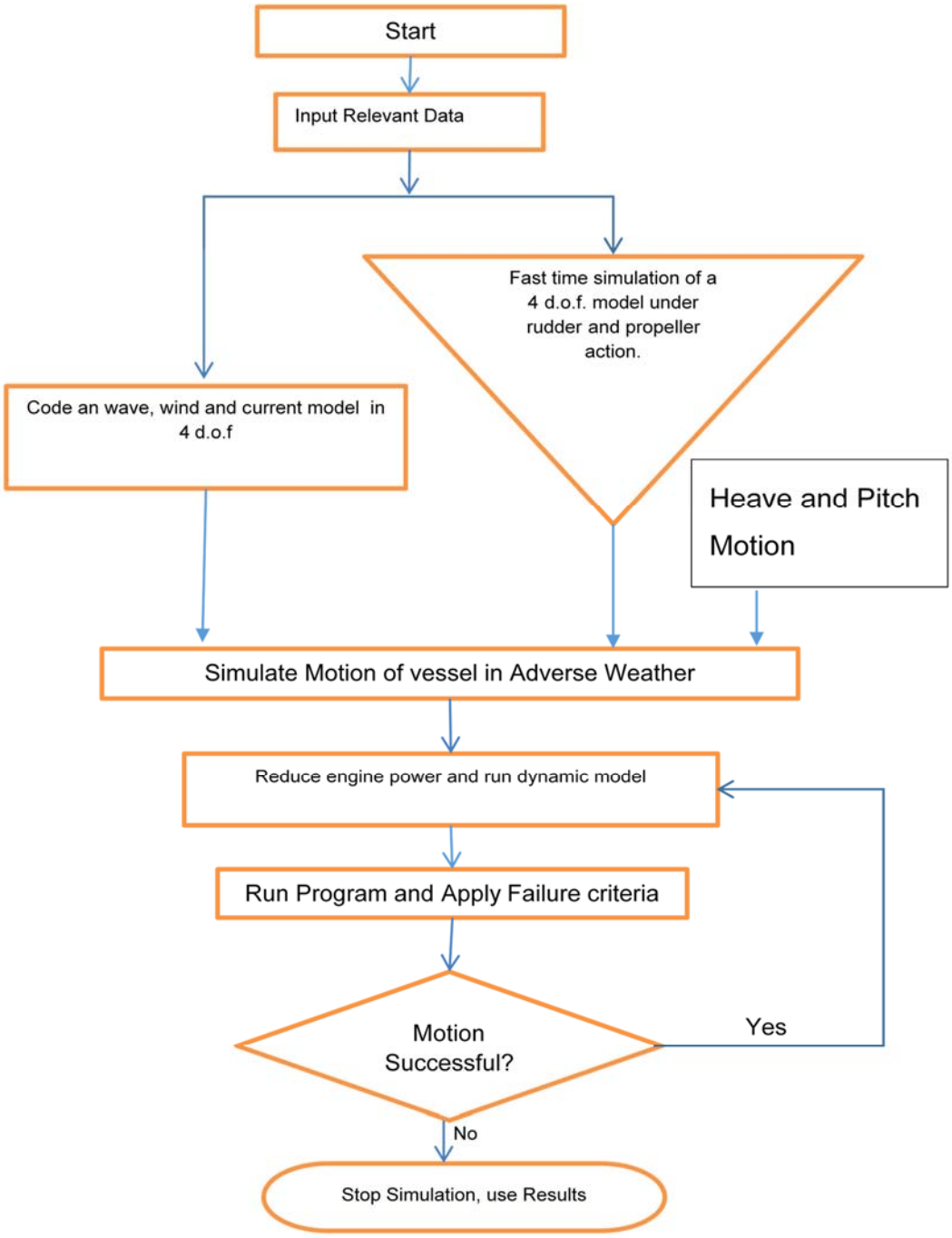

Figure 3-1 Overall Structure of the Methodology

As was explained earlier, most manoeuvring theory assumes that the ship is moving calm water and the IMO standards, ITTC (2017) requires that trial site should be

located in waters of adequate depth with low current and tidal influence as possible, and manoeuvring trial should be performed in the calmest possible weather conditions. IMO (2002), requires trials to be conducted to be conducted with a sea state not greater than 4, some ships may require, sea states as low as 1 in order to provide accurate full scale data). Hence, the manoeuvring model is normally derived for a ship moving at positive speed, under a zero-frequency wave excitation assumption such that added mass and damping can be represented by using hydrodynamic derivatives (constant parameters).

One of the objectives of this research is the development of a fast-time simulation program that can model the manoeuvring performance of a given ship when attempting the defined criteria manoeuvres in the identified environmental conditions, for establishing an acceptable level of power at which the ship can manoeuvre safely in anticipated adverse weather conditions. In order to determine the hydrodynamic coefficients, free running test model experiments may be conducted for the different manoeuvring motions of the ship in calm water, or otherwise derived from established formulations.

A program was developed for a basic ship running in calm water in four degrees of freedom (surge, sway, roll and yaw), using dynamic equations derived from Newton's Second Law of Motion, as expressed in Son and Nomoto (1981) and applying relevant equations for the accelerations, and deriving the velocities and positions by numerical integration (Runge-Kutta or Euler Method), as demonstrated in later chapters. The modular approach, promoted by the Japanese Modelling Group (Yasukawa and Yoshimura (2015)) was used in order to obtain the forces and moments of the bare hull as a combination of the forces and moments separately obtained, due to the hull, the propeller and the rudder.

Algorithms were developed for the purposes of controlling the ship's rudder, i.e., the ship could be controlled to return to a given heading after a deviation due to external environmental loading. Also, the control of the rudder is such that the rudder turns at a specified rate and adjusts its position and direction of motion to enable the ship to maintain a prescribed heading, also capable of turning into head wind and waves. Also, programs were written to enable the vessel to be run in a manner that executes given formal manoeuvres, and for this work, the Turning circle and Zigzag

manoeuvers. Since each manoeuvring regime required a different rudder control algorithm, when running the code, the user is prompted to take some action. The user's response directs the code to execute the manoeuvring motion needed. The plots from these Manoeuvres could be used to carry out an analysis of the ship's manoeuvring characteristics. For this test case, the calm water manoeuvring output was compared with the plots of Son and Nomoto (1981) that did similar motion simulation with same experimental results in order to validate the functionality of the code for calm water manoeuvring motion as in Figure 6-1 and Figure 6-4.

Then, the environmental forces and moments were obtained by combining some expressions for wave forces and moments computationally derived based on the conventional Strip theory assumptions, as given in Lewis (1989), considering the body as a slender body in order to reduce the 3-D condition in to a 2-D case for convenience of computation and with the wind forces derived using the method of Blendermann (1995), ensuring they run separately and successfully too, and then finally combining these external forces program code with the code for the ship's calm water simulation process. The Strip theory was applied in a manner that the person that want to use it for any new Ship of a different dimension can utilise the algorithm by dividing the ship in to an even number of sections that can enable the Simpson's 1/3 Rule.

For this work, the main simulation is that of a container ship manoeuvring in calm water executing the defined manoeuvres and another which turns the ship initially into head waves and wind (i.e. 180deg). One of the reasons a container ship was chosen being that container ships represents 4% of all maritime vessels but generated 20% of emissions from international shipping, Psaraftis and Kontovas (2009), and run at speeds of between 20 and 24 knots, thus a reduction in CO_2 emissions in this category of vessels will impact on the overall CO_2 emissions from international shipping. Again, it relatively has lower metacentric height and more susceptible to adverse weather disturbances (unlike oil carriers for example which are relatively stiffer), thus the need to have some method of investigating the effects of adverse weather when the ship is fitted with reduced installed power or derated.

This simulation program was principally meant for application to new ship at its early design stage, at which most of the significant hull details are known with reasonable

confidence, and also for the evaluation of an old ship undergoing a major refit to increase its loading capacity or derate its engine for the purpose of improving its Energy Efficiency Design Index, being one of the recommendations from ABS (2013). It is programmed with equations which considered some inevitable simplifications, however, taking relevant physics into account, made to be as accurate as practicable within the scope of the available technological resources, robust and backward compatible, inexpensive and can be applicable and easily affordable to any shipyard and administration.

This tool runs fast and many trial runs can be done in a short period to establish a low limit for power reduction considering an adverse environment and can be done for various sea state. Assuming a ship already in service was purchased, and a new owner feels that it will be in use in this new route for a foreseeable long future period and they decide to derate the engine to improve its EEDI, while considering its safety, they can do that by applying this method using, Eshipman or a similar program. Running the model in severally, reducing the power by a small percentage after each run until they reach an unsafe margin as illustrated in Figure 3-1. This will enable someone carrying out say, a free running physical model or CFD based model tests using a commercial software for same purpose (in a bid to obtain a more acceptable time and possibly more accurate result) to determine a reasonable starting point as Eshipman have been used to determine the a region of acceptability, and thus reduce the number of trials. After determining the minimum safe level, a factor of safety and sea margin could be added based on a percentage of the new accepted new MCR.

Studies of the manoeuvring characteristics of ships in waves have recently attracted much interest and all ships must have at least some inherent control characteristics that enable it to:

- Manoeuvre safely in ports and restricted waterways,
- Stop within a reasonable distance,
- Maintain its desired course in the open sea with any ocean currents, etc.

These minimum capabilities are needed under all conditions of loading, at both high speeds and the moderate speeds associated with restricted waters, and in wind and

waves as well as in calm sea state. Good manoeuvrability requires reliable and prompt changes of heading on demand, which implies predictable turning response to rudder movement and correspondingly prompt checking of the turn when rudder position is reversed, allowing for inertial and added mass effects.

When dealing with the control of ships fitted with control devices, under the influence of environmental forces, due consideration is given to:

a. The characteristics of the ship's response to the controls,

b. The rate at which the error between the ship's actual path and the desired path can be detected and what corrective action can be initiated, and

c. The size of the control forces and moments transmitted to the ship by the rudder

The International Maritime Organization , as a preliminary action towards assembling standardised data and developing criteria for minimum standards, provides guidelines that the manoeuvring performance of all new ships of 100 metres in length and over, are to be estimated, tested, and verified. The guidelines state that all ships should have manoeuvring qualities which enable them to keep to a course, to turn and to check turns, to operate at acceptably slow speeds and to stop, all in a satisfactory manner. This publication called for the estimation and verification for both fully loaded and trial conditions for the following characteristics:

1. Turning circle characteristics, 2. Yaw checking ability, 3. Initial turning ability, (4). Course-keeping ability, (5). Slow steaming ability and, (6). Stopping ability.

These definitive manoeuvres have been developed and approved in order to demonstrate the efficacy of the elements of the control loop and to reduce as much as possible the influence of the error between the ship's actual path and the desired path. These manoeuvres basically establish the stability and control characteristics of a ship independent of its helmsman or autopilot. The three manoeuvres commonly applied for merchant ships and naval ships are:

(a) Turning circle manoeuvre, which determines the basic turning qualities of the ship.

(b) Zigzag, Z, or the so-called Kemp/overshoot manoeuvre, Kempf (1944), which is second in importance to the Turning manoeuvre and is meant for determining the ship's control characteristics in terms of its course changing ability.

(c) Direct or reversed spiral manoeuvres which serves mainly to determine the natural stability characteristics of a ship.

In this research, the source code is equipped with pre-programmed capabilities for making zigzag and turning circle manoeuvres and allows several variables to be input or modified by the user. Calm water condition results were compared with IMO standard recommendations. Full scale measurements of manoeuvrability and full scale manoeuvring trials procedure were provided in ITTC (2002), ITTC (2014) and ITTC (2017).

The Turning Circle Manoeuvre is normally carried out in calm water scenario and is achieved by applying a rudder angle at an initial speed. According to IMO, the approach speed is to be at least 90 percent of the ship's speed corresponding to 85 percent of the maximum engine output, but some tests should also be carried out at low speed (below 8 knots), and before the execution of the turning circle manoeuvre, the ship must have run at constant engine(s) setting with minimum rate of change of heading (steady course) for at least two minutes, ITTC (2017). It is necessary to do a turning circle of at least 540 degrees in order to enable the determination of the main parameters which are the standard measures of manoeuvrability such as tactical diameter, advance, transfer, and loss of speed on steady turn, time to change heading 90 degrees and time to change heading 180 degrees. The turning circle is probably the oldest manoeuvring test. The test can be used as an indication on how well the steering machine and rudder control performs during course-changing manoeuvres.

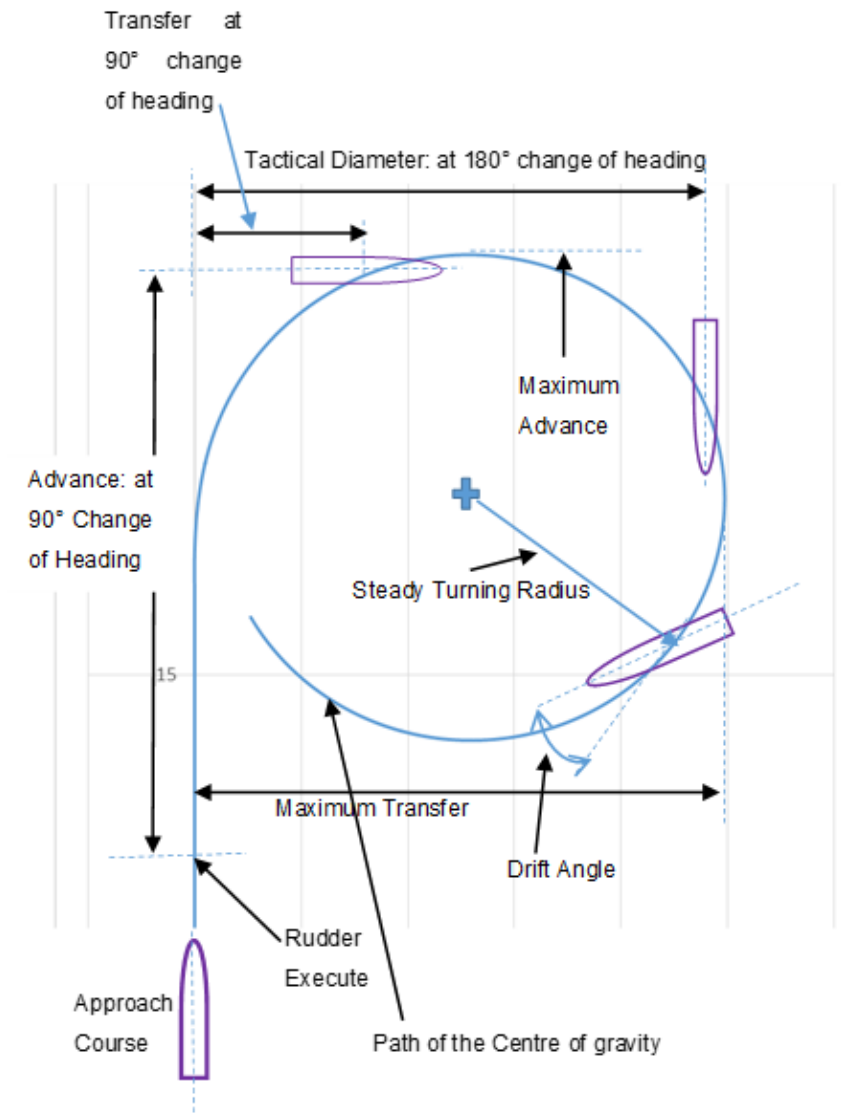

Figure 3-2 Turning circle: definitions (ITTC (2002)).

The results of a zigzag manoeuvre indicate the level of the ability of a ship's rudder to directionally control the ship. It is traditionally known that the manoeuvring trial provides the greatest amount of directly useful information on the combined effects of the hull form parameters (including draught and trim), rudder performance, and control system operation. It is usually referred to as, for example, a 20 – 10 manoeuvres, with the first degree representing the actual set rudder angle (i.e. 20 degrees), and the second, the heading or angle (i.e. 10 degrees) that the ship should be allowed to attain before reversing the rudder. Figure 3-3, illustrates a sample of a 20 – 20 zigzag manoeuvre with the key parameters labelled.

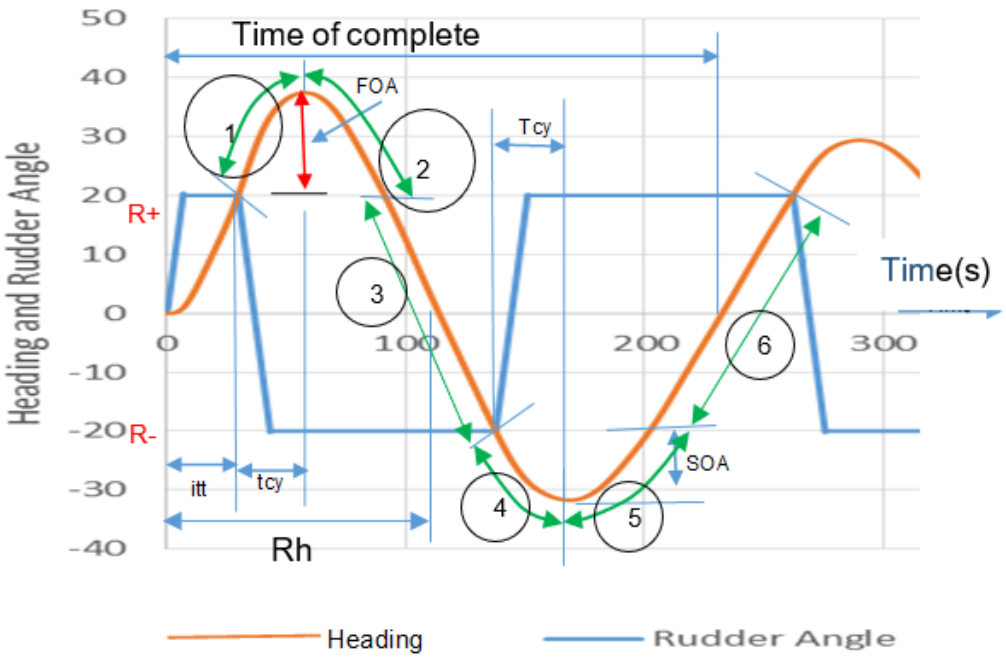

Figure 3-3 Example Analysis of a Zig-Zag Manoeuvre with Defined Regions

Legend to Figure 3-3 (definition of terms are given below):

- Tcy is the 'time to check yaw'.
- Itt is the 'initial turning time'.
- FOA is the 'First overshoot angle'.
- SOA is the 'Second overshoot angle'.
- Rh represents the 'reach'.
- Numbers 1 to 6 are regions on the Ship's path used to generate the simulator's logics in the programming of the zigzag motion, the conditions are tabulated in the truth Table 3-1. The Researcher used a self-formulated simplified algorithm for simulating the zigzag motion and in the process had some challenges which raised doubts as to whether issues were from some faulty data, formulation or poor algorithm. This truth table was included to guide anyone interested in writing such algorithm in the future on the simplest logic to follow, so that one area of doubt is completely ruled out.

Table 3-1 – Logic cases for zig-zag regions (see also, Woodward (2009) for another possible logic table)

Region	*1*	*2*	*3*	*4*	*5*	*6*
psi(i)> R+	*True*	*True*	*False*	*False*	*False*	*False*
Psi(i) > R-	*True*	*True*	*True*	*False*	*False*	*True*
Psi(i)<R-	*False*	*False*	*False*	*True*	*True*	*False*
Case True	*2*	*2*	*1*	*1*	*1*	*1*

The illustration in Figure 3-3 is used to generate the above logic table which will make it easier for the zigzag motion code to be understood. In the above logic table, the command rudder angles are R+ and R-, and are equal to the command ship heading in the zigzag algorithm (e.g. 20/20 or 10/10 zigzag). Different combinations are possible only by changing the numbers (say, 20/10 for a rudder angle of 20degree and a ship's heading of 10 degree). The process for executing the zigzag manoeuvre in the code is consistent with known method as follows:

(a) Steady the ship with the rudder at a zero-angle deflection.

(b) Deflect the rudder at a rate (no less than 2.33 degree/sec according to SOLAS II-1 Regulation 29-3.2) to a preselected angle, say for example 20 degrees, and hold until a preselected change of heading angle, say 20 degrees, is reached.

(c) At this point, deflect the rudder at maximum rate to the opposite (checking) angle of 20 degrees and hold until the executed change of heading angle on the opposite side is reached. This completes the overshoot test.

(d) If a zigzag full test is to be completed, again deflect the rudder at maximum rate to the same angle as in the first direction. This cycle is to be repeated through to the third, fourth, or more executions although the characteristics though the first overshoot is the most important as it is a measure of the vessel's course checking ability, ABS (2006).

This was traditionally done until a total of 5 rudder deflection steps have been completed. This entire process has been implemented in the code which allows the user to input the required peak angles and then the motion is executed as an iterative loop in time steps, applying conditions that initiated rudder movement in the desired direction at a given deflection rate. The relevant results of a zig-zag test are: initial

turning rate, execute heading angle, time to check yaw, heading, reach, time of a complete cycle, angular speed and unit time.

Definition of these important terms determined during the zigzag test are:

- Time to check yaw: the time between the rudder execute and the time of the maximum heading change in the original direction.
- Initial Turning Time: the time taken to change course or heading in response to rudder execute. Time taken to change yaw in a particular direction
- Overshoot angle: This is a very crucial parameter determined using this test. Overshoot angle is defined as the excess angle of heading reached by ship in its previous direction (after rudder is applied). Least overshoot angle is most desirable for better controllability.
- Yaw rate/turning speed in the changed direction.
- Reach: The time between the first execute and the instant when the heading angle is zero.

Common values for the rudder angle are 20/20 and 10/10. However, other combinations can be applied. For larger ships a rudder angle of 10 degrees are recommended to reduce the time and water space required. The set requirements can be found in L. (2015).

In this study, the 20 - 20 zigzag manoeuvre was presented as it is generally preferred because, according to Lewis (1989):

i. It has been used for many years, so that a considerable body of statistical data now exists.

ii. Ship handlers often use 20 degrees of rudder when initiating and checking turns.

iii. With some ships, 10 degrees of rudder may not suffice for checking turns; that is, no useful reliable data will be obtained.

iv. Inexact setting of the rudder angle in a trial is less harmful in a 20-20 than in a 10-10-degree zigzag manoeuvre.

However, just as the results of the spiral manoeuvre give some indication of the control effectiveness (yaw-angle rate versus rudder angle), so do the results of a zigzag test which depends somewhat on the stability characteristics of the ship as well as on the effectiveness of the rudder.

The direct and reversed spiral test was not traditionally specified as they does not provide a good test of the machinery extremes which can require significant trials time. The data gathered, however, was critical to determining the controls-fixed dynamic stability of the ship. Practical time and cost considerations usually limit physical manoeuvring trials to the fewest number that can reliably demonstrate that a ship has sufficient and adequate controllability.

3.2 Rigid Body Motion Assumptions

Ship motion equations were derived from rigid body dynamics equations; however, some assumptions were made to simplify them in order to achieve the objective of a fast processor time. The formulations from which the forces and moments were computed, including the assumptions, are explained in this section.

In reality, the body of a ship is composed of a very large number of small parts and components assembled together through welding, mechanical fastening etc., in order to form the structure. Also included are machinery and systems of the whole ship into which cargo, fuel, water etc., are then added and thus creates the overall weight of the ship and of its distribution. These components are subject to various forms of deformations over the length of the ship, microscopic relative motions, changes in geometrical shapes, separations; other motions of internal liquids in tanks and other internal liquid contents with free surfaces for which, ship motion causes sloshing, free surface effects, etc., which affects the ideal otherwise quasi-static loading on the vessel in motion and of its stability condition. However, for this work, the ship together with its content are modelled as a whole rigid body in order to simplify the process of computation. This implies that the said deformations and associated loading effects are assumed to be negligible.

Considering the dynamic motions of a rigid body within a body-fixed Cartesian coordinate system whose origin is at the centre of gravity which is in the region of the mid-ship, with the assumption that the ship is transversely symmetrical about its longitudinal centre-plane (implying that the centre of gravity has coordinates, $\mathrm{x_G}, 0, \mathrm{z_G}$) and the products of inertia about the body axis system ($\mathrm{I_{xz}}$, $\mathrm{I_{yz}}$, $\mathrm{I_{xy}}$.) are ignored, which results in six degrees of freedom nonlinear equations motion, as is given in, Fossen (1994), as follows:

$$X = m[(\dot{u} - vr + wq) - x_G(q^2 + r^2) + z_G(pr - \dot{q})] \quad \textit{3-1}$$

$$Y = m[(\dot{v} - wp + ur) + z_G(qr - \dot{p}) + x_G(qp - \dot{r})] \quad \textit{3-2}$$

$$Z = m[(\dot{w} - uq + vp) - z_G(p^2 + q^2) + x_G(rp - \dot{q})] \quad \textit{3-3}$$

$$K = I_x\dot{p} + \left(I_z - I_y\right)qr + m[-z_G(\dot{v} - wp + ur)] \quad \textit{3-4}$$

$$M = I_y\dot{q} + (I_x - I_z)pq + m[z_G(\dot{u} - vr + wq) - x_G(\dot{w} - uq + vp)] \quad \textit{3-5}$$

$$N = I_z\dot{r} + \left(I_y - I_x\right)pq + m[x_G(\dot{v} - wp + ur)] \quad \textit{3-6}$$

Where, X, Y, Z, represent surge, sway, and heave forces, K, M, N, represents roll, pitch and yaw moments, $\mathrm{x_G} = \mathrm{x_{rot}} - \mathrm{x_{CG}}$ is the distance from the centre of rotation of the ship to the centre of gravity; u, v, and w, are surge, sway and heave velocities; p, q and r, are roll, pitch and yaw angular velocities and the other items are defined in the nomenclature. This is to demonstrate the existence of the six degrees of freedom equation which is further modified to create lower degrees of freedom equations. In the present state of manoeuvring studies, it is practically scarce and expensive to conduct experiments that give results of forces and moments in a coupled six degrees of freedom test for a manoeuvring ship due to required measurement techniques and the application of a coupled six degrees of freedom equation is almost impossible even when the fluid, propeller and rudder forces have not yet been introduced (Tello Ruiz *et al.* (2012)), thus it is an acceptable practice to perform a coupled 3 degrees of freedom (surge, sway and yaw) experiment and then a coupled pitch and heave with an uncoupled roll, or recently, a coupled four degrees of freedom (surge, sway, yaw and roll) as was the case of the experimental result from which most of the data for this research was extracted and in Dong *et al.* (2015).

3.3 A Modular Modelling Approach

The method of creating the algorithm that computes the forces and moments acting on the ship is discussed here. This model was proposed by Ogawa and Kasai (1978) from the Mathematical Modelling Group (MMG) of the Society of Naval Architects of Japan. The equations of motion of the system are set up considering the forces and moments which come into action when the vessel is disturbed from its equilibrium position. Hence for dynamic equilibrium, the exciting force or moment is resisted by the inertial, the damping and the restoring reactions of the system.

A modular approach does treat the forces and moments acting upon the individual elements, such as the hull, rudder, propeller and any external disturbances (wind, wave, current) as self-contained modules. Thus, the complete system is modelled by summing up the individual components. In other words, the MMG model breaks the hydrodynamic forces into hull, propeller, rudder forces, and their interactions, thereby forming the overall system of equation as in equations 3-7 to 3-10 (see also Yasukawa and Yoshimura (2015)). It is possible to alter a single module without altering the manoeuvring coefficients of any of the other modules, apart from input / output formats and protocols, etc., thereby potentially providing a more flexible research and design tool as in Dand (1987), who applied this method to include shallow water effects and compared this method with the whole-ship regression model. Also, simulations can be performed with different rudder dimensions or characteristics, in a bid to investigating the effect on manoeuvrability; however, a single rudder is still assumed (as is a single propeller, etc.).

The forces and moments determination contained within each module were constructed with reference to the physical processes that are involved; this provides a far more rigorous structure than does a regression model. Due to the roll coupling effect when high speed fine form vessel is steered in calm water, which will increase in adverse weather condition; for the starting part of this work, the researcher initially considered four degrees-of-freedom; i.e. surge (X); sway(Y) and yaw (N) and roll (P), since the experimental data is available for ease of verification. The Simulation for the four degrees of motion (Surge, sway, roll and yaw) in calm water was successfully developed and run to give satisfactory output. Then the remaining two degrees of freedom (heave and pitch) was inputted using charts and formulae from

recognised authors when the environmental loading formulations were added to the calm water scenario.

The modular approach does suffer however from some difficulties associated with connections and data pathways between the modules. The behaviour of one module will inevitably affect that of another module, for instance, if the dimensions of the rudder is adjusted, it will affect the hull motion characteristics due to change in drag. Also, as pointed out by Dand (1987), data derived from experimental tank tests on resistance propulsion, and seakeeping are in many cases not suitable for direct application to this model. Other issues do arise from the general shortage of data with which to construct the separate modules, especially as most formal tests and experiments do not generally cover the complete breadth of operating environments that are frequently encountered in service. This is principally due to cost and technological limitations for instance, there are limitations to the measurement of coupled motions, to some extent, and coupled motion analyses normally give more realistic results, also measurement of main ship motion characteristics in adverse wind and wave is an expensive venture.

Taking into account the limitations regarding experimental studies on manoeuvring in waves, this work attempts to use known experimental data from Son and Nomoto (1981) for the calm water manoeuvring motions and empirical expressions from Araki and Motoki. (2013), for a manoeuvring ship in waves as done with the system based method. This latter involves obtaining hydrodynamic forces mainly calculated by solving partial differential equations of potential flow using Computational Fluid Dynamics software or by obtaining hydrodynamic forces with towing tank or free running model test basin experiments and employing them to tune the empirical manoeuvring and wave models. The ship motions (acceleration, velocity, and position) are then calculated by solving ordinary differential equations with initial conditions, in the time domain using a numerical method with a suitable assumed time step.

Recently, many authors such as Mohammadafzali (2016), He *et al.* (2016), etc., used the modular approach in order to evaluate the manoeuvring performance in waves as proposed by the Japanese modelling group (MMG) who have carried out several investigations to prove its results are close to real experimental results and recently

being used by many researchers. Hence, such a methodology has been investigated in the present work by comparing the measured characteristics in calm water against the output from the code assuming calm water condition. Also, the functionality of the method in wind and waves at designated significant wave height (from the Beaufort Scale) for determining the speed loss in head wind and comparing with published works for the same class of ship. This helps to serves as a comparison that shows the functionality of a major part adverse weather algorithm.

The forces and moments acting on a ship's hull can be broadly grouped into four categories, namely, the:

a) inertial forces,

b) damping forces,

c) restoring forces and,

d) exciting forces.

The **inertial** forces may produce a resistance when the ship is set in motion by what-so-ever-cause; the **damping** forces act in opposition to the ship's motion such that they reduce or dampen the motions of the vessel due to wave excitation. The **restoring** forces act to always bring the ship back to its initial still water equilibrium position from its displaced position caused by the wave exciting moments. The **exciting** forces can be generally sub-divided further into two components: firstly, those due to the control surfaces, such as the rudder and propeller, which provide and enhance manoeuvrability; and secondly, those due to external disturbances, such as winds, waves and ocean currents; these result in the external forces and moments. There is an assumption that certain oscillatory forces and moments produced by wave excitation (such as: Oscillation of propeller thrust, torque and required power above their time average values which may result in engine overloading (beyond the allowed margin), and propeller pitching which reduces the available time-averaged thrust and thus the available power due to the dynamic characteristics of the ship in response to wake change under the influence of wave effects) are negligible. Thus, neglecting these mentioned oscillatory forces and moment due to propeller pitching, the equations of motions of a ship under the influence of environmental forces and moments are as follows:

$$\textit{Surge,} \quad X = X_{HF} + X_{FK} + X_{RF} + X_{WF} + T(1 - t_p) - R \qquad \textit{3-7}$$

$$\textit{Sway,} \quad Y = Y_{HF} + Y_{FK} + Y_{DF} + Y_{RF} + Y_{WF} \qquad \textit{3-8}$$

$$\textit{Roll,} \quad K = K_{HF} + K_{FK} + K_{DF} + X_{RF} + K_{WF} \qquad \textit{3-9}$$

$$\textit{Yaw,} \quad N = N_{HF} + N_{FK} + N_{DF} + N_{RF} + N_{WF} \qquad \textit{3-10}$$

Where the subscripts are identified as follows:

HF – Hull forces

FK – Froude-Krylov forces

RF – Rudder forces

DF – Diffraction forces

WF – Wind forces.

It was required to compute the propeller thrust and rudder force components, develop a control algorithm and add to the hydrodynamic forces and moments simulation.

The simulation is done a specified number of times while the engine is set at the 100% MCR at different environmental conditions up to the 5.5m significant wave height, wind speed of 19m/s and current of 3m/s, and repeatable success is ensured. For this research, the criteria for success being that the velocity of the ship at any instant in time should not reduce below 4 knots (2.06 m/s). Then the approach is to reduce the installed power (MCR for this research is from the subject ship's design data) by say, 5% by multiplying the MCR by 0.95, and to repeat as above, until a point is reached where the simulation stops under some defined criteria, e.g., when with a reduced installed power, the speed drops below 2.06m/s, or is not able to turn into the waves (i.e. the program simply gives infinite numbers).

3.4 Some Basic Parameters Estimation Methods

As was mentioned for this reference vessel, there is a considerable amount of available data, a good amount of the data that has been used in this work has been taken from various referenced texts, and others were derived using approximate

formulae. However, for a new vessel in its early design stage, such reliable data may not be readily available, thus, some formulae, as given below, are presented here to aid another user of this program in the estimation for another design of vessel. These are as follows:

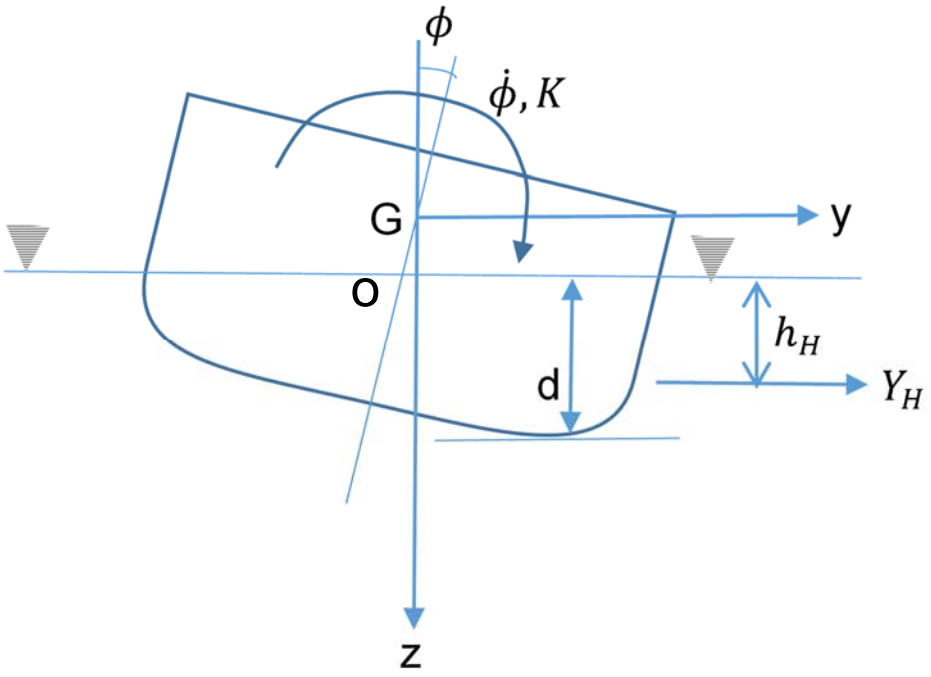

Figure 3-4 Coordinate system illustration

Heel damping moment: $N_{\dot{\phi}} = \alpha\dot{\phi} = \frac{2\pi(I_{xx}+J_{xx})}{T_R}\kappa\dot{\phi}$ *(Takashina (1980)).* *3-11*

And the z-coordinate Z_H, of the point, upon which the lateral force Y_{Hull} acts can also be derived by:

$$z_H = 0G + h_H = -\frac{g.GZ(\phi)}{Vr} \text{ Takashina (1980)} \quad 3\text{-}12$$

$$x'_R = \frac{x_R}{L_{pp}} \; and \; x'_R = z_R/d \quad 3\text{-}13$$

where *d* is the moulded depth of the ship and the prime indicates the non-dimensional form of the terms. The principal moments of inertia are given by:

$$I_x = I_{xCG} + m(y_G^2 + z_G^2) \quad 3\text{-}14$$

$$I_y = I_{yCG} + m(x_G^2 + z_G^2) \quad 3\text{-}15$$

$$I_z = I_{zCG} + m(x_G^2 + y_G^2) \quad 3\text{-}16$$

Kristensen and Lützen (2013), presented some expressions for estimating the wetted surface area (S) for some types of ships, and for single screw container vessels:

$$S = 0.995\left(\frac{\nabla}{T} \times 1.9L_{wl} \times T\right) \quad 3\text{-}17$$

where $\mathrm{l_{wl}} = 1.01 \times \mathrm{l_{pp}}$ is the length of the ship along the summer load water-line.

A ship's natural period (T) for various free motions according to Zăgan *et al.*) can be approximated by:

$$T_{pitch} = 2\pi \times \sqrt{\frac{\rho\nabla k_{yy}^2 + A_{55}}{\rho g\nabla(GM_L)}} \quad 3\text{-}18$$

$$T_{heave} = 2\pi \times \sqrt{\frac{\rho\nabla + A_{33}}{\rho g A_w}} \quad 3\text{-}19$$

Tsujimoto *et al.* (2008), pointed out that mean wave period from Beaufort Scale is given by $\mathrm{T} = 3.86\sqrt{\mathrm{H}}$ where H is height in metres (m) and T is the period in Seconds (s). This serves for ease of computation such that once the formulae is used, one only needs to change the wave height (as per the required Beaufort number value) and the expression will give the equivalent Beaufort scale period.

Generally, for estimating the rigid body moments of inertia for the transverse and longitudinal; the radii of gyration can be taken as 0.4B and 0.25Lpp respectively. However, Bureau Veritas proposes the following expression for the radius of gyration in roll:

$$K_{xx} = 0.289 \times B \times \left(1.0 + \left(\frac{2 \times KG}{B}\right)^2\right) \quad 3\text{-}20$$

KG being the height of the centre of gravity, G, above the keel

The longitudinal radius of gyration of a long homogeneous rectangular beam with a length L is about

$$K_{yy} = 0.29 \times L \times \left(\sqrt{\frac{1}{12} \times L}\right) \qquad 3\text{-}21$$

MAN (2011), stated as follows: that for ships with a single propeller, that the wake fraction coefficient $\mathrm{w_p}$ is normally in the region of 0.20 to 0.45, corresponding to a flow velocity to the propeller V_a of 0.80 to 0.55 of the ship's speed V_s.

Also, $\mathrm{t_p} = 0.5 \times \mathrm{C_p} - 0.12$, where C_p is the hull prismatic coefficient and t_p is the propeller thrust deduction coefficient. The thrust deduction coefficient t_p and the propeller wake fraction w_p both tends to increase with the increase in hull block coefficient and are generally larger for single screw ships than for twin-screw ships MAN (2011). The propeller diameter D_p, if not known can be estimated as a function of the maximum draught (t_{max}) as follows:

For container ships: $D_p = 0.623 \times t_{max} - 0.16$

However, for this research, these formulations from MAN were not applied as the specific value for the specimen ship were given.

Chapter 4 Manoeuvring Performance of Ship in Calm Water

As discussed earlier in section 3.1, it was usual practice to carry out manoeuvrability tests in a calm water condition, and the existing regulations and criteria are based on this practice. Thus the body motions of a ship while it is manoeuvring are mostly expressed in terms of its surge, sway and yaw behaviour with the assumption of a fixed draught, and with the effects of pitch, heave and roll being ignored as manoeuvring as a test study, is generally recommended to take place in calm waters i.e., a calm environment (Wind< Beaufort 3 and sea state< 2 - ABS (2006)), deep, unrestricted water (> 4x mean draught), full load (summer load line draught), even keel condition, and a steady approach at the test speed (min 90% full speed) in accordance with IMO guidelines IMO (2002) and ITTC (2017). However, in relatively rough operational weather and at higher speed conditions, the effects of pitch, roll, and heave, particularly for high speed vessels would be required. This is the first

essential step to setting a firm foundation for extending the code as discussed later, to accommodate a range of adverse weather conditions.

Also, a modular concept being adopted in this study implied that the non-dimensional hydrodynamic derivatives obtained in a calm water condition were used to compute the forces and moments in this state, and which were then applied to the equations of hull motion by adding it to the other external forces and moments for the computation of the motion dynamics in the adverse weather condition. To this end, the methodology was initially developed, and which is capable of simulating the manoeuvring of a ship in calm water situations in order to test the ability of the ship to meet with the minimum set criteria in ITTC (2002), ITTC (2014) and L. (2015). It is structured in such a manner that allows a user to select required manoeuvring motion (Turning Circle, zigzag, straight line or a turn into head wind and wave).

Figure 4-1 below is a process flow schematic that should enable the reader to understand the overall structure of the program when reading through the various explanations that are given further in this work to provide a better understanding of the program.

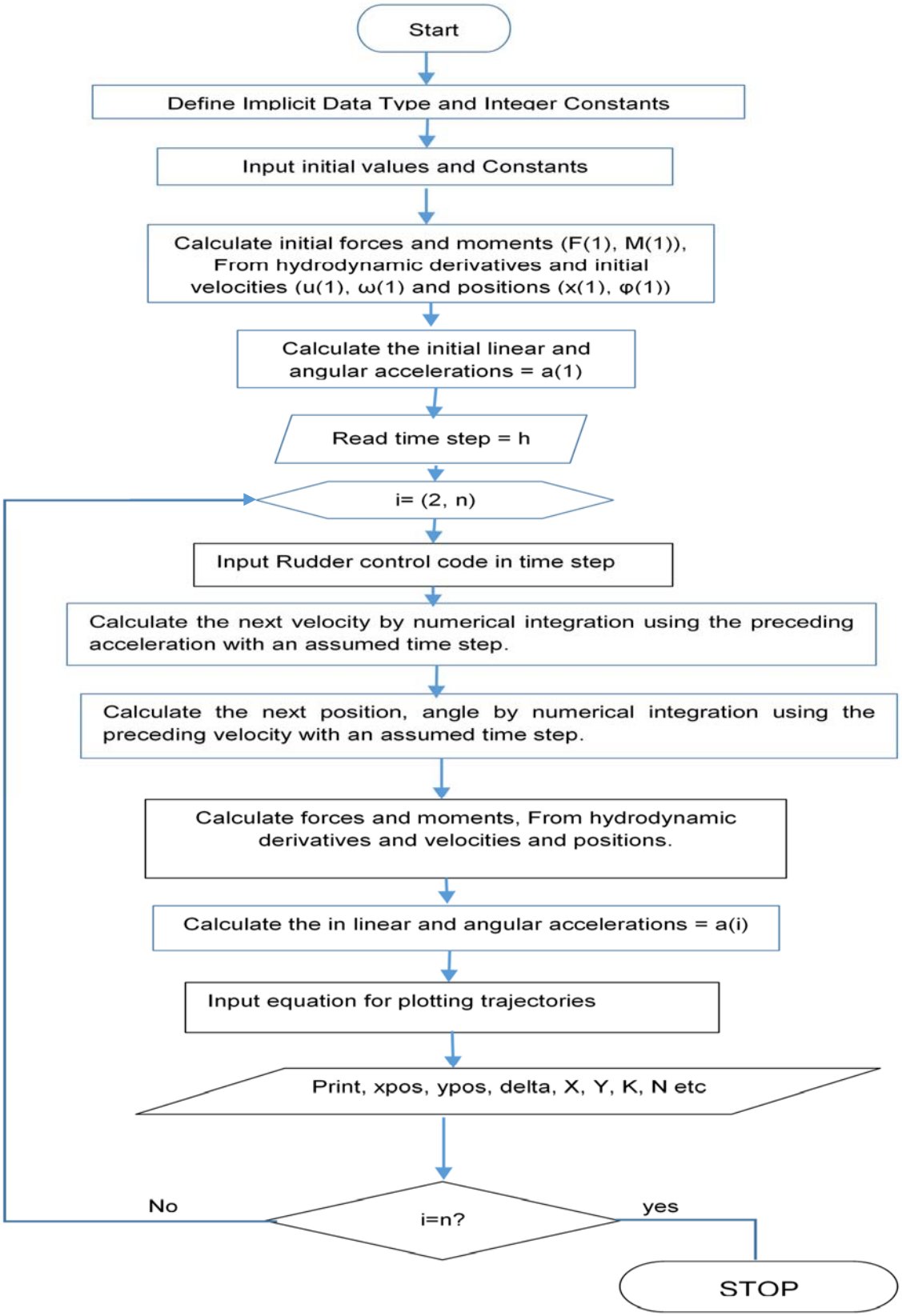

Figure 4-1 Overall Program Structure

The calm water resistance and the hydrodynamic hull forces Y_{HF}, K_{HF}, and N_{HF}, depend on the drift and heel angles in Equations (4-5 to 4-8). These hydrodynamic

forces and moments are generated as a reaction to vessel's motion and generally have linear component which is by virtue of the inviscid nature of the fluid, represented by potentials and non-linear components generated by virtue of the its viscous nature. Data were provided from towing tank model tests of the vessel SR-108 container ship (a vessel that has a great deal of published realistic data) taken from the work of Son and Nomoto (1981), and used for this research. The main reason for this being that the output from the initial program when the algorithm is written for the ship operating in calm water can be easily validated. However, known empirical formulae for certain parameters were written down in the code and 'commented', such that they can be activated and applied in the future versions of this work in order to make for the ultimate objective of being able to apply the program, using a known ship hull form, with relevant properties and general details being available at the design stage, thus the result of the simulation of the ship at reduced installed power will only be seen as a deviation from the full power condition which will be with minimal error. Otherwise, using the generic formulations will result in compounded error which adversely impair the final judgment.

4.1 Description of Specimen Ship

The designer of a new ship will have the full dimensions and parameters of the ship they are designing. They will be able to carry out model tests to determine the hydrodynamic derivatives for the hull and rudder of the ship. On the other hand, some scholars have developed empirical formulae for deriving the hydrodynamic derivatives using ship's dimensions and other relevant design parameters. Due to the need to ensure that the equations and algorithms applied in this method are functionally correct, there was a need to use a ship with established hydrodynamic data and manoeuvring characteristics. This will additionally make for ease of validation. The aim is to determine by how much the installed power of this ship can be reduced to before it starts getting unsafe under prescribed additional environmental loading.

The vessel used for this research is an S-175 Container ship (Figure 4-2 and Figure 4-3) whose model test results can be found in ITTC publications, hydrodynamic data were obtained from towing tank model tests of the vessel SR-108 container ship (a sister ship) taken from the work of Son and Nomoto (1981). It was considered as an

ice class ship when performing EEDI calculations, because this has implications for warming up the cold region and upsetting the ecosystem (Schröder *et al.* (2017)), if appropriate considerations are not made.

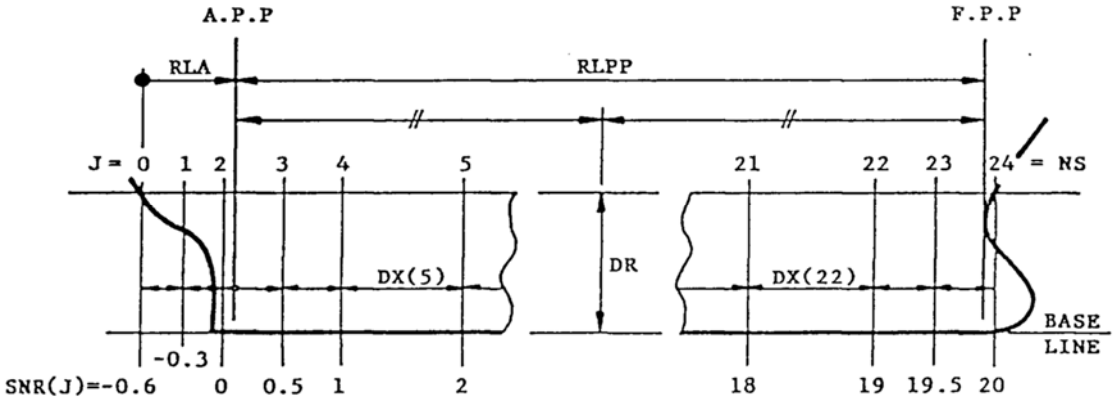

Figure 4-2 Definition of Longitudinal station Values

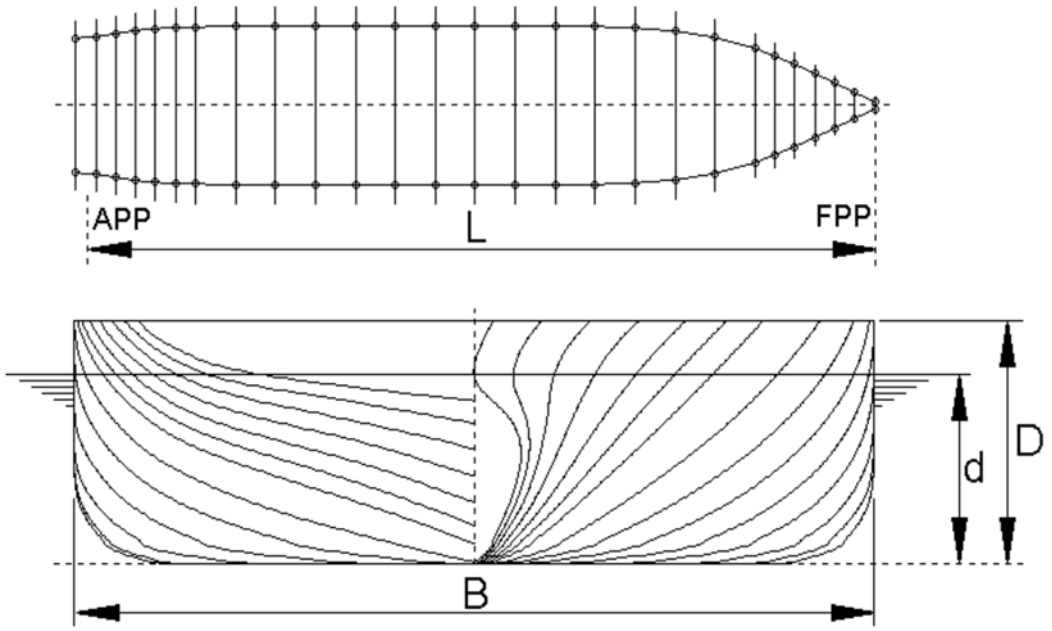

Figure 4-3 Hull Form Definitions Journee (2001)

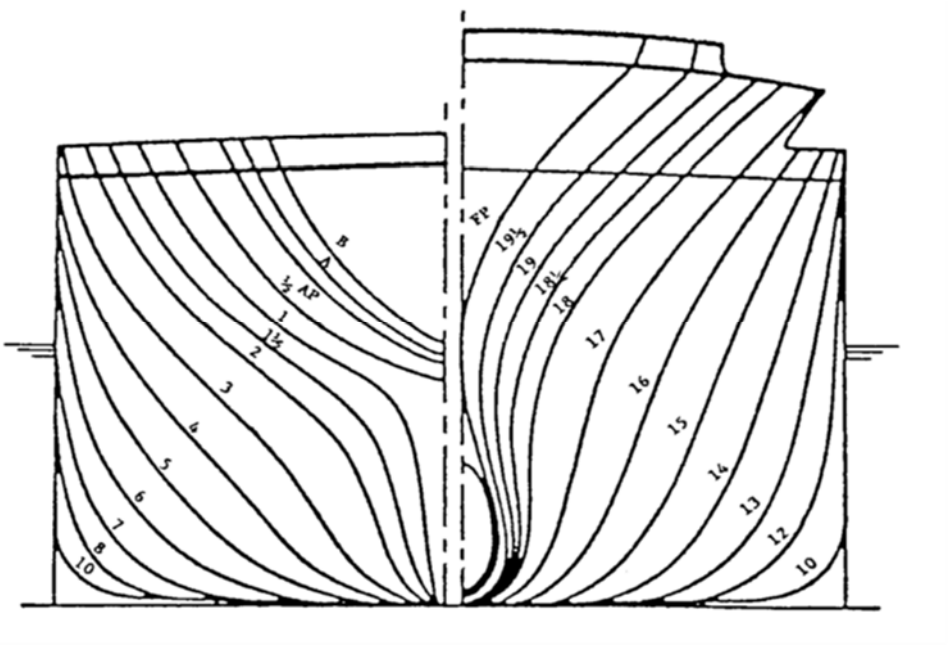

Figure 4-4 Available conventional Body Plan of S-175 Container Ship

Due to insufficient available parameters, the given parameters were used in order to obtain the hull girder transverse section areas by the use of AutoCAD software for digitising and then replotting the hull body plan in order to obtain the unit lengths of the individual submerged sections to obtain the results used in the subsequent analyses, The AutoCAD drawing is shown below:

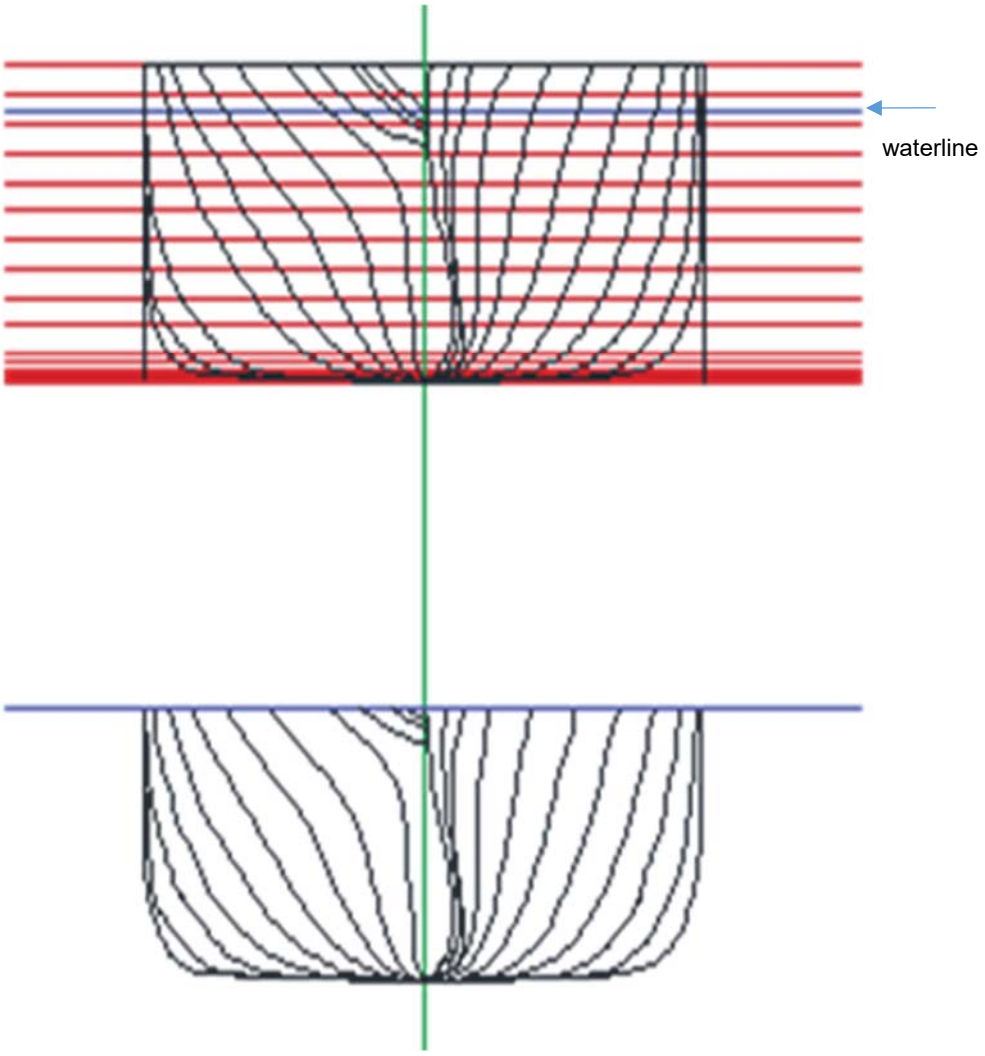

Figure 4-5 Auto-Cad version of body Plan

Table 4-1 Ship's Main Dimensions, characteristics and Dynamic Properties

Description	*Value*
LBP	*175m*
Breadth moulded	*25.4 m*
Depth Moulded	*11 m*
Draught Forward	*8.0m*
Draught Mean	*8.5 m*
Draught Aft	*9.0m*
Displacement Volume	*21222 m3*
Deadweight	*2628.88*
LCG aft of mid-ship	*2.5 m*
Longitudinal radius of gyration	*0.236 L*
Two-node frequency	*1.6 Hz*
Block coefficient	*0.572*
Midship coefficient	*0.98*
KM	*10.39m*
KB	*4.6154m*
KG	*10.09m*
Rudder Area	*33.0376m²*
Propeller Diameter	*6.533 m*
Aspect Ratio of rudder	*1.8219*
Pitch/diameter ratio	*1.009*

The main reason for using this container ship being that the output from the initial program when the algorithm is written for the ship operating in calm water can be easily validated to confirm that the code algorithms are correct. The other reasons for using a container ship as a development case being that it is one of the principal means of marine transportation, and they consume more fuel than other marine vehicles of same tonnage per mile because they are required to sail relatively faster in order to accommodate the tight customer schedules.

4.2 Dynamics Equations for Ship Manoeuvring Motions

This section considers the forces and moments that are acting on the ship moving forward at a set initial speed in calm water (the speed is recalculated as the motion proceeds and may demonstrate the speed drop in rough weather). However, the following diagram do illustrate the various conditions that will be dealt with in this work. Two Cartesian coordinate systems are shown in Figure 4-6. The linear

displacements (as used in the computation of the trajectories) are represented in the earth-fixed axes, and the equations of hull motions are described in the ship body-fixed coordinates. Thus, the hydrodynamic forces acting on a ship are described in the body-fixed frame. The origin of the body-fixed frame is at the intersection of the longitudinal centreline and the mid-ship section, with the water line, and the positive z axis is downward.

Figure 4-6(a), is with the wave fixed with its origin at a wave trough, the η – axis in the direction relative to the wave travel; and (b) is with the upright body fixed with its origin at the centre of gravity of the ship.

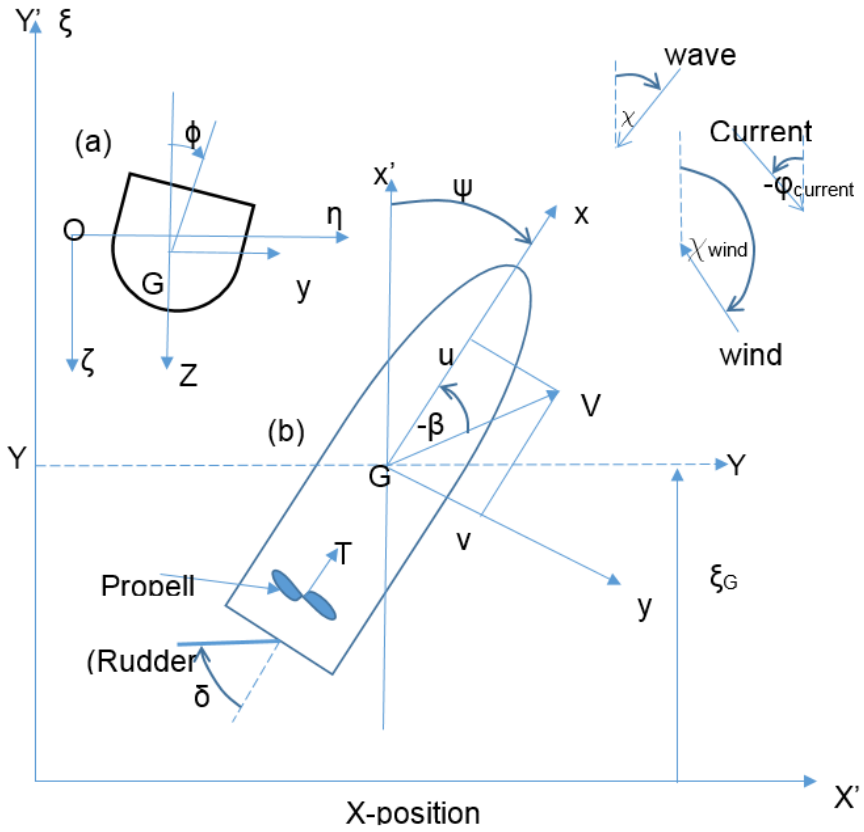

Figure 4-6 Earth-fixed and body-fixed coordinate system

In calm water, if the order of the forward velocity is assumed to be first order, then the sway and yaw motions would be defined as being the second order because the forward velocity is much larger than the sway or yaw velocities, the heave, roll, and pitch motions would be considered to be of the third order; therefore, ship manoeuvring motions in calm water are usually simplified to 3DOF motions (surge-sway-yaw). However, in practice roll motion can be observed during sharp turning in calm water because of the rudder and centrifugal forces. Therefore, the roll motion is

included and thus a 4DOF mathematical model (surge-sway-roll-yaw) is used. Son and Nomoto (1981), gave the simplified equations of motion as:

$$X = (m - X_{\dot{u}})\dot{u} - (m - Y_{\dot{v}})vr \quad \textit{4-1}$$

$$Y = (m - Y_{\dot{v}})\dot{v} + (m - X_{\dot{u}})ur - Y_{\dot{r}} \quad \textit{4-2}$$

$$K = \left(I_x - K_{\dot{p}}\right)\dot{p} + WGM_T\phi \quad \textit{4-3}$$

$$N = (I_z - N_{\dot{r}})\dot{r} + N_{\dot{v}} \quad \textit{4-4}$$

The resulting hull forces and moments in the above-mentioned basic equations for manoeuvring motions were expressed as hydrodynamic derivatives shown in equations 4-5 to 4-8. Their numeric values can be obtained from model experiments and or from Computational Fluid Dynamics software simulations (as in Zhang *et al.* (2010), that used Ansys FLUENT software). The values used in this work was from the experimental result of Son and Nomoto (1981).

$$X = X_{uu}u^2 + (1-t)T + X_{vr}vr + X_{vv}v^2 + X_{rr}r^2 + X_{\phi\phi}\phi^2 + X(\delta) + c_{RX}F_N \sin\delta + \left(m + m_y\right)vr. \quad \textit{4-5}$$

$$Y = Y_v v + Y_r r + Y_p p + Y_\phi \phi + Y_{vvv}v^3 + Y_{rrr}r^3 + Y_{vvr}v^2 r + Y_{vrr}vr^2 + Y_{vv\phi}v^2\phi + Y_{v\phi\phi}v\phi^2 + Y_{rr\phi}r^2\phi + (1 + a_H)F'_N \cos\delta - (m + m_x)ur. \quad \textit{4-6}$$

$$K = K_v v + K_r r + K_{\dot{\phi}}\dot{\phi} + K_\phi \phi + K_{vvv}v^3 + K_{rrr}r^3 + K_{vvr}v^2 r + K_{vrr}vr^2 + K_{vv\phi}v^2\phi + K_{v\phi\phi}v\phi^2 + K_{rr\phi}r^2\phi + K_{r\phi\phi}r\phi^2 - (1 + a_H)z'_R F'_N \cos\delta + m_x I_r ur - W(GM)\phi. \quad \textit{4-7}$$

$$N = N_v v + N_r r + N_p p + N_\phi \phi + N_{vvv}v^3 + N_{rrr}r^3 + N_{vvr}v^2 r + N_{vrr}vr^2 + N_{vv\phi}v^2\phi + N_{v\phi\phi}v\phi^2 + N_{rr\phi}r^2\phi + N_{r\phi\phi}r\phi^2 + (x'_R + a_H x'_H)F'_N \cos\delta. \quad \textit{4-8}$$

Also, practical limitations of physical measurement techniques and the state of refinement of the present theory do not justify the inclusion of higher order terms (Lewis (1989)). The terms of the manoeuvring derivatives were non-dimensioned in the code for ease of working between model test data and actual ship test data using the relationships.

The coefficient values of $\mathrm{a_H}$, $\mathrm{x'_H}$ and $(1 - \mathrm{t_R})$ are dependent on the block coefficient ($\mathrm{C_B}$) and are given by $\mathrm{a_H} = 0.627 \times \mathrm{C_B} - 0.153$, $\mathrm{x_H} = -\mathrm{L} \times (0.4 + 0.1 \times \mathrm{C_B})$, from

Kijima *et al.* (1990) and $1 - \mathrm{t_R} = 0.28 \times \mathrm{C_B} + 0.55$, from Matsumoto and Suemitsu (1980), respectively. z_H is the z-coordinate of the point, upon which the lateral force Y_{Hull} acts. The normal rudder force F_N was defined in terms of the rudder area, aspect ratio and the effective speed of water flow over the rudder which will differ significantly from the forward speed of the ship, as will be shown later. The first order Euler method was applied when the program was run in three degrees of freedom that did not include the roll restoring force, and it works well. When the roll motion was included as in equations (4-1 to 4-4), the first order Euler method got really unstable and as such the program could not be run. The Runge-Kutta's solution of second order differential equations Stroud (2011) was applied to enable this to be run successfully.

As an alternative, the solution for the three degrees of freedom given in Lewis (1989) and Betancourt (2003), was extended to include the roll angle, however, considering the non-linear Taylor expansion for each force or moment (equations 4-5 to 4-8) with the dynamic response terms of the corresponding equation (4-1 to 4-4) given by Son and Nomoto (1981) and solving the resulting simultaneous equations will give the rate of change of surge, sway, roll and yaw velocities over time in dimensional form as:

$$\dot{u} = X/(m + m_x) \qquad 4\text{-}9$$

$$\dot{v} = -\frac{(I_x+J_x)(I_z+J_z)Y+(-m_yI_y)(I_z+J_z)K+(m_y\alpha_y)(I_x+J_x)N}{(m+m_y)(I_x+J_x)(I_z+J_z)-(-m_yI_y)^2(I_z+J_z)-(m_y\alpha_y)^2(I_x+J_x)}. \qquad 4\text{-}10$$

$$\dot{p} = -\frac{-(-m_yI_y)(I_z+J_z)Y+K(m+m_y)(I_z+J_z)-K(m_y\alpha_y)^2+(-m_yI_y)(m_y\alpha_y)N}{(m+m_y)(I_x+J_x)(I_z+J_z)-(-m_yI_y)^2(I_z+J_z)-(m_y\alpha_y)^2(I_x+J_x)}. \qquad 4\text{-}11$$

$$\dot{r} = -\frac{-(m_y\alpha_y)(I_x+J_x)Y+K(-m_yI_y)(m_y\alpha_y)+N(m+m_y)(I_x+J_x)-N(m_yI_y)^2}{(m+m_y)(I_x+J_x)(I_z+J_z)-(-m_yI_y)^2(I_z+J_z)-(m_y\alpha_y)^2(I_x+J_x)}. \qquad 4\text{-}12$$

This provision made for either Euler or Runge-Kutta Integration to be applied, however, around a given range of wave frequencies, the Euler method gets unstable, therefore, the Runge-Kutta method for second order differential equation was used in this research, and applying an assumed time step. The Euler method computation multiplies the time step by the instantaneous acceleration and then adds to the previous (or initial) value of the variable; the resulting variable (velocities) is then equal to the new calculated value. Also applying Euler Integration in order to find the

displacement by multiplying the desired velocity by a specified time step and then adding to the previous (or initial) value of the variable.

The Runge-Kutta 4th order (RK4) formulation for second order differential equation using the initial conditions and solving for the next step, is as follows:

$\mathrm{u}(1) = \text{initial ship velocity}$, which is computed from the result of equation 4-50. $\mathrm{v}(1) = 0$, $\mathrm{r}(1) = 0$, $\mathrm{p}(1) = 0$, $\phi(1) = 0$, $\psi(1) = 0$

$$\dot{\mathrm{u}} = \mathrm{f}_1(\mathrm{u}, \mathrm{v}, \mathrm{r}, \mathrm{p}, \mathrm{t}, \phi, \psi, \phi) \quad \textit{4-13}$$

$$\dot{\mathrm{v}} = \mathrm{f}_2(\mathrm{u}, \mathrm{v}, \mathrm{r}, \mathrm{p}, \mathrm{t}, \phi, \psi, \phi) \quad \textit{4-14}$$

$$\dot{\mathrm{r}} = \mathrm{f}_3(\mathrm{u}, \mathrm{v}, \mathrm{r}, \mathrm{p}, \mathrm{t}, \phi, \psi, \phi) \quad \textit{4-15}$$

$$\dot{\mathrm{p}} = \mathrm{f}_4(\mathrm{u}, \mathrm{v}, \mathrm{r}, \mathrm{p}, \mathrm{t}, \phi, \psi, \phi) \quad \textit{4-16}$$

$$k_{i1} = 0.5h^2 f(u_i, v_i, p_i, r_i, p_i, \phi_i, \psi_i) \quad \textit{4-17}$$

$$k_{i2} = 0.5h^2 f(x(i) + 0.5h * u(i) + 0.25k1(i), u(i) + k1(i)/h) \quad \textit{4-18}$$

$$k_{i3} = 0.5h^2 f(x(i) + 0.5h * u(i) + 0.25k1(i), u(i) + k2(i)/h) \quad \textit{4-19}$$

$$k_{i4} = 0.5h^2 f(x(i) + h * u(i), v_1 + k3(i), u(i) + 2 * k3(i)/h) \quad \textit{4-20}$$

$$P = (k_{i1} + k_{i2}k + k_{i3})/3 \quad \textit{4-21}$$

$$Q = (k_{i1} + 2 * k_{i2} + 2 * k_{i3} + k_{i4})/3 \quad \textit{4-22}$$

$$x(i+1) = x(i) + h * u(i) + P \ \textit{(new positon)} \quad \textit{4-23}$$

$$u(i+1) = u(i) + Q/h \ \textit{(new velocity)} \quad \textit{4-24}$$

$$udot(i) = f(u(i), v(i), r(i), p(i), \phi(i), \psi(i), \phi(i)) \quad \textit{4-25}$$

$\mathrm{x(i)}, \mathrm{u(i)}$ and $\mathrm{udot(i)}$, are instantaneous positions, velocities and accelerations for the next time step and h is the time step. This is shown for the surge direction and the others follow similar pattern of solution. The other degrees of freedom were computed accordingly in the code.

For plotting the path of the ship in continuous motion considering Figure 4-6, the Instantaneous values of the linear velocities of the ship relative to the earth axes, instead of relative to the ship axes as initially stated, are obtained by:

$$\dot{x}_{0o}(t) = u\cos\psi(t) - v(t)\sin\psi(t) \qquad 4\text{-}26$$

$$\dot{y}_{0o}(t) = u(t)\sin\psi(t) + v\cos\psi(t) \qquad 4\text{-}27$$

The drift angle is given by:

$$\beta = \psi - tan^{-i}(\frac{\dot{x}_{0o}}{\dot{y}_{0o}}) \qquad 4\text{-}28$$

Where $\dot{x}_{0o}(t)$ and $\dot{y}_{0o}(t)$ are components of the instantaneous resultant velocity of the origin, O, of the ship along a fixed set of earth axes, x_0 and y_0, respectively.

For potting the actual trajectories, equations 4-26 and 4-27, are numerically integrated relative to the fixed earth axes and the orientation of the ship.

$$xpos = x_0 + h(u\cos\psi - v\sin\psi\cos\phi) \qquad 4\text{-}29$$

$$ypos = y_0 + h(u\sin\psi + v\cos\psi\cos\phi)) \qquad 4\text{-}30$$

Where *h* is the assumed time step.

A summary of some of the assumptions made in order to simplify the equations for the calm water hydrodynamic conditions gives:

a) The rotational velocity and acceleration about the y-axis are zero. (q = 0 and $\dot{q}$ =0)
b) The translational velocity and acceleration in the z direction are zero. (w=0 and $\dot{w}$=0)
c) The vertical (heave and pitch) motions were decoupled from the horizontal plane motions and are negligible.
d) The product of the mass moment of inertia I_{xz} is very small and can be neglected.
e) The surge equation (equations 4-1), is substituted by a dynamic equation, which is a function of u, v, and δ (equation 4-5).
f) The longitudinal centre of gravity, (LCG) and the longitudinal centre of buoyancy, (LCB) are both at mid-ship.

g) The vertical centre of gravity, (VCG) is on the centreline.
h) The only important forces and moments acting on the ship that are induced by the rudder were those due to any rudder deflection. Rudder drag forces at zero deflection are ignored, forces and moments due to $\dot{\delta}$ and $\ddot{\delta}$ can be assumed to be negligible.

4.3 Rudder Forces and Moments

The rudder is the primary device that is used to maintain directional control of the ship and it is most commonly positioned astern where it interacts with the propeller and the flow from it. The use of a rudder is not limited to producing a directional turning moment, but it also does provide a damping against turning motion, thus giving a stabilising effect on the ship motion. The ability to change the heading of the ship (course-changing), and the ability to bring the ship back onto a straight line from the previous condition in which was turning (course checking) are achieved using the available steering system, which is the rudder in this case. Its magnitude and control functionality should be capable of maintaining course in waves and wind from any direction. Its effectiveness is defined by the hydrodynamic transverse force that is generated on it, and associated reactive force on the hull, at a given angle of turn. The forces and moments generated by the rudder are hereby shown in Figure 4-7.

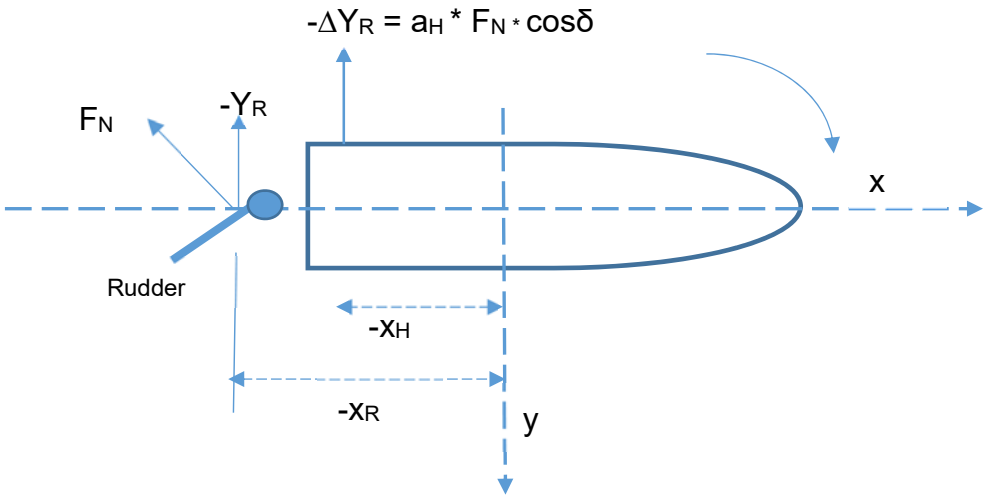

Figure 4-7 Diagram of rudder forces and hull-rudder interaction (Hooft *et al.* (1994)).

The rudder is of a symmetrical streamlined cross-section which is to be acted upon by surface pressures resolving into lift and drag forces when held at an angle of

attack relative to the flow of water. It is required to design the rudder in a manner that it produces maximum lift for a minimum drag, on the assumption that the lift (sideways force) behaves in a consistent manner for all likely angles of attack. In order to determine the forces acting on the rudder, the actual velocity and direction of the relative flow at the rudder need to be determined from the general motion of the ship. The lift force, F_N acting on a rudder is given by:

And the above are related by the expression:

$$F_N = constant \times \rho A_R V^2 f(\propto) \qquad 4\text{-}31$$

Where

A_R is the projected area of the rudder, in m^2, *V* is the average velocity of the water past the rudder Ship's velocity in m/s, ρ is the density of the water, ∝ is the angle of attack. The *constant* is a function on the cross-sectional and profile shape of the rudder, experimentally determined. The Manoeuvring Modelling Group report, Son and Nomoto (1981), gives the normal rudder force as

$$F_N = \left(\frac{6.13\Lambda}{\Lambda + 2.25}\right)\left(\frac{A_R}{L^2}\right) V_R^2 sin(\alpha_R) \qquad 4\text{-}32$$

And the components in surge, sway, roll and yaw as:

$$\text{Surge: } X_R = -(1 - t_R)F_N sin\delta \qquad 4\text{-}33$$

$$\text{Sway: } Y_R = -(1 + a_H)F_N cos\delta . cos\phi \qquad 4\text{-}34$$

$$\text{Roll: } K_R = z_{HE}(1 + a_H)F_N cos\delta \qquad 4\text{-}35$$

$$\text{Yaw: } N_R = -(x_R + a_H x_H)F_N cos\delta . cos\phi \qquad 4\text{-}36$$

Where:

$$V_R = \sqrt{u_R^2 + v_R^2} \qquad 4\text{-}37$$

$$u_R = u_p \varepsilon \sqrt{1 + \frac{8\kappa K_T}{\pi J^2}} \qquad 4\text{-}38$$

$$v_R = \gamma v + c_{\delta r} r + c_{\delta rrr} r^3 + c_{\delta rrv} r^2 v \qquad 4\text{-}39$$

$$\alpha_R = \delta + tan^{-1}(\frac{v_R}{u_R}) \qquad 4\text{-}40$$

$$F'_N = \frac{F_N}{0.5 \times \rho \times A_R \times u_R^2} \qquad 4\text{-}41$$

F'_N, is the non-dimensioned form of the Normal Rudder Force.

It worthy to note that most rudders for ships are hydraulically limited to a maximum turning angle of 35 degrees (and physically to 37degrees) on one side to avoid stalling (which occurs at angles between 35 and 45 degrees (Muckle and Taylor (2013)), excessive loss of speed and large heel on turn.

Below a ship's manoeuvring speed, the manoeuvrability of the rudder is insufficient because of relatively reduced velocity of the water arriving at the rudder. It is normally difficult to ascertain the minimum safe manoeuvring speed of the ship as the velocity of the water arriving at the rudder depends on the propeller's slip stream. This method may efficiently give a vital information at the design stage or before any anticipated modification.

4.4 Propeller Thrust Model

The propeller of this subject ship is a 5-bladed fixed pitch propeller with known physical shape and dimensions as obtained from the experimental data of Son and Nomoto (1981). The engine power (MCR) is translated into the motion of the ship by appropriate formulation.

Here, a propeller thrust model is defined that considers, the propeller loading in terms of both the resultant torque (through its experimentally determined effective propeller inflow velocity coefficients) and provides a realistic simulation of the revolutions, torque and thrust within the time-domain being declared. The propeller thrust is assumed to act only along the longitudinal direction of the ship's hull. No oblique flow

effects were considered, even when manoeuvring, except for the wake fraction and thrust deduction factor corrections.

As a result, and by assumption, no side forces are exerted during manoeuvres and, the non-dimensional force is given by

$$K_T = \frac{T_P}{\rho n^2 D_p^4} \quad 4\text{-}42$$

$$K_T = 0.527 - 0.455J \text{ (Brasel and Dworak (2014))} \quad 4\text{-}43$$

$$K_Q = \frac{Q_p}{\rho n^2 D_p^5} \quad 4\text{-}44$$

$$Q_P = 2\pi \times I_{prop} \times \dot{n} + \rho \times n^2 \times D^5 \times K_Q \quad 4\text{-}45$$

$$J = \frac{u_p V}{nD} \quad 4\text{-}46$$

$$u_p = u\left[\left(1 - w_p\right) + \tau\left\{\left(v + x_p r\right)^2 + C_{pv} v + C_{pr} r\right\}\right] \quad 4\text{-}47$$

$$X_p = (1 - t)\sum(T_P) = R_T \quad 4\text{-}48$$

Where T_P is the Propeller thrust, the terms K_Q and K_T are the torque and thrust coefficients, and Q_P the propeller torque respectively. To determine T_P, the Holtrop and Mennen (1982) method was used to determine the total resistance, R_T, then the expression in equation 4-48 was applied to obtain T_p and this value was used to calculate K_T and its result agreed with that from equation 4-43. Thus equation 4-43 was used for the simulation. Plots that show the calculated value of total resistance by Holtrop and Mennen (1982) method, the engine manufacturer's formulation and the resistance component from experimental result are shown in section 4.5.

4.5 Main Engine Machinery Model

The method of modelling the main engine and of how its installed power is translated into the forward motion of the ship by the propeller is explained below. The main propulsive engine for this vessel is modelled as being at constant revolutions per minute (rpm), (so that power loss in waves can be determined by ship speed loss (m/s) due to propeller slip and added resistance, etc.) slow speed diesel engine with direct shafting to the propeller. The reason being that the aim of the work is to run the ship at its maximum continuous output engine power, and then enter seas with the

waves and winds appropriate to adverse environment conditions, and to subject the ship to the various manoeuvring motions, and then to subsequently reduce the level of installed power until the failure criteria is reached. The details of the propulsive machinery are given in Table 4-2.

Table 4-2 Objective S-175 Container Ship Engine and EEDI Parameters

Engine Parameter	*value*	*unit*
Bore	*600*	*mm*
Stroke	*2400*	*mm*
No. of Cylinders	*6*	*-*
Maximum Continuous Rating (MCR)	*14280*	*kW*
Torque	*1095*	*Nm*
Engine Speed @ 100% of MCR	*105*	*rpm*
Specified fuel oil consumption (100% MCR)	*169*	*g/kW h*
Engine power @ 80% MCR	*11424*	*kW*
Combined Waste Heat Recovery @ full Load (TWHR)	*1180*	*KW*
Combined Waste Heat Recovery @ 75% Load (TWHR)	*787*	*KW*
Specified fuel oil consumption (80% MCR)	*163.85*	*g/kW h*
Turbocharger type	*High efficiency*	*-*
Propulsion Efficiency η_p	*84.35*	*%*
Power @ 90% MCR	*12852*	*kW*
Speed @90% MCR	*99.8*	*rpm*
Specific fuel oil consumption (@90% MCR)	*167.4*	*kw*
Power to CO_2 *conversion factor for Heavy Fuel Oil (HFO) ISO 8217 Grade a RME to RMK* (C_F)	*3.114*	*t-*CO_2 */ t-Fuel*

The Engine power of the ship was not given in the paper from which the most data for this research was taken. The resistance was approximately calculated by the method of Holtrop and Mennen (1982), using only the available parameters and used to calculate the effective power as in equation 4-49. Then an engine with closely matching rating was selected from the manual of MAN (2014) and the rest of the computations and analyses were done based on that engine.

$$\textit{The Effective Power} = EP = R_T \times V_s \qquad 4\text{-}49$$

The initial propeller Speed (n_m) in revolutions per minute will thus computed from the value of the given MCR (P_M) MAN (2011):

$$n_m = C \times \sqrt[3]{\frac{P_M}{(D_p)^5}} \text{ thus,} \qquad 4\text{-}50$$

$$P_{MCR} = (\frac{n_s}{C})^3 * D_p^5 \qquad 4\text{-}51$$

where D_p is the diameter of the propeller, P_M, the Engine power (Maximum continuous rating) and C is a constant given by M.A.N Diesel, which is dependent on the number of propeller blades as follows:

Table 4-3 Propulsion Constant MAN (2011) for future guidance

Number of Propeller Blades	*3*	*4*	*5*	*6*
Constant (C)	*125*	*115*	*104*	*93*

For the subject ship, C was derived to be = 104, considering the known engine Power and using equation 4-50. Plots that show the calculated value of total resistance by Holtrop and Mennen (H&M) method, the engine manufacturer's formulation (MAN) and the resistance component from experimental result (Son and Nomoto (1981)) are shown in Figure 4-8.

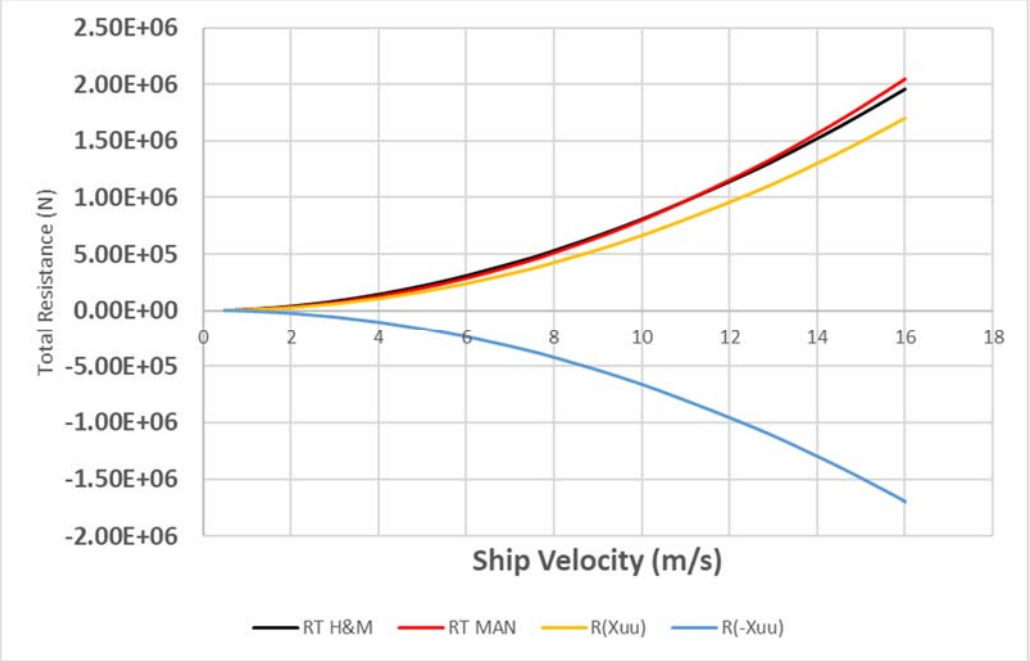

Figure 4-8 Total Resistance Vs Ship'v velocity characteristics.

Thus inputting the initial speed was done in this order (Figure 4-9):

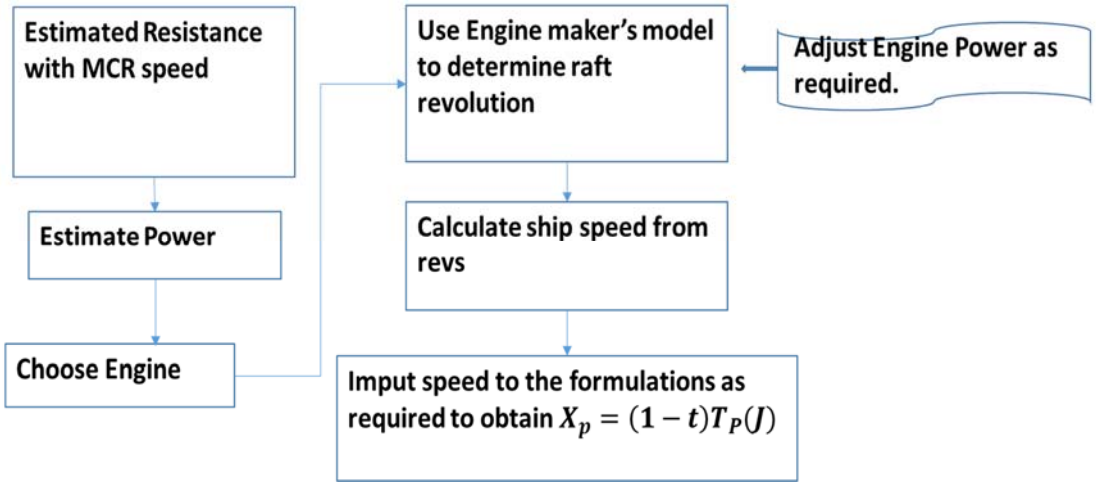

Figure 4-9 Method of inputting the ship speed to the modelling equations.

The specific fuel oil consumption (SFOC) curve is given below (Figure 4-10):

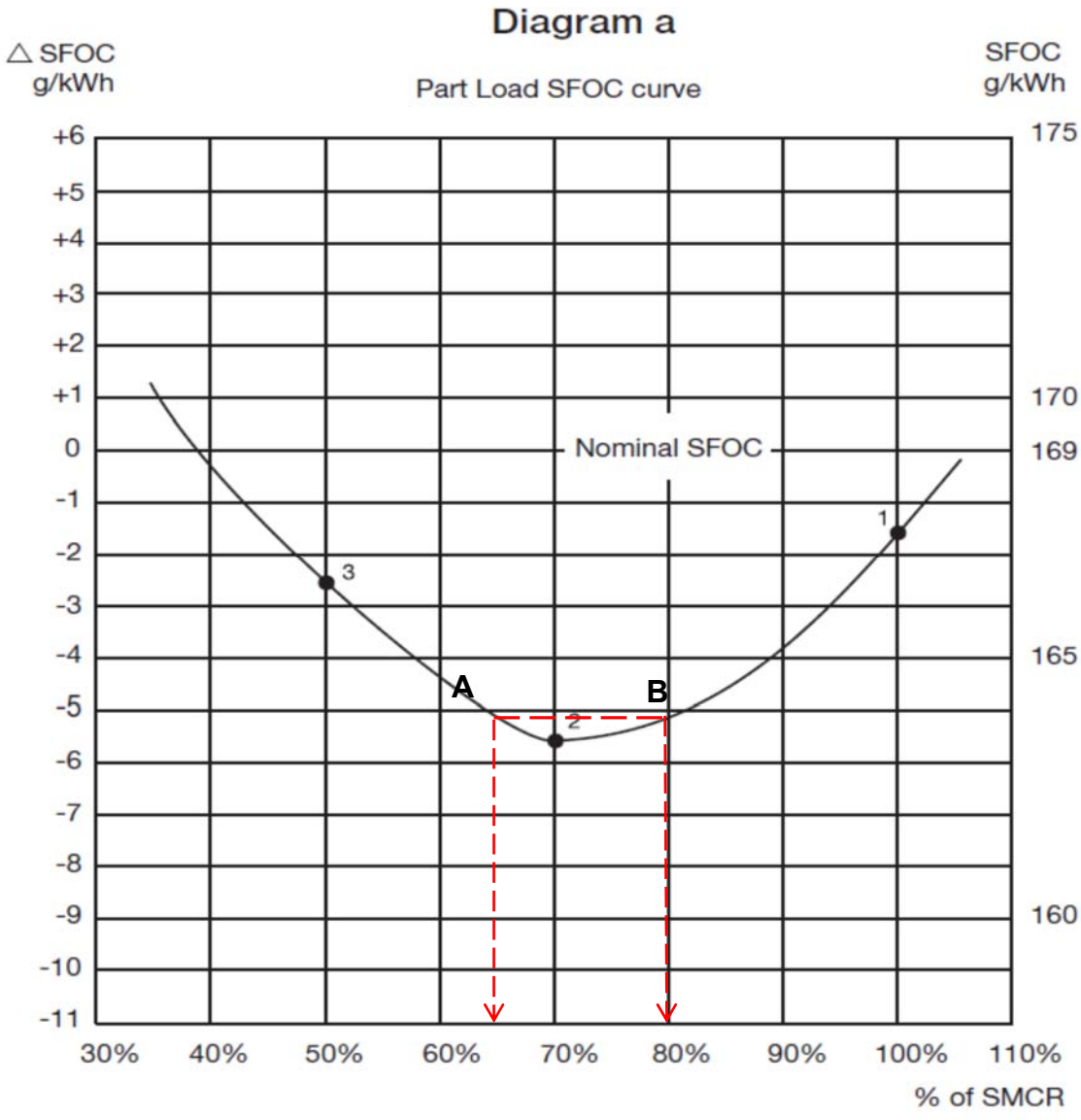

Figure 4-10 Example of SFOC for derated 6S60ME-C8.2/-GI with fixed pitch propeller and high efficiency turbocharger MAN (2014).

The above specific fuel oil consumption (SFOC) figures seen in the curve are with a tolerance of 5% (at 100% SMCR) and are based on the use of fuel with a lower calorific value of 42,700 kJ/kg (approximately 10,200 kcal/kg) at ISO conditions. These values are known from the Engine parameters; however, the calculation is made in such a manner that the given engine speed of 105 rpm, comes as a function of the MCR power of 14280kW (equation 4-50). Thus, adjusting the power alone will now determine the ship's speed and consequently behaviour of the ship in motion, and the subsequent loops will recalculate a new ship speed each time that the power is reduced, from which results were extracted. Also, this plot of the specific fuel consumption cannot be represented by a single equation for ease of programming. However, each of the sides from the 70% minimum SFOC was represented be equations below, and then suitable conditional command used to determine the appropriate fuel oil consumption for each percentage of power.

The plot is represented by the following equations with the coefficient of determination, $\mathrm{R}^2 = 0.9998$:

$$\mathrm{sfoc} = 26.57 \times \ \%\mathrm{smcr}^2 - 47.466 \times \%\mathrm{smcr} + 183.56 \ ; \ 0.35 \geq \%\mathrm{smcr} \leq 0.7 \qquad 4\text{-}52$$

$$\mathrm{sfoc} = 38.677 \times \ \%\mathrm{smcr}^2 - 52.407 \times \%\mathrm{smcr} + 181.08 \ ; \ \%\mathrm{smcr} > 0.7 \qquad 4\text{-}53$$

And plotting the percentage of Engine load vs the total WHRS given, a reasonable relationship was obtained as, $\mathrm{TWHR} = 1572 \times \%\mathrm{smcr} - 392$, to enable an approximate automatic computation of the waste heat recovered at the other load points not given in the literature.

Where $\%\mathrm{smcr}$ is the multiplying factor for power (between 0 and 1); e.g., at 70% MCR, $\%\mathrm{smcr} = 0.7$.

Normally, at a manoeuvring speed of about 3.5-4.5 knots, a correspondingly low propulsion power will be needed judging from the propeller law. However, in heavy weather the amount of power required to sustain this range of speed will be higher due to the increased resistance on the ship.

The mass flow rates of fuel for the ship is given by:

$$\dot{m} = \frac{\text{sfc} \times \text{power}}{1000} \left(\frac{\text{kg}}{\text{hr}}\right) \quad \textit{4-54}$$

Thus the mass flow rate at 100% MCR:

$$\dot{m}1 = \frac{169 \times 14280}{1000} = 2413.32 \left(\frac{\text{kg}}{\text{hr}}\right) \quad \textit{4-55}$$

and at 80% MCR:

$$\dot{m}2 = \frac{163.85 \times 11424}{1000} = 1871.82 \left(\frac{kg}{hr}\right) \quad \textit{4-56}$$

This calculation was done only to demonstrate the application of equations 4-52 and 4-53 for calculating the fuel consumption.

4.6 Energy Efficiency Design Index Consideration (EEDI)

In this section, an explanatory definition of EEDI is given, the perspectives for derating a ship's engine during a major refit or for a new build explained, and the overall implications to the derated ship discussed.

In a generic format EEDI being a measure of a ship's energy efficiency in grams of carbon-dioxide per ton.nautical mile ($\frac{\text{g of } CO_2}{\text{ton.nm}}$), is defined as :

$$EEDI = \frac{Impact\ to\ Environment}{Benefit\ for\ Society} \left(\frac{g}{t.nm}\right)$$

By this, increasing the cargo capacity and, or reducing the fuel consumed per mile for a given cargo capacity will reduce the EEDI, i.e., provide for improved efficiency. For the purpose of this work, deration of the engine will be explained citing the following circumstances that amount to reducing engine's power using ship 'X' as sample:

a. Ship '**X**', an existing ship to have its engine power reduced either by electric/electronic limiter, or by mechanically disabling one or more, say, cylinder output.

b. A new sister ship, in terms of hull form and minimum cargo carrying capacity, to Ship '**X**' is to be built, however, with a reduced engine capacity.

c. A new ship is to be built with same deadweight as Ship '**X**', however with a new improved hull form, energy recovery/saving provisions and reduced engine capacity.

d. A new ship with same engine power (i.e. overall fuel consumption) as ship '**X**', built with a larger cargo carrying capacity, or an existing ship, modified for increased cargo capacity.

This research in its present state does pay more attention to the first three considerations. For scenario '**c**', is the most expensive option and a most desirable condition where both the propulsion and systems will be optimised with the hull characteristics that might lead to improved dynamic behaviour; however, there is also the need to study the dynamic characteristics of the ship in adverse weather condition with a view to making adequate powering. Scenario '**b**' will imply that there may be required, a bigger steering capacity, which means slightly increased weight, however, this will be more than offset by the reduced weight of engine and possible further reduction in weight due to possible reduced weight of the auxiliary machinery owing to the reduced engine size. Also, there is a chance of increasing the deadweight of the ship owing to the resultant reduced weight and space due to reduced machinery capacity, and this will further reduce the EEDI values. Thus '**a**' and '**b**' are the two conditions that would require more detailed investigation that will lead to adequate powering decision in '**a**' and optimised powering and steering system decision in '**b**'.

Eshipman was used to compute the Attained EEDI of the ship as per its 100% MCR; then a new EEDI for the ship after the reduction of the MCR to 75% of its original value. These computations were made on the assumption that:

- it is of the ice class with its correction factor f_i given in equation 4-59
- There is a waste heat recovery system which meets electricity generation and heating requirements when vessel is at high loads.
- There are no further Innovative energy efficient technology.

- The cubic capacity correction factor are as given in IACS (2013).

Germanischer Lloyd (2013), give the following formulation for the required EEDI:

$$\text{Attained EEDI} = \frac{\sum P \times sfc \times C_F}{f_{cf} \times \text{capacity} \times V_{ref} \times f_w} \quad \textit{4-57}$$

$$\text{required EEDI} = a \times b^{-c} \quad \textit{4-58}$$

$$f_i = \frac{0.0377 \times L_{pp}^{2.329}}{\text{capacity}} \quad \textit{4-59}$$

$$f_w = a_w \times \ln(\text{capacity}) + b_w \quad \textit{4-60}$$

Where f_w is the weather correction factor with a_w and b_w given as 0.0208 and 0.633 for container ship, $\sum P$ is the sum of the engine power at 75% SMCR (for instance, for the full power consideration, $\sum P$ is 75% of the full power, and for the 80% derated power consideration, $\sum P$, is 60% of the original full power), C_F is the fuel to CO_2 conversion factor V_{ref} is the reference speed determined at 75% of the SMCR, (EShipman computed this to be equal to 11.2m/s for the full MCR consideration and 8.825 for the 80% MCR power consideration). f_{cf} is the product of all the capacity factors (for this research, others are considered as 1.0 except the ice class correction factor f_i), a is given as 174.22, b is the deadweight and c was given as 0.201 for container ships. The results of the computations are given in section 6.2.

4.7 Controller for the Rudder(s) and Propulsion

This section discusses the manoeuvring tests that can be achieved and highlights some control principles relating the motions of the ship to the various control hardware. There was a validation of the ability of the algorithm to bring the ship to a specified heading after performing a pre-defined turning direction, from an initial arbitrary heading. It is known that most ships do ideally have an inherent course keeping stability property, which implies that it naturally does not tend to continue to turn and gets back into a straight-line motion after the external disturbance that caused some small deviation vanishes, when its rudder is returned into the in-line position. The rudder is required to automatically bring the ship back to its desired

heading after a slight deviation, and as well to steer the ship to a new course if required. In order to achieve these functions efficiently, a control system was used to operate the rudder through its steering gear. For the manoeuvrability of the vessel to be tested, there is provision for the manual input of rudder angles, however, a simple rudder control system algorithm was incorporated in the simulator such that the algorithms for instigating the identified manoeuvres could take input from the current rudder and ship positions.

The speed of the engine needs to be sustained and as such, a control system needs to compensate for drop in speed, especially due to additional forces and moments that are imposed on the ship. To this end, one P+D (Proportional + Derivative) controllers are required for the rudder control. The Heading controller acting on the rudder(s) is responsible for operating the rudders so as to keep the ship heading in the desired direction. The speed controller is a P+I controller responsible for ensuring that the rotation of the propeller at the appropriate RPM is sustained in order to keep the ship at the desired speed within an acceptable tolerance. For this research, the speed controller was not applied since the revolutions per minute was kept constant, however, a limiter was put in place to limit the linear velocity. The ship's linear velocity does change with environmental condition, thus a computation converts the instantaneous velocity to revolutions per minute, and some limiter is put in place to avoid excessively high and very low velocity.

The functionality of the rudder can be ascertained from time and gain constants, 'K' and 'T'. The index 'K' indicates the ratio of a steady turning angular rate to a corresponding helm angle i.e., the angular velocity eventually reached, and may be called the index of "turning ability". The 'T' index of that indicates the course stability, and defines the rapidity with which a ship approaches the terminal angular rate, $K\delta_0$. The quality of a ship often relates to her behaviour after she is disturbed by an external force and as a result deviates from a straight-running course with the rudder(s) set amidships, and is also known as "stability on course" and is dependent on the index, T, and which determines the ease with which course-keeping is maintained.

The more manoeuvrable ships are observed to have higher 'K' and lower 'T' values, with tankers tending to be found in the upper group. The smaller the index 'K', the

smaller is the turning rate that is produced by a given helm angle. The smaller the index T, the more stable is a ship on a set course and the quicker is her response to steering commands.

SOLAS II-1/29.3 requires that the main steering gear is capable of putting the rudder over from 35° on one side to 35° on the opposite side with the ship at its deepest seagoing draught and when running ahead at maximum ahead service speed, and also under the same conditions, from 35° on either side to 30° on the opposite side in no more than 28 s; for all ships, with the steering gear that is operated by power units.

To this end the minimum rate of turn for the rudder about its axis when using the steering gear should be 2.321°/s (65°/28s). The automatic control of a ship's system can be represented as follows:

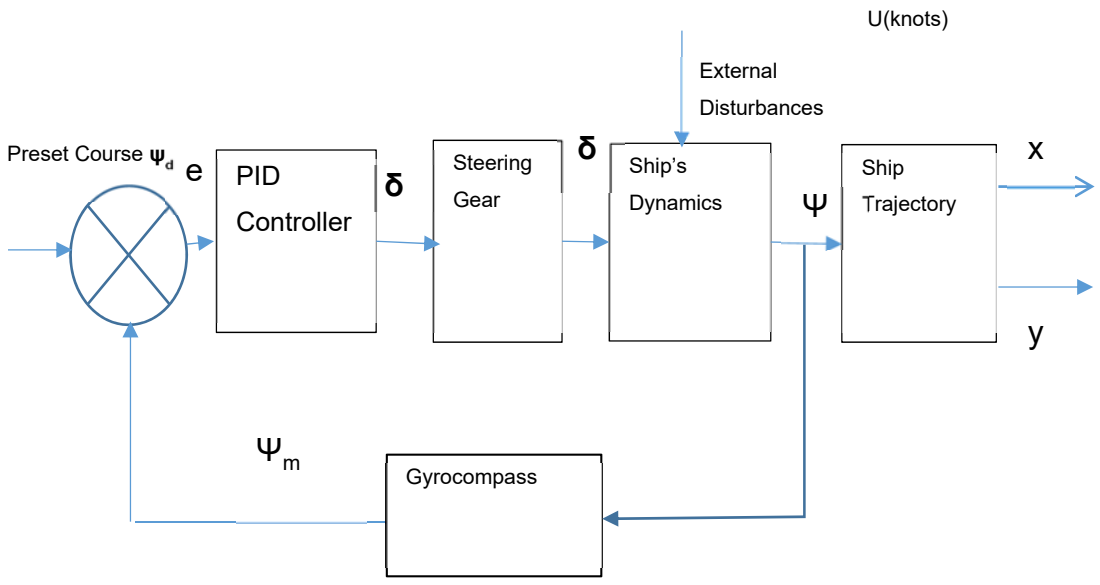

Figure 4-11 automatic control of a ship's system

The Rudder dynamics applied for this work is a first order model. As mentioned earlier, steering gears are designed to operate between 35 degrees Starboard to 35 degrees port angles at a speed which varies between 2.33deg/sec to 7 degs/sec, depending on each design requirement. The minimum value being determined by the SOLAS rule stated earlier. However, for this study a higher rate more than 2.5°/sec was applied.

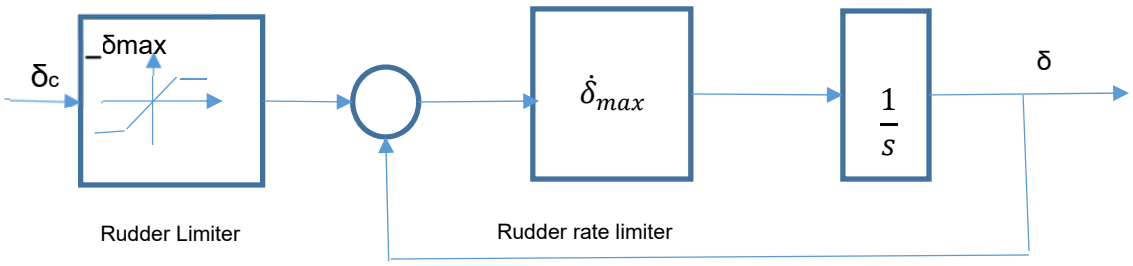

Figure 4-12 The Steering Gear Proportional+Derivative model

$$T_E\dot{\delta} = \delta_E - \delta;$$

T_E is the time constant of the steering gear and δ_E is the command ruder angle. The rudder was programmed to respond to a change in yaw angle for a zigzag motion, and when it is desired to move in a straight line in adverse weather condition, it is programmed to respond to both drift and yaw angle.

Chapter 5 Influence of Environmental Conditions

In the preceding sections of this thesis, the discussions on the ship's simulation and the formulations applied in the formulation for testing methodology have been based on the assumptions of a flat and motionless sea which is the normal basis on which ship resistance calculations for design purposes are carried out. The performance of the ship in adverse weather condition is the key consideration in this research thus, the aims and objectives of this chapter are to discuss the environmental loads on ships and its effects on ship's motion. And then to discuss the adopted formulation(s) and any corrections that were applied in order to aid the development of the proposed methodology. In most accident reports in coastal areas, environmental conditions such as strong wind and, sometimes strong current were mentioned, but usually no large waves as the areas were protected Shigunov (2018). The interim guidelines Shigunov (2012a) and Shigunov (2012b), requires that a minimum advance speed set to 4 knots be attainable to provide sufficient time for leaving the coastal area and some margin for ocean current.

The major constituent of additional resistance problems with ship controllability that comes from the environment is the wave resistance and its associated motion effects followed by wind effects which also do play a significant role. Local winds are a result of the complex interactions between thermal energy transfer from the sun and any existing global weather pattern of the earth that produces varying degree of pressure fluctuations that result in the various magnitude and directions of winds, and it is known that sea waves are primarily the result of the transference of the kinetic energy of the local winds to the sea surface. If the wind is sustained the wave will grow in height and length and eventually become gravity waves that can travel far beyond the reach of the wind thus wave and wind do have very strong relationship when dealing with environmental loading, and it is required to define a sustained wind speed value that has a return period of 100 years and related to a reference level of 10 metres above sea level for design purposes in the determination of global loads (Germanischer Lloyd (2013)). In restricted waters where ship's operating speed is generally low, with currents which are non-uniform, tidal current consideration becomes an additional concern, as they are most likely to produce controllability problems especially in bends where significant current velocity gradients tends to occur.

There are numerous proposals and scientific formulations regarding the predictions of environmental loading on ships. Since Eshipman is a manoeuvring simulation platform for testing this method, the effect of tidal current is included in its development.

The ability of ships to manoeuvre in an adverse environmental conditions can be examined in several different scenarios, such as:

a. Requirement to manoeuvre at reduced speeds in restricted waters.

b. Need to manoeuvre in coastal areas when there is the possibility of increasing storms and, or high tidal current velocity.

c. The need for a ship to manoeuvre in adverse conditions in the open seas.

As mentioned in section 2.1, the criteria for ship propulsion and steering abilities which included that the ship should be able to: (1) maintain course in waves and wind from any direction and (2), sustain advance speed of at least 4.0 knots in waves and wind from any direction according to (Shigunov (2012a) and Shigunov (2012b)), who also suggested that the weather conditions were not made severe on the assumption that ship masters do not normally stay near the coast in an increasing storm and either search for a shelter or leave to the open sea and take a position with enough room for drifting.

The recommended environmental conditions to be applied in a scenario where escape is impossible includes wind speed of 15.7 m/s at significant wave height 4.0 m for ships with Length between perpendiculars (L_{pp})=200 m, to wind speed = 19.0 m/s and significant wave height=5.5 m, for *Lpp*=250 m and greater (IMO (2017)). These were said to have been derived by benchmarking of tankers, bulk carriers and container ships in the EEDI database against these two criteria. However, for this research, the case of wind speed = 19.0 m/s and significant wave height=5.5 m was applied for the 175m ship. The required minimum advance speed of 4.0 knots was assumed to provide some minimum speed over ground for timely escape of the coastal area, and include some margin to take into account current. Also, from experience at sea, most of the steering systems are programmed such that the autopilot is deactivated once the ship speed goes below 5knots, and manual steering

is used. In the open sea, a key requirement is the ability of ship to change its heading into a favourable one with respect to the environment and sustain this heading.

5.1 Estimation of the Wind Force model

The wind loading (both the ambient natural winds and the self-created wind owing to the forward motion of the ship at its set speed) on ships on the exposed members of the structure may account for approximately 15% of the combined loading from wind current and waves Patel (2013) and as such is to be given due consideration. The wind forces and moments are higher in deep seas leading to relatively larger effect on the base overturning moment, thus the wind induced overturning roll moment is a determining factor for the dynamic stability of ships, Taylan (2003). When considering manoeuvrability at low speeds, especially in a physically constrained area or in a congested traffic; the rudder effectiveness in directionally controlling the ship is reduced due to reduced flow across its surfaces. As a result, accurate wind load data, regarding both speed and direction is of great importance for preparing the algorithm for ship manoeuvring simulators.

Though the wind resistance of ships does not generally influence the design as much as it did in earlier times, when streamlined superstructures were more usual. Ships and offshore platforms usually exhibit very complex above water geometries that includes masts, towers, bulwarks, funnels, deck houses, etc. that may have a significant effect on the vortex formations, the local turbulence and the flow separation points, and thereby on the complex nature of the overall aerodynamic loads. So, simplifications are made by including load factors. However, the importance of obtaining accurate knowledge of the ship's wind resistance characteristics is unchanged for the purpose of reaching optimum design of the propulsion plants and for the analysis of design validation.

There has been considerable research towards investigating the effects of wind loading on the manoeuvring performance of ships as it often becomes very critical and poses risks of grounding and collision, when a ship is in an area of traffic congestion as when around a busy harbour or some other areas with high traffic density, and also subject to high and gusty wind loads. Most of these researches

were carried out experimentally. However some authors such as Blendermann (1994), have proposed coefficients of lateral and longitudinal resistance, and induced rolling moments and Isherwood came up with some equations derived from linear multiple regression models generated from their experimental results.

Two kind of winds speeds are considered in the design of offshore structures. One is the sustained wind speed, which is defined as the average wind speed over a time interval of 1 minute measured at an elevation of 10 metres above still water level. The second being the gust speed, is a sudden (usually temporary) increase of the wind's speed, and is of real concern as its magnitude may be usually unpredictable. A wind gust comes quite suddenly and abruptly, it usually comes in 2-minute intervals. According to U.S. weather observing practice, gusts are reported when the peak wind speed reaches at least 16 knots and the variation in wind speed between the peaks and lulls is at least 9 knots. The duration of a gust is usually less than 20 s. Azad *et al.* (2010) and Djamila *et al.* (2014).

DNV-GL (2015), provides an expression for the instantaneous wind pressure which was applied in the wind loading computation, given by:

$$q = \frac{1}{2}\rho|v_{mw} + \overline{u} - \dot{x}|(v_{mw} + \overline{u} - \dot{x}) \qquad 5\text{-}1$$

where $\bar{u}$ is the gust speed and direction variation, v_{mw} is the mean wind speed and direction, q is the dynamic pressure ($q = \frac{1}{2}\rho V_w^2$ is the expression of the basic wind pressure dynamic component that is then associated with the structural geometry).

$\dot{x}$ the instantaneous velocity of the ship (i.e., V_s). Density of dry Air at 15°C is ρ = 0.001224 [kN·s^2/m^4] =1.224kg/m^3

A relation between the wind speed and direction in the earth fixed reference system and the ship reference system is given by:

$$u_w = V * cos\beta + V_{wind} cos(\varphi_{wind} - \psi) \quad 5\text{-}2$$

$$v_w = -V * sin\beta - V_{wind} cos(\varphi_{wind} - \psi) \quad 5\text{-}3$$

$$V_w = \sqrt{u_w^2 + v_w^2} \quad 5\text{-}4$$

$$\beta_w = atan\left(\frac{-v_w}{u_w}\right) \quad 5\text{-}5$$

where u_w is the surge direction (longitudinal) wind velocity, V_w, is the sway direction (transverse) wind velocity, ψ is the yaw angle, β is the drift angle, ϕ_{wind} is the compass angle of the direction of the wind. Figure 5-1 shows the wind effects with parameters defined in texts below:

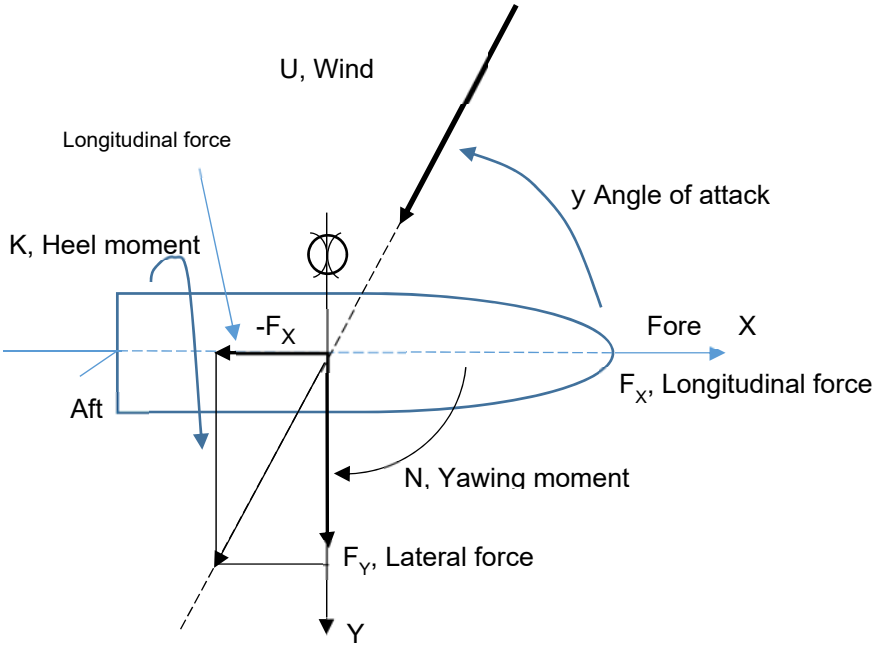

Figure 5-1 Illustration of Wind forces and moments.

The surge force coefficient is that due to the drag force along the vessel's axis through the centre of pressure, the sway force coefficient is from the drag force along the vessel's sway axis and the yaw moment coefficient is from the wind induced yaw moment. Because the side view area of a container ship, particularly with its superstructure, will not normally be fore and aft symmetrical, the side wind force will

result in both sway and yaw components. However, a fully laden container ship will have a more centrally located centre of pressure. The resultant wind force and moment is a combined value of the two sets of force and moment coefficients

The American Bureau of Shipping (ABS) provides the following table on Wind Pressure Height coefficient above the design water surface modified from a velocity profile, to a force profile in Table 5-1 :

Table 5-1 Wind Pressure Height coefficient above the design water surface (Hooft et al.).

Height(m)	*Height(ft)*	*Height coefficient (C_h)*
0-15.3	*0-50*	*1.0*
15.3-30.5	*50-100*	*1.1*
30.5-46.0	*100-150*	*1.2*
46.0-61.0	*150-200*	*1.3*
61.0-76.0	*200-250*	*1.37*
76.0-91.5	*250-300*	*1.43*
91.5-106.5	*300-350*	*1.48*

The basic form of these velocity profiles is:

$$V_h = v_{ref}\left(\frac{h}{h_{ref}}\right)^{1/n} \qquad \textit{ABS (2005)} \qquad 5\text{-}6$$

Where,

V_h = wind velocity at elevation h above the mean sea level.

v_{ref}= wind velocity at the stated reference height

h_{ref} = reference height (10 m or 33ft in American Petroleum Industry standard, (ABS, 2005 .142)).

$1/n$ = exponent of the velocity profile. In specific terms:

$$V_w = v_w\left(\frac{10}{h}\right)^{1/7}$$

V_w = the wind velocity at 10 m height (m/s)

v_w= the wind velocity at elevation h (m/s) and,

h = elevation above ground/water surface (metres)

Yang Xingyan (2013), proposed equation 5-7 for estimating the value of the windage area for some large tonnage ships:

$$logY = \alpha_w + \beta_w \times logX \qquad 5\text{-}7$$

where Y represents A_x or A_y depending on the value of α_w and β_w as can be read from the Table 5-2, and X is the dead weight tonnage or gross tonnage.

A_x = transverse (fore and aft view) projected area,

A_y = longitudinal (side view) projected area,

Table 5-2 Tables of α_w and β_w for various Ship Types.

Ship Type	*X*	*Loaded* A_x		*Ballast* A_x		*Loaded* A_y		*Ballast* A_y	
		α_w	β_w	α_w	β_w	α_w	β_w	α_w	β_w
Gen Cargo	*DWT*	*0.228*	*0.667*	*0.099*	*0.615*	*0.507*	*0.616*	*0.479*	*0.662*
Bulk Carrier	*DWT*	*0.944*	*0.370*	*0.629*	*0.469*	*1.218*	*0.425*	*0.970*	*0.530*
Container	*DWT*	*0.136*	*0.609*	*0.574*	*0.526*	*0.417*	*0.703*	*0.731*	*0.625*
Oil Tanker	*DWT*	*0.469*	*0.474*	*0.251*	*0.551*	*0.556*	*0.558*	*0.650*	*0.592*
RORO	*DWT*	*1.029*	*0.435*	*0.917*	*0.473*	*1.453*	*0.464*	*1.541*	*0.456*
Passenger	*GT*	*0.947*	*0.426*	*0.986*	*0.416*	*0.059*	*0.680*	*0.656*	*0.667*
Ferry	*GT*	*0.728*	*0.473*	*0.710*	*0.484*	*0.564*	*0.674*	*0.569*	*0.679*

As mentioned earlier, in calm weather, the ship will experience some heel moment when making a sharp turn at high speed. Thus in adverse weather condition with high windward force on the emerged side of the ship as shown below in Figure 5-2, there is increased windage area that is non-negligible and would increase the roll effect, especially with large motions.

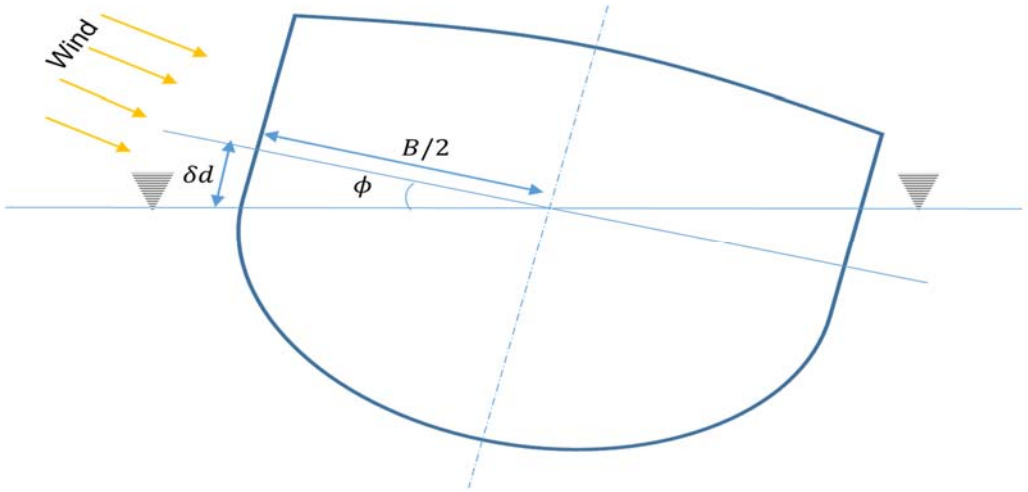

Figure 5-2 Effect of Wind in Adverse weather condition

This does create increased forces and moment effects especially with beam wind which may results in greater drifts and increased probability of a capsize. This increased moment is probably a principal contributory factor that has caused some of the accidents that have occurred when manoeuvring in conditions in areas under adverse wind conditions Ueno *et al.* (2012).. When computing the environmental effect on ship motion, many authors do consider the ship as having a constant draft and thus do not put the roll effect into perspective. On a reasonable assumption that the vessel remains wall-sided over the length of the ship at as the ship rolls, then the change in draft (δd) and the area (δA_y) at an instant in time over the ship's length can be given by:

$$\delta d = \frac{B}{2} \times tan\phi \qquad 5\text{-}8$$

$$\delta A_y(i) = \frac{B}{2} \times tan\phi(i) \times L_{pp} \qquad 5\text{-}9$$

Thus, for the time domain simulation, 5-7 becomes

$$A_y(i) = 10^{(\alpha_w + \beta_w \times logX)} \pm \frac{B}{2} \times tan\,\phi(i) \times L_{pp} \qquad 5\text{-}10$$

There is need to include this effect in the simulation of the vessel's manoeuvring in the adverse weather conditions, so proper observations can be made unto taking

acceptable preventative measures some result of including this effect is given in section 6.1.1. Heave and pitch will create similar effect, however, their effect will mostly affect the forward speed and sideway drifts, and is neglected here.

Following the coordinate system shown in Figure 5-1, and considering the fact that the ship will have to turn at some point:

$$F_X = C_X \times qA_{Fw} \cos\gamma \qquad 5\text{-}11$$

$$F_Y = C_Y \times qA_{Lw} \sin\gamma \qquad 5\text{-}12$$

$$N = C_N \times qA_{Lw}L_{oa} \sin\gamma \qquad 5\text{-}13$$

$$K = C_K \times qA_{Lw}H_s \sin\gamma \qquad 5\text{-}14$$

$$Z = C_Y \times qA_{Fw} \qquad 5\text{-}15$$

$$M = C_M \times qA_{Fw}H_F \qquad 5\text{-}16$$

$\mathrm{H_L} = \mathrm{A_{Lw}/L}$ is the above sea level height of geometric centre of the front at projected area, $\mathrm{A_{Lw}}$.

$\mathrm{L_{oa}}$, the length overall

$\mathrm{H_S} = \mathrm{A_{Fw}/B}$ is the height of geometric centre of the side area, $\mathrm{A_{Fw}}$.

Blendermann (1994), provides coefficients of lateral and longitudinal resistance, cross-force, and rolling moment:

$$C_X(\gamma_w) = -CD_l \frac{A_{Lw}}{A_{Fw}} \times \frac{\cos\gamma_w}{1 - \frac{\delta}{2}\left(1 - \frac{CD_l}{CD_t}\right)\sin^2(2\gamma_w)} \qquad 5\text{-}17$$

$$C_Y(\gamma_w) = -CD_l \times \frac{\sin\gamma_w}{1 - \frac{\delta}{2}\left(1 - \frac{CD_l}{CD_t}\right)\sin^2(2\gamma_w)} \qquad 5\text{-}18$$

$$C_K(\gamma_w) = \kappa C_Y(\gamma_w) \qquad 5\text{-}19$$

$$C_N(\gamma_w) = \left[\frac{S_L}{L_{oa}} - 0.18\left(\gamma_w - \frac{\pi}{2}\right)\right] C_Y(\gamma_w) \qquad 5\text{-}20$$

where:

$$CD_l \frac{A_{Lw}}{A_{Fw}} = CD_{lAF} \text{ and} \qquad 5\text{-}21$$

$$CD_l = CD_{lAF}(\gamma_w) \frac{A_{Fw}}{A_{Lw}} \qquad 5\text{-}22$$

Where:

A_{Lw} Is the lateral projected area, A_{Fw} is the transverse projected area and SL is the horizontal distance to centroid of ALw from datum (midships), δ is a cross force parameter obtained from Table 5-3.

Fossen (1994), indicated that values of coefficients are in the range: C_x [0.5, 0.95]; C_y [0.7, 0.95]; C_n [0.05, 0.2].

Table 5-3 parameters for Blenderman's method

Type of Vessel	*CD_t*	*CD_{lAF} (0)*	*CD_{lAF} (π)*	*δ*	*κ*
Container	*0.9*	*0.55*	*0.5*	*0.4*	*1.4*

The Beaufort scale, which is used in Met Office marine forecasts, is an empirical measure for describing wind intensity based on directly visually observed sea conditions. Wave specifications and equivalent wind speeds (well-developed wind waves of the open sea) in Table 5-4, and parameters for demonstrating the methodology were taken considering this table.

Table 5-4 Beaufort Wind Scale

B.scl	*WSm (Knots)*	*m/s*	*WSlim (Knots)*	*WSlim (m/s)*	*DesT*	*PrbwH*	*PmwH*	*SS*	*SDT*
0	*0*	*0*	*<1*	*<1*	*Calm*	*-*	*-*	*0*	*Calm (glassy)*
1	*2*	*1*	*1-3*	*1-2*	*Light air*	*0.1*	*0.1*	*1*	*Calm (rippled)*
2	*5*	*3*	*4-6*	*2-3*	*Light breeze*	*0.2*	*0.3*	*2*	*Smooth (wavelets)*
3	*9*	*5*	*7-10*	*4-5*	*Gentle breeze*	*0.6*	*1.0*	*3*	*Slight*
4	*13*	*7*	*11-16*	*6-8*	*Moderate breeze*	*1.0*	*1.5*	*3-4*	*Slight - Moderate*
5	*19*	*10*	*17-21*	*9-11*	*Fresh breeze*	*2.0*	*2.5*	*4*	*Moderate*

B.scl	*WSm (Knots)*	*m/s*	*WSlim (Knots)*	*WSlim (m/s)*	*DesT*	*PrbwH*	*PmwH*	*SS*	*SDT*
6	*24*	*12*	*22-27*	*11-14*	*Strong breeze*	*3.0*	*4.0*	*5*	*Rough*
7	*30*	*15*	*28-33*	*14-17*	*Near gale*	*4.0*	*5.5*	*5-6*	*Rough-Very rough*
8	*37*	*19*	*34-40*	*17-21*	*Gale*	*5.5*	*7.5*	*6-7*	*Very rough - High*
9	*44*	*23*	*41-47*	*21-24*	*Strong gale**	*7.0*	*10.0*	*7.0*	*High*
10	*52*	*27*	*48-55*	*25-28*	*Storm*	*9.0*	*12.5*	*8*	*Very High*
11	*60*	*31*	*56-63*	*29-32*	*Violent storm*	*11.5*	*16.0*	*8*	*Very High*
12	*-*		*64+*	*33+*	*Hurricane*	*14+*	*-*	*9*	*Phenomenal*

$B_{.scl}$ – Beaufort wind scale

W_{sm} – Mean wind speed,

W_{slim} – Limits of wind speed,

D_{esT} – Wind descriptive terms,

P_{rbwH} – Probable wave height (in metres*),

Pr_{mwH} – Probable maximum wave height (in metres*),

S_s – Sea state,

S_{DT} – Sea descriptive terms.

Other sources of wave and wind data does exist, such as the British Maritime Technology (BMT) Global Wave Statistics and various wave statistics that represent average yearly wave environments for selected regions, in the form of so-called scatter diagrams such as the North Atlantic, etc. However, they are not directly useful for this research. The sea state used for the determination of $EEDI_{weather}$ and weather coefficient, f_w are determined at state Beaufort 6 with the mean wind speed given as 12.6m/s, mean wind direction as 0 degree (head wind), significant wave height as 3.0m, mean wave period as 6.7s and the mean wave direction as 0 degree (head sea); (Germanischer Lloyd (2013)).

5.2 Wave Effects

Ship speed estimation and performance trials are normally done in still water, however, it is already a known phenomenon that ocean going ships do meet sea conditions that does influence the resistance of the ship. This added resistance will not have a constant value in the ocean which is an irregular sea and will be varying approximately as the magnitude of the wave elevation and will lead to speed loss. There are other situations where extreme motions will prompt the master to reduce speed and avoid severe slamming, or propeller racing, etc. The inclusion of the wave forces is a relevant and forthright decision though, it is worth considering which components should be applied for instance, the first order wave forces are important for the prediction of the emergence of the propeller and the rudder, which will reduce the steering control effectiveness; or the integration of the mean second order wave forces which does subject the ship to a steady force component essential for ship manoeuvring capabilities such as turning circles, zigzag and spiral motion. Numerous phenomena are involved while the ship is manoeuvring in waves and the combination of them are very important and must be evaluated for some scenarios, types of ships, and zones of operability. Conversely, identifying phenomena which are relatively insignificant to the problem under consideration will indeed simplify the mathematical model and its application.

Ship motions in waves are principally affected by:

a. the magnitude of the exciting force,

b. Roll resonance and,

c. the magnitude of the damping effects

Due to angular dispersion, or spreading, the many wave systems will tend to come from different directions creating very confused seas, and the combined effect would generally show in the form of short-crestedness. Relatively lower magnitudes of following and quartering waves do not generally cause problems, however, severe following and quartering waves are always avoided due to lower freeboard at the stern and the associated risk of damage to the rudder, stern slamming and parametric roll. Also, in head sea condition in rough weather, there will be some critical speed or rate of encounter of a wave system of a particular wave length to

ship length ratio, usually approximately 1 to 1.25 that will produce a maximum pitching motion , in which circumstance powering conditions are mostly impaired due to loss of propulsive efficiency Gillmer (1982).

One of the requirements of this research work is to apply adverse environmental conditions that would be close to real life scenarios in which a vessel may operate. This would include combined wave and wind conditions. To make for simplicity, the waves will be made to come in one direction for each set of simulation, and for this research, the ship will turn into head sea (i.e. 180 degrees). Mean direction of the waves and wind may be considered to deviate by about 30°, which has been known to be more critical for steering and propulsion than aligned wave and wind directions through frequent practical observations. Hence,

a. Some wave amplitude formulation is described, and,

b. Additional forces and moments on the ship due to the wave effects used in the code is explained.

For a regular long crested wave, the wave height can be given by

$\zeta_w = \zeta_a \sin(\omega_e t - kx)$, where ζ_a is the wave amplitude

The wave spectrum recommended by the International Towing Tank Conference ITTC) is the 1978 recommendation for open ocean spectral formulation based on the Bretschneider Spectrum and is given by

$$S(\omega) = \frac{A}{\omega^5} exp\left(-\frac{B}{\omega^4}\right) in\ m^2/(rad./sec) \qquad 5\text{-}23$$

Where $S(\omega)$ is the spectral density, A and B are constants, ω is the angular velocity of the wave. And for known wave height and the characteristic period,

$$A = \frac{173 \times \zeta_{\frac{1}{3}}^2}{T_1^4}\left(\frac{m^2}{s^4}\right) \text{and } B = \frac{691}{T_1^4}\ (s^{-4}) \text{ and } T_1 = \frac{2\pi m_0}{m_1}$$

$$\zeta_{ij} = \sqrt{2 * S(\omega_i \theta_j) * \delta\omega * \delta v} \qquad 5\text{-}24$$

$$\zeta_i = \sum \zeta_{ij} \qquad 5\text{-}25$$

$$W_F(i) = \frac{\pi}{2} cos^2(\theta(i)) \qquad 5\text{-}26$$

Where, ζ_{ij}, is a component wave height of the irregular wave, ζ_i is the magnitude of the main wave height, $W_F(i)$ is the weighting function, $\zeta_{1/3}$ is the significant wave height.

The exciting forces considered here include the **Froude-Krylov forces** being the forces on the freely floating unrestrained ship due to undisturbed wave potential, and the corresponding **diffraction forces** from the hull surface, in which the disturbance that occurs as the ship changes the pressure field.

For a ship that is manoeuvring in waves, the effect of fluid memory is ignored in this research due to the assumption that the error for a low frequency manoeuvre will be relatively small. Hence it is assumed, that the hydrodynamic forces at any instant in time are dependent on the instantaneous forces, accelerations and velocities.

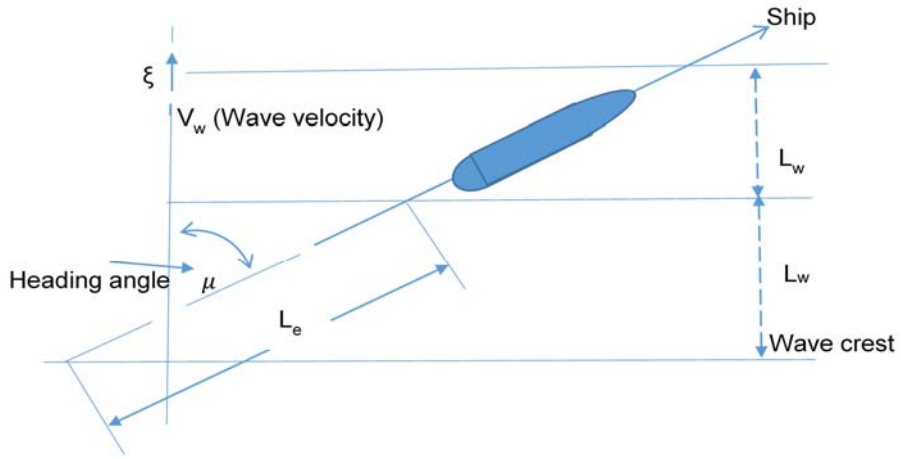

Figure 5-3 Vessel moving in a regular wave train Bhattacharyya (1978)

Effective wavelength $L_e = \frac{L_w}{cos\mu}$ *5-27*

Frequency of encounter $\omega_e = \omega_w(1 - \frac{\omega_w V}{g} cos\mu)$ *5-28*

Where L_w, is the wavelength (in metres), g is the gravitational acceleration, V, the ship speed (in meters per second), k, the wave number (in rad/metre) and, ω the circular frequency (in rad/s). In this work are related by the deep-water dispersion relationship

$$\omega^2 = gk \quad 5\text{-}29$$

Considering a ship moving in water with acceleration or deceleration, quantities of fluid moving around the hull creates additional hydrodynamic forces acting on the hull. This is for convenience of computation, imagined and treated as the hydrodynamic added mass which increases the total system mass and inertia moment. In order to establish the mathematical model for ship motion, the added components needed to be determined. For a specific ship, they can be obtained experimentally. However, for ship simulation, especially at the initial design stage it is necessary to estimate this by a known reliable theoretical approach such as the Equivalent ellipsoid and Strip theory methods, or by the use of charts experimentally determined by model tests.

The following models are used to compute the Froude-Krylov forces and moments given in Araki *et al.* (2013), and is nonlinear because the wave-induced forces and moments are functions of a longitudinal relative position of the ship to a wave trough.

$$X_{FK} = -\rho g \zeta_w k cos\chi . \sqrt{F_c^2 + F_s^2} + sin(k\xi_G + \varepsilon_F) \quad 5\text{-}30$$

$$Y_{FK} = \rho g \zeta_w k sin\chi . \sqrt{K_c^2 + K_s^2} + sin(k\xi_G + \varepsilon_F) \quad 5\text{-}31$$

$$K_{FK} = \rho g \zeta_w k sin\chi . \sqrt{F_c^2 + F_s^2} + sin(k\xi_G + \varepsilon_F) \quad 5\text{-}32$$

$$N_{FK} = \rho g \zeta_w k sin\chi . \sqrt{N_c^2 + N_s^2} + sin(k\xi_G + \varepsilon_F) \quad 5\text{-}33$$

where: $X_{FK}, Y_{FK}, K_{FK}, N_{FK}$, are the surge, sway, roll and yaw forces and moments from the Froude Krylov components of the Wave effects.

$$\varepsilon_F = tan^{-1}\left(\frac{F_s^2}{F_c^2}\right) \quad 5\text{-}34$$

$$\varepsilon_k = tan^{-1}\left(\frac{K_s^2}{F_c^2}\right) \quad 5\text{-}35$$

$$\varepsilon_N = -tan^{-1}\left(\frac{N_s^2}{N_c^2}\right) \quad 5\text{-}36$$

$$\left.\begin{matrix} F_c \\ F_s \end{matrix}\right\} = \int_{AP}^{FP} e^{-\frac{kd(x)}{2}} S(x) C_1 \left\{\begin{matrix} cos(kx\,cos\,\chi) \\ sin(kx\,cos\,\chi) \end{matrix}\right\} dx \quad 5\text{-}37$$

In the Froude-Krylov force and moments formulation, the subscripts ‘c’ in equations 5-30 to 5-37, is used to identify those components that has only cosine functions and ‘s’ identifies those that includes sine function.

$$\left.\begin{matrix} K_c \\ K_s \end{matrix}\right\} = \begin{bmatrix} K_{1C} - \frac{K_{2C}}{k^2} \\ K_{1S} - \frac{K_{2S}}{k^2} \end{bmatrix} \quad 5\text{-}38$$

$$\left.\begin{matrix} K_{1C} \\ K_{1s} \end{matrix}\right\} = \int_{AP}^{FP} \left\{\frac{B(x)}{2}\right\}^3 e^{-kd(x)} C_1 \left\{\begin{matrix} cos(kx\,cos\,\chi) \\ sin(kx\,cos\,\chi) \end{matrix}\right\} dx \quad 5\text{-}39$$

$$\left.\begin{matrix} K_{2C} \\ K_{2s} \end{matrix}\right\} = \int_{AP}^{FP} B(x)\,(1 - (1 - kd(x))e^{-kd(x)}) C_1 \left\{\begin{matrix} cos(kx\,cos\,\chi) \\ sin(kx\,cos\,\chi) \end{matrix}\right\} dx \quad 5\text{-}40$$

$$\left.\begin{matrix} N_C \\ N_S \end{matrix}\right\} = \int_{AP}^{FP} e^{-kd(x)}\, C_1 \left\{\begin{matrix} cos(kx\,cos\,\chi) \\ sin(kx\,cos\,\chi) \end{matrix}\right\} dx \quad 5\text{-}41$$

The diffraction forces and moments are computed from the following formulae:

$$Y_W^{Diff}(u,\xi'_G,\chi) = \zeta_w\omega\omega_e sin\chi(\int_{AE}^{FE}\rho\, S_y(x)e^{\frac{-kd(x)}{2}}\, sin(k(\xi'_G + xcos\chi))\, dx -$$

$$(\zeta_w\omega usin\chi\left[\rho S_y(x)e^{\frac{-kd(x)}{2}}\, cos\, k(\xi'_G + xcos\chi)\right]_{AE}^{FE} \qquad 5\text{-}42$$

$$K_W^{Diff}(u,\xi'_G,\chi) \qquad 5\text{-}43$$

$$= -\zeta_w\omega\omega_e sin\chi(\int_{AE}^{FE}\rho\,(S_y(x)l_n)e^{\frac{-kd(x)}{2}}\, sin(k(\xi'_G + xcos\chi))dx)$$

$$-(\zeta_w\omega usin\psi[\rho S_y(x)l_n(x)e^{\frac{-kd(x)}{2}}\, sin(k(\xi'_G + xcos\chi))]_{AE}^{FE})$$

$$N_W^{Diff}(u,\xi'_G,\chi)$$

$$= \zeta_w\omega\omega_e sin\chi * \int_{AE}^{FE}\rho\, S_y(x)(e^{\frac{-kd(x)}{2}})x\, sin(k(\xi'_G + xcos\chi))\, dx \qquad 5\text{-}44$$

$$-\ (\zeta_w\omega usin\chi[\rho S_y(x)(e^{\frac{-kd(x)}{2}})x\, cos(k(\xi'_G + xcos\chi))]_{AE}^{FE})$$

Where Y_W^{Diff}, N_w^{Diff} and K_w^{Diff} are the sway, yaw and roll diffraction forces and moments (due to diffraction element of the wave effect), and FE and AP does represent forward and aft perpendiculars respectively.

The wave diffraction for surge, X_{Diff}, is generally small due to the conventional strip theory assumption of ship slenderness and thus cannot be calculated due to such limitation and as such was therefore neglected.

For the wave forces and moments code, the following have been assumed:

1. The wave encounter angle is assumed to be the same as the wind encounter angle (and fixed to the initial wind angle) when simulating in order to determine the speed drop in wind and waves and differed by 30 degrees when simulating the turning motions – however, the encounter frequency will change as the ship's forward speed changes in the time domain loop.

2. The longitudinal position of centre of ship gravity from a wave trough ξ_G is assumed to be constant and computed in sections as the distance of each section from the ship's mid-ship section.

5.3 Further Seakeeping Performance

In section 5.2, the roll forces and moments were considered to be as a result of Froude-Krylov and diffraction effects. There is need to investgate the effect of reducing the power on heave and pitch motions as this will give an indication of the level of power where this responses can be high and cause such effects as propeller emergence which will lead to propeller racing and loss of efficiency, bow immersion, etc. Thus an engine will not be derated to run with such power as its maximum continuous rating when such a defined weather condition is to be encountered.

Since this research is considering a scenario where a significant wave height in excess of 2.5 metres, with wind and ocean current involved, there is the need to include the computation of these motions in this method. Some researchers have done some investigation on pitch and heave motions such as Tasai (1961), who applied the strip theory method to calculate the damping force and the added mass of ships, Jensen and Dogliani (1996) who investigated the wave-induced ship's hull vibration with non-linear effects due to changes in added mass, hydrodynamic damping and waterline breadth with sectional area immersion in waves, using non-linear, quadratic strip theory approach formulated in the frequency domain considering various ship headings. Majority of the authors that performed pitch and heave responses either carried it out for stationary vessels or in motion at ship's rated speed.

In this research, a frequency domain calculation of heave and pitch motion was applied, but this was done at different power levels, so that the effect of waves on the ship motion at reduced engine power can be investigated. It considers wave induced motion as being the only source of heave excitation. The exciting force for the heaving motion is determined by integrating the additional components of buoyancy due to the several waves simultaneously acting along length of the ship, and for a unit length (strip) of a ship's hull, the exciting force is given by:

$$F = v\rho \times g \times 2y \times \zeta \times dx \qquad 5\text{-}45$$

Where ζ is the ordinate of the effective wave profile, thus allowing for the heading (relative to the waves) for this case, given by:

$$\zeta = \zeta_a e^{-k'T_m} cos(k'x - \omega_e t) \qquad 5\text{-}46$$

$k' = 2\pi/L'_w = k\cos\mu$ is the effective wave number, $L'_w = L_w/\cos\mu$, is the effective wavelength, L_w being the absolute wavelength for an arbitrary relative angle μ, k, is the normal wave number, μ is the direction of the ship's heading in relation to the waves, and T_m is the mean depth of the effective wave from the still water free surface.

Based on the usual strip theory assumption that the ship is wall sided in the region of the load waterline, and that while the individual wave approaches the ship, the time, t, is recorded when the wave crest is at amidships. The exciting force for heaving is calculated on the assumption that the ship remains still as far the vertical motion is concerned and the waves pass slowly along the length of the ship; and the expression for the uncoupled heave exciting force for a surface profile, taken as the effective wave profile is given in Korvin-Kroukovsky and Jacobs (1957):

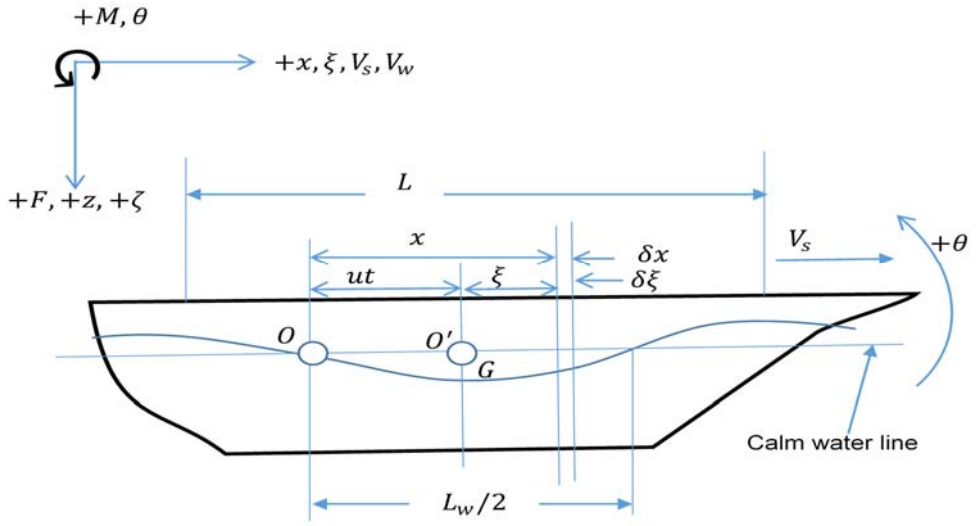

Figure 5-4 Coordinate System for Heave and Pitch Response

$$F = \left(2\rho g \zeta_a \int_{-L/2}^{L/2} y \cos k'x \, dx\right) \cos \omega_e t \qquad 5\text{-}47$$

where ω_e is the encounter frequency (i.e. the frequency of the radiated waves)

This equation is used as the surface profile assumption implies a greater exciting force which will make the design behaviour to be on the safer side. The equation of motion for uncoupled pitching of a ship can be written as

$$a\frac{d^2\theta}{dt^2} + b\frac{d\theta}{dt} + c\theta = M_0\, cos\omega_e t \qquad 5\text{-}48$$

where: $a\frac{d^2\theta}{dt^2}$ is the inertial moment such that, a, is the virtual mass and $\frac{d^2\theta}{dt^2}$ is the angular rigid body acceleration in pitching.

$b\frac{d\theta}{dt}$ is the damping moment, such that, b, is the damping moment coefficient and $\frac{d\theta}{dt}$ is its angular velocity.

$c\theta$ is the restoring moment, such that, c, is the restoring moment coefficient and θ, is the angular displacement in pitching.

$M_0\, cos\omega_e t$ is the exciting moment which varies with the encounter frequency, ω_e.

However, for this research, a coupled solution in the form of equation 5-49 is used for the computation of the motion, the following parameters defined here were applied.

The general equation for a coupled heave and pitch motion is given by Lewis (1989):

$$F(t) = (m + a_z)\ddot{z} + b\dot{z} + cz + d\ddot{\theta} + e\dot{\theta} + h\theta \text{ , where:} \qquad 5\text{-}49$$

$$m = \int m_n d\xi \qquad 5\text{-}50$$

$$a_z = \int a_n d\xi \qquad 5\text{-}51$$

$$b = \int b_n d\xi \qquad 5\text{-}52$$

$$c = \int c_n d\xi \qquad 5\text{-}53$$

$$d = -\int a_n d\xi \qquad 5\text{-}54$$

$$e = -\int b_n \xi d\xi + 2u\int a_n d\xi + u\int \frac{da_n}{d\xi}\xi d\xi = 1\int b_n \xi d\xi + u a_z \qquad 5\text{-}55$$

$$h = -\int c_n \xi d\xi + u\int b_n d\xi + u\int c_n\, \xi d\xi \qquad 5\text{-}56$$

m, is the total physical mass of the ship, a_z is the heave added mass, a_n is the section added mass in heave, b is the damping coefficient for heaving, $\ddot{\theta}$ is the pitch acceleration, $c = \int c_n d\xi$, the restoring force coefficient; d, e and h are pitch coupling terms.

The exciting heaving force $\mathrm{F(t)}$ considering a coupled effect is derived from

$F = F_1 cos\omega_e t + F_2 sin\omega_e t = F_0 cos(\omega_e t + \sigma)$ where:

$\mathrm{F_1}$ is the inertial reaction force of the fluid.

$\mathrm{F_2}$ is the hydrostatic restoring force.

$F_0 = F_1^2 + F_2^2$ *(Amplitude of the exciting force relative to the wave motion).* *5-57*

$\sigma = -\tan^{-1}(\frac{\mathrm{F_2}}{\mathrm{F_1}})$ *(phase lag of the exciting force relative to the wave motion)* *5-58*

$\mathrm{F_0}$ and σ are found from the complete forcing function obtained by:

$F_1 = \int \frac{dF_1}{dx} dx$ *and* $F_2 = \int \frac{dF_2}{dx} dx$ *5-59*

where

$\frac{dF_1}{dx} = \zeta_a e^{-kz}(-\omega_e^2 a_n + c_n)\, sin(k\xi) + \zeta_a e^{-kz}\left(-b_n - u\frac{da_n}{d\xi}\right) cos(k\xi)$ *and* *5-60*

$\frac{dF_2}{dx} = \zeta_a e^{-kz}(-\omega_e^2 a_n + c_n)\, cos(k\xi) - \zeta_a e^{-kz}\left(b_n - u\frac{da_n}{d\xi}\right) sin(k\xi)$ *5-61*

where z represents the mean draught of each section strip of the ship.

Also, the angular motion in pitch is written as;

$$M(t) = \left(I_{yy} + A_{yy}\right)\ddot{\theta} + B\dot{\theta} + C\theta + D\ddot{z} + E\dot{z} + Hz \quad 5\text{-}62$$

$$A_{yy} = \int a_n \xi^2 d\xi \quad 5\text{-}63$$

$$B = \int b_n \xi^2 d\xi \quad 5\text{-}64$$

$$C = \int c_n \xi^2 d\xi - uE \quad 5\text{-}65$$

$$D = d \text{ above} \quad 5\text{-}66$$

$$E = -\int b_n \xi d\xi - u a_z \text{ and} \quad 5\text{-}67$$

$$H = -\int c_n \xi d\xi \quad 5\text{-}68$$

$$M = M_0 \cos(\omega_e t + \tau) = \int \frac{dF}{d\xi} d\xi \quad 5\text{-}69$$

where M_0 is the amplitude of the exciting moment, and τ is the phase lag of the exciting moment relative to the wave motion and given by:

$$M_0 = M_1^2 + M_2^2 \text{ and } \sigma = -tan^{-1}(\frac{M_2}{M_1}) \quad 5\text{-}70$$

$$M_1 = \int \frac{dM_1}{dx} dx \text{ and } M_2 = \int \frac{dM_2}{dx} dx \quad 5\text{-}71$$

Where M_1 is the pitching moment due to inertial reaction force of the fluid (F_1) and M_2 is the hydrostatic restoring force due to the hydrostatic restoring force (F_2).

Due to the fact that the solutions to the given equations of motion include both amplitudes and phase lags, they are best written in complex form as they can deal with the negative roots. Thus considering forcing functions such as:

$$\bar{F} = F_0 e^{-i\sigma} \quad 5\text{-}72$$

$$\bar{M} = M_0 e^{-i\sigma} \quad 5\text{-}73$$

where $\bar{\mathrm{F}}$ and $\bar{\mathrm{M}}$ are the forcing functions in complex form, of which $\mathrm{P}, \mathrm{Q}, \mathrm{S}, \mathrm{R}$ are given by:

From equation 5-49,

$$P = (m + a_z)\omega^2 + iB\omega + c \qquad 5\text{-}74$$

$$Q = -d\omega^2 + ie\omega + h \text{ and} \qquad 5\text{-}75$$

and from equation 5-62,

$$S = -\left(I_{yy} + A_{yy}\right)\omega^2 + iB\omega + c \qquad 5\text{-}76$$

$$R = -D\omega^2 + iE\omega + H \qquad 5\text{-}77$$

From which the solution for the complex pitch and heave motions were obtained as:

$$\bar{z} = \frac{\bar{M}Q - \bar{F}S}{QR - PS} \qquad 5\text{-}78$$

$$\bar{\theta} = \frac{\bar{F}R - \bar{M}P}{QR - PS} \qquad 5\text{-}79$$

Thus the final solution to the motions are given by

$$\bar{z} = z_a(\cos\delta + i\sin\delta) \qquad 5\text{-}80$$

$$\bar{\theta} = \theta_a(\cos\varepsilon + i\sin\varepsilon) \qquad 5\text{-}81$$

The computation was repeated for different power levels and the resulting heave and pitch responses represented in a graphical form in Figure 6-23.

The tuning factor is the ratio of the frequency of encounter to the natural frequency which is given by:

$$\Lambda = \frac{\omega_e}{\omega_z}, \qquad 5\text{-}82$$

ω_z the natural frequency of the heaving motion.

The phase angle between the wave motion and heaving motion is given by

$$\varepsilon = \varepsilon_1 + \varepsilon_2 \qquad 5\text{-}83$$

where ε_1 is the phase angle between the wave motion and the exciting force caused by the waves, and:

$$\varepsilon_2 = \frac{2\kappa\Lambda}{1-\Lambda^2} \qquad 5\text{-}84$$

is the phase angle between the exciting force and the heaving force.

The relative heave motion of the ship with respect to the wave is thus given by:

$$s = \zeta_a[cos\ \omega_e t - \frac{z_a}{\zeta_a} cos(\omega_e t - \varepsilon)] \qquad 5\text{-}85$$

The magnitude of the maximum resultant relative heave motion of the ship with respect to the wave surface occurs when

$$-sin\omega_e t + \frac{z_a}{\zeta_a}(sin(\omega_e t)\ cos\,\varepsilon - cos(\omega_e t)\ sin\,\varepsilon = 0 \qquad 5\text{-}86$$

Experiments conducted by Gerritsma (1957) showed that the hydrodynamic added mass for the heave motion is of the order of magnitude as that of the mass of the vessel, and the larger the Block coefficient, the more the added mass. Thus, where the heave added mass is not known, an acceptable estimate can be made.

The heave natural frequency can be obtained by the expression

$$\omega_3 = \sqrt{(\frac{\rho g A_{wp}}{M_s + m_{a3}})}\ Rad/sec$$

Where A_{wp} is the ship's water-plane area, M_s is the mass of the ship and m_{a3} is the heave added mass.

5.4 The Influence of Ocean Current

Current forces basically, acts on the underwater part of the hull. The parameters being utilise to compute these forces are normally obtained from calm water resistance assumption, i.e. the current effect on the ship in a water without waves or wind. In reality, various independent phenomena are responsible for the occurrence of current which includes the ocean circulation system, resulting in a steady current, the cyclical change in lunar and solar gravity, causing tidal currents, wind and differences in density of the water etc. The effect of current and strong wind does pose a very specific manoeuvring problem especially for ships with large windage

area, such as, container ships, RoRo vessels, car carriers and also for bulk carriers because the speed is limited due to navigational restrictions. The Kuroshio is a north-flowing ocean current on the west side of the North Pacific Ocean that runs from South to North off the coast of Japan and can reach a speed of 4-5 knots thus practically, a ship heading south in the current with a command speed of 15 knots it is a common experience to have the propulsion plant producing shaft horsepower normally required for speeds of 18-19 knots. Also on the other hand, when heading North in favour of the current, there is a negative slip resulting in speed increase of 1 – 3 knots for a set horsepower. Any of these conditions if encountered in an area with navigational restriction could affect the manoeuvring performance of a ship if the prime mover and control devices are not properly considered during any planned modification.

In waters where manoeuvrability at reduced speed is essential due to navigational restrictions, (e.g. during approaching or departure ports, or in areas where reduced water depths with high current speeds) through the water and thus, rudder efficiency is reduced. Low-speed manoeuvrability criteria may lead to enhanced requirements for steering devices.

The variation in the velocity of current is very slow, and thus current loading is being computed as a steady state phenomenon. Considering Figure 4-6 and the expression for the current velocities given in Fossen (1994), the relative surge and sway velocities between the ship and the current are given by :

$$u_c = V_s \cos\beta + V_{curr}\cos(\psi_c - \psi) \quad 5\text{-}87$$

$$v_c = -V_s \sin\beta - V_{curr}\cos(\psi_c - \psi) \quad 5\text{-}88$$

V_{curr} and ψ_c are the current velocity and direction, respectively.

The velocities of the Ship Relative to the currents are given by

$$u_{ship} = u + V_{curr}cos(\psi - \psi_c) \quad 5\text{-}89$$

$$v_{ship} = v + V_{curr}\, sin(\psi - \psi_c) \quad 5\text{-}90$$

And the forces;

$$X_{current} = 0.5 \times R_{wx} \times \rho_{water} \times A_T u_{current}^2 \quad 5\text{-}91$$

$$Y_{current} = 0.5 \times R_{wy} \times \rho_{water} A_L v_{current}^2 \quad 5\text{-}92$$

Where:

$X_{current}$ and $Y_{current}$ are the resultant longitudinal and lateral current forces respectively.

R_{wx} and R_{wx} , are the longitudinal and lateral current resistant coefficients, ρ_{water} is the water density derived from plots in Fossen (2011) in Figure 5-5.

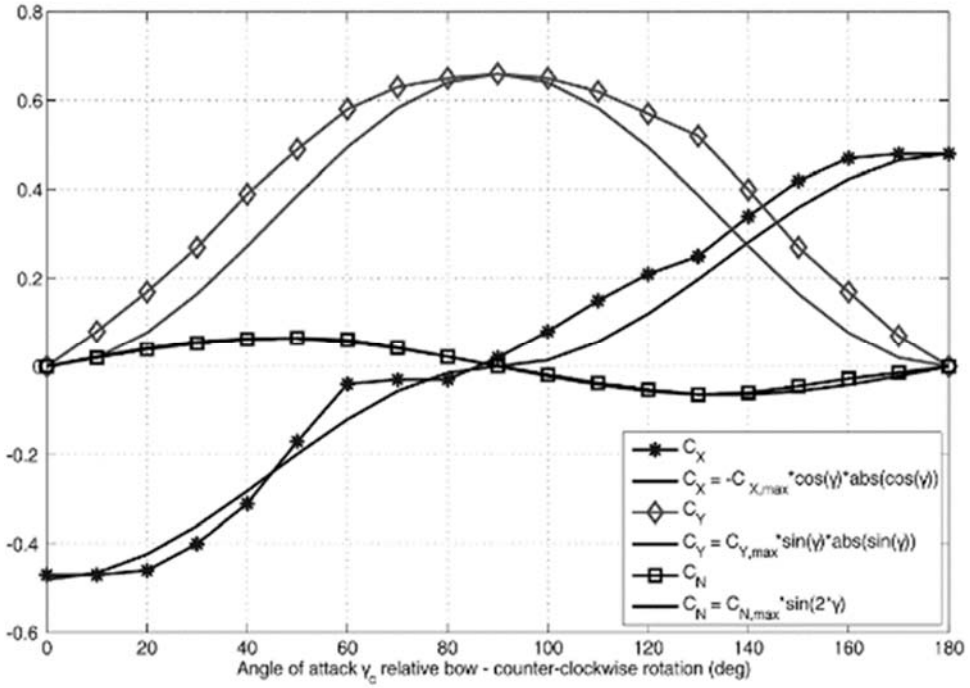

Figure 5-5 Experimental Current coefficient for a tanker (Fossen (2011)).

A_T, is the submerged transverse current projected area = $A_T = B \times d/2$.

A_L, is the submerged lateral current projected area =$A_L = L \times d/2$

Chapter 6 Analyses and Discussion

Manoeuvring is usually an operation which is carried out when a vessel entering or exiting coastal waters of a country, in the process, it may cross several ships on its route, while proceeding towards or departing from a berth or jetty of a port. The operation is also carried out while crossing canals and traffic zones. Most incidence of collisions and grounding of ships are reported during manoeuvring of the vessels in restricted waters (either traffic, channel or depth restriction), and hence the manoeuvring operation is considered most crucial time a ship faces in her voyage, both from ship's and seafarer's perspective. The design of the ship's hull, its propulsion, rudders and control systems must be matched to ensure that they meet some minimum standards so that full control of the ship is achieved and thus reducing the chances of such incidences substantially.

During manoeuvring, the full power (electrical and mechanical) must be available such that can be put to use to pull or push the ship away from danger. Though in most cases, tug boats are used to assist the vessel during manoeuvring, however, there are limitations. There are some weather conditions in which the tug boat cannot approach the ship to secure her lines, thus, a ship must have some manoeuvring characteristics with its hull, main and auxiliary machineries designed and built such that it is able to start, stop and steer safely. To possess these capabilities, the design of the hull, propulsion system, rudder and associated control systems must exceed certain capacity and when matched must ensure stable and reliable functionality.

It is very important to test for these capabilities at the design stage to avoid incidences that may occur when the ship is subjected to some normally encountered adverse environmental conditions. On the flip side, it is also very important to reduce carbon-dioxide emissions by improved efficiency at the design stage, which if to be achieved by a reduction in installed power may adversely affect the ship's manoeuvring capability. The tests to predict the capabilities of the ship at the design stage are usually achieved through detailed captive or free running tests in the laboratory or designated basins, and or by use of Computational Fluid Dynamics techniques. These techniques are relatively expensive and time consuming. It will be beneficial if limits can be set at the design stage using a much cheaper program, with

acceptable accuracy, which will reduce the cost of detailed testing, and thus, mean reduced cost to ship owner, builder, Classification Society, etc.

In order to make for this option that can give acceptably accurate results, much faster and less expensive, EShipman was developed. The program was initially tested using the parameters of a ship with known data, and manoeuvring characteristics (as in Figure 6-1 and Figure 6-2) in the calm weather condition so that comparisons could be made to see if its results do agreed with the experimental result of the parent authors.

6.1 Validation and Discussion

Eshipman was principally meant for application to new ship at its early design stage, at which most of the significant hull details are known with reasonable confidence. It is programmed with equations which considered some inevitable simplifications, however, taking relevant physics into account, made to be as accurate as practicable within the scope of the available technological resources, robust and backward compatible, inexpensive and can be applicable and easily affordable to any shipyard and administration.

The manoeuvring trial motion algorithm was applied for the Turning Circle tests and for the Zigzag trial while the ship was under full power. The predicted trajectories are in the earth fixed reference frame. The plots given in Figure 6-1 and Figure 6-4 demonstrates that the program results in this condition showed some agreement of the calm water manoeuvring performance of code, the differences as seen in Table 6-1 might be due to some of the formulated parameters and assumptions applied when developing EShipman. For the Calm Water scenario, the ship is subjected to the usual manoeuvring trials such as the Zigzag Manoeuvre and the Turning Circle Manoeuvre.

For this work, the Metacentric heights (GM) used for the calm water simulation are 0.3m and 0.5m in order to compare with the result of Son and Nomoto.

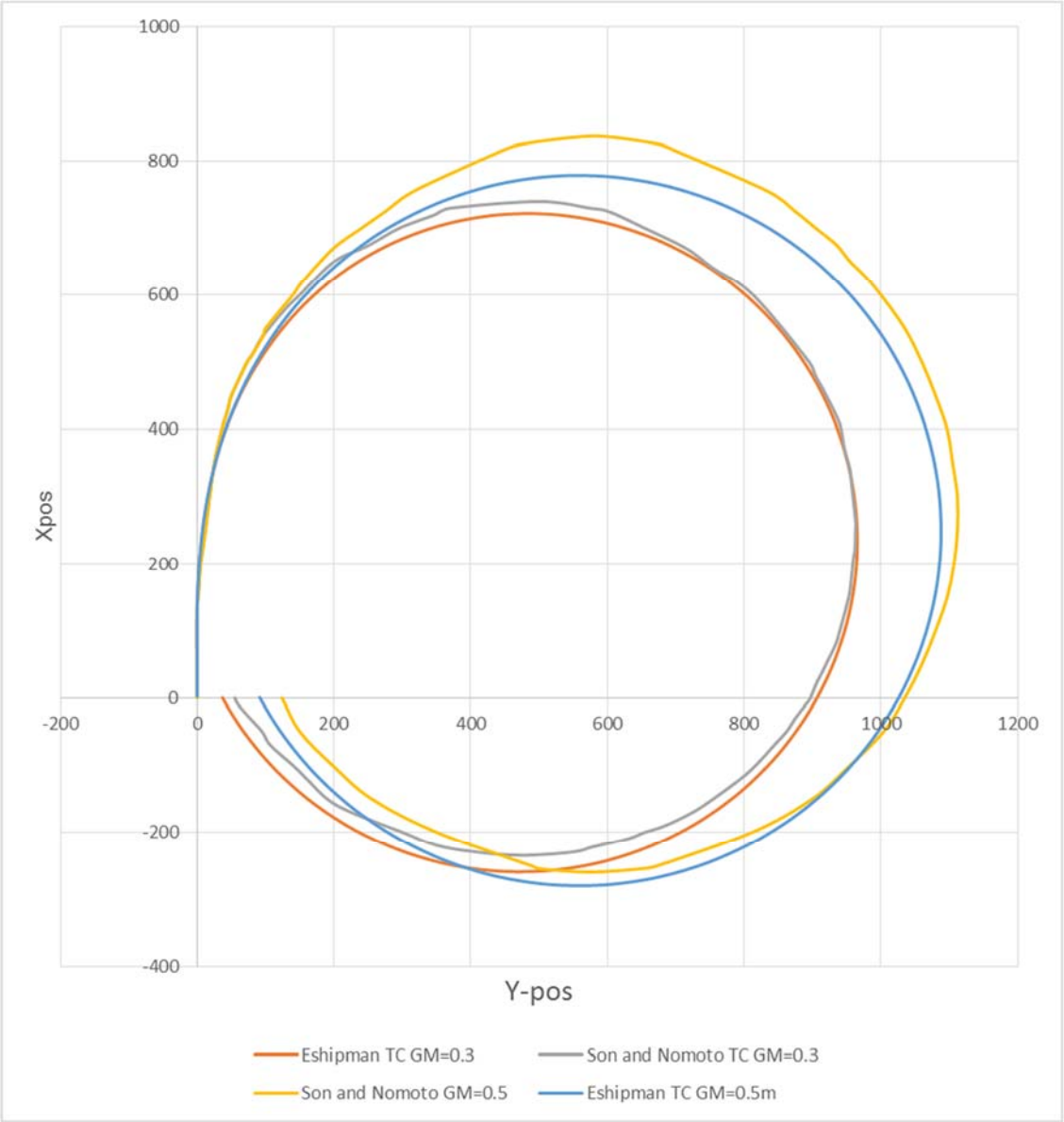

Figure 6-1 Calm water turning circle plot at 100% MCR (GM = 0.3m, rudder angle=15 degrees) (Son and Nomoto (1981), and Eshipman).

Table 6-1 Tactical Diameter Comparison for Figure 6-1.

	T/D from EShipman	T/D from Son and Nomoto
GM=0.3 m	937m	945m
GM=0.5 m	1097	1080

As can be seen from Figure 6-1, the simulation was carried out and rudder command was given at the origin. This implied that it will take some seconds to reach the set angle of 15 degrees, thus the ship did some bit of straight line motion before it began

to turn. The *X-pos* is the Distance travelled by the vessel in the surge direction. *Y-pos* is the distance travelled by the vessel in the sway direction of the ship. Son and Nomoto's plot was meant to verify the yaw-sway-roll-rudder coupling due to the turning of the rudder of a high speed vessel, thus the turning circle motion was done with the rudder at 15 degrees, with the ship at its maximum speed (24.15 knots). For the purpose of validating the functionality of Eshipman, some turning circle motions were carried out under identical conditions and as can be seen, the plot from Eshipman shows good agreement with the Son and Nomoto's motion. The slight difference being probably due to the some empirical formulations and reasonable assumptions made in the absence of accurate data.

However, it is to be noted that the tactical diameters of both are above 5.0 times the ship's length, which is outside the range of 4 to 5 times ship's length recommended by the IMO for calm water manoeuvring. As was earlier mentioned, this is because, Son and Nomoto applied a rudder angle of 15 degrees which is lower than the recommended maximum angle. Thus, another motion was executed with Eshipman with the rudder at 35 degrees while on full load as can be seen in Figure 6-2 below.

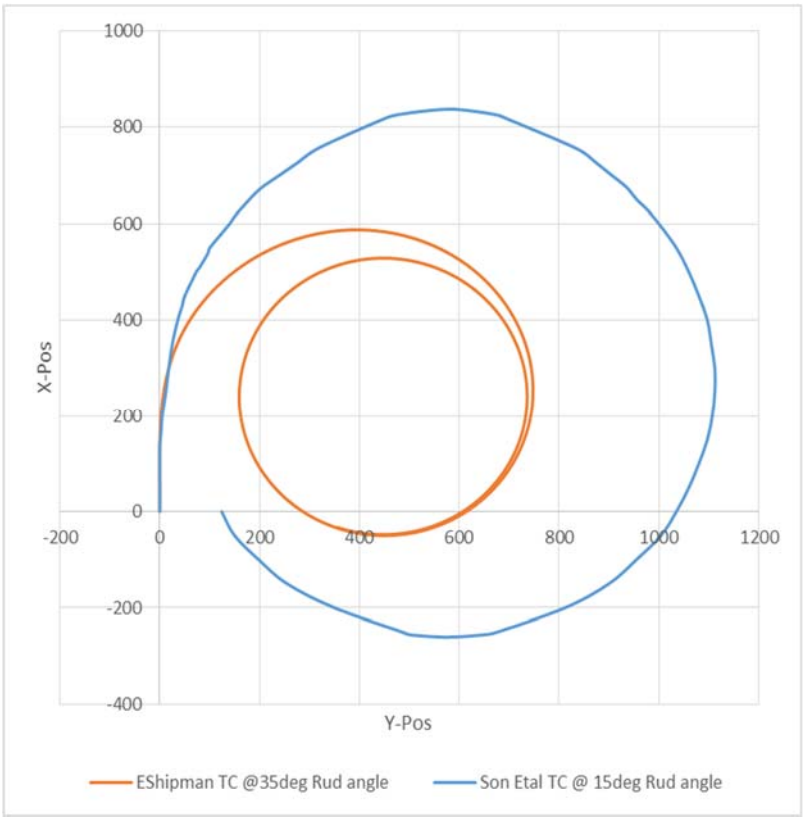

Figure 6-2 Calm water turning circle plot (GM = 0.3m), Rudder angle=35deg for Eshipman and 15deg for Son and Nomoto.

EShipman was used to compute a turning circle motion to demonstrate one of the ship's manoeuvring characteristics as in Figure 6-2, the tactical diameter produced by this test program is about 4.21 times the length of the ship and advance of 3.3 times the Ship's length, when the rudder angle at 35 degrees, which is below the upper limit of the IMO recommended range, ITTC (2017), ABS (2006).

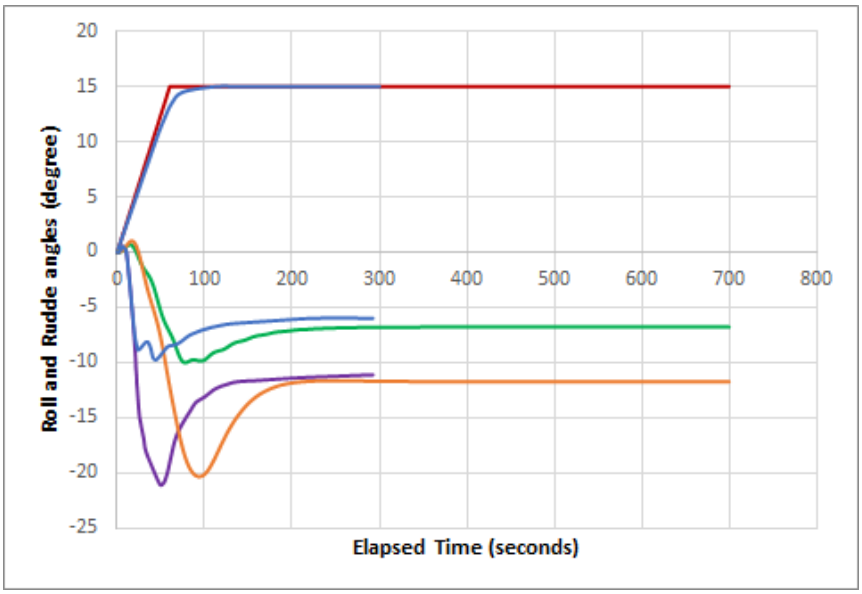

Figure 6-3 Roll angles from Eshipman, rudder rate of 3 degrees per second

The plots in Figure 6-3 were used to demonstrate the functionality of Eshipman by comparing the roll angle obtained from the experimental work of Son and Nomoto for a ship making a turning circle motion with the rudder turned to an angle of 15 degrees. It was noted that the peak roll is higher for the computed result by 1 degree for the condition with GM=0.5 but virtually equal for GM=0.3. However, for the rest of the motion, at the steady angles difference of about 1 degrees with the computed value higher. The four degrees of freedom model used for developing this program is said to have higher accuracy at roll motions less than 10 degrees. Thus the roll motions that at 10 degrees or more tend to produce misleading higher figures.

The Zigzag and the 'Turning into head wind and waves' manoeuvring was shown here just to demonstrate the presence of its algorithm in the test program, the turning circle motion was used in the subsequent discussion of this thesis. As was earlier explained, the zig-zag manoeuvre was performed by reversing the rudder alternately by a rudder angle to either side. The rudder angle was held constant until the heading was changed to 20 degrees, then the rudder is reversed, and repeated until

a total of 5 rudder steps have been completed. For the container Ship, operating at full power in calm water condition, the zigzag motion plot is as shown in (Figure 6-4).

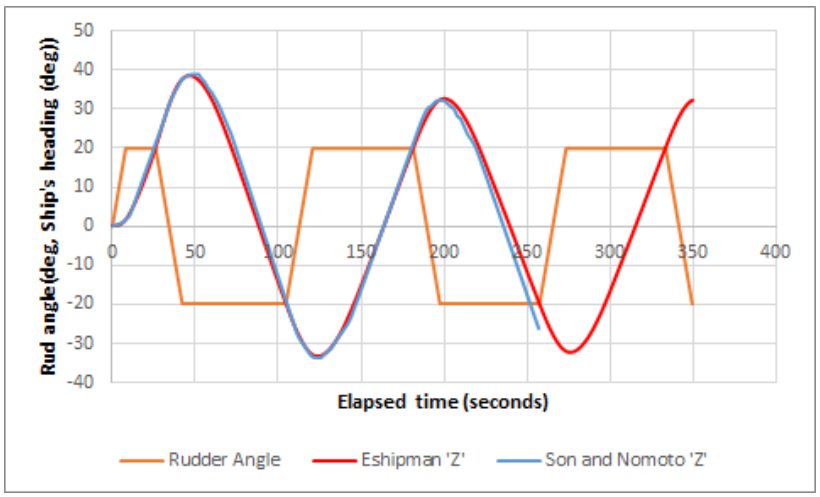

Figure 6-4 calm water zig-zag plot at 100% MCR, GM=0.3m, Vo=24.15knots form Eshipman & Son and Nomoto (1981)

Table 6-2 Comparison of the Essential parameters from Figure 6-4

Parameter	*Son and Nomoto*	*Eshipman*
Time to check yaw	*25*	*24.5 secs*
the initial turning time	*26*	*26*
First overshoot angle	*18.7*	*18.7°*
Second overshoot angle	*-13.5*	*-13.5*

Table 6-2 shows the essential parameters extracted from a zigzag motion for the purpose of analysis. These indices show very little error between both plots for the first four ‘execute’ of rudder, though the error starts widening for the fifth ‘execute’, the performance is good enough to make reasonable judgement and this demonstrates that the program for the zigzag manoeuvring motion, including the rudder algorithms do function satisfactorily.

For this vessel moving at full power, this 20/20 zigzag motion plot, the elapsed time to reach the first overshoot was 49 seconds and a 17.0 degree overshoot.

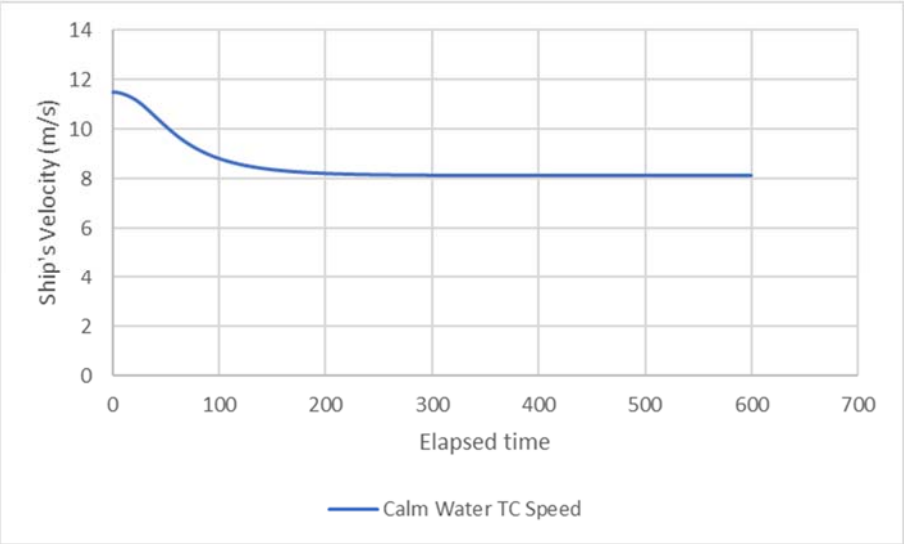

Figure 6-5 ship speed vs time characteristics while performing a turning circle motion in calm weather

Figure 6-5, shows the ship speed variation with time while executing a turning circle manoeuvre. With the ship in calm water, the speed dropped to about 8.1 m/s (15.74 knots), where it becomes asymptotic. Thus it does not approach the low safe limit of 4 knots.

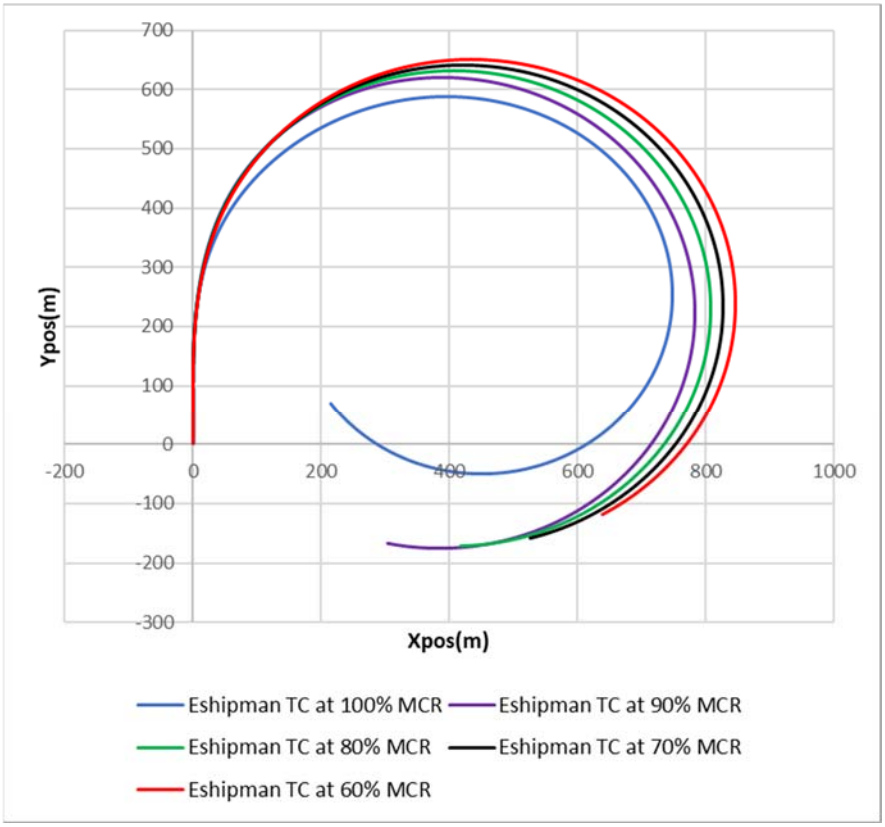

Figure 6-6 EShipman Simulation of Turning Circle motion of vessel in calm weather at designated MCR percentages.

Figure 6-6 demonstrates that in calm weather condition, EShipman is able to perform a turning circle manoeuvring in which the turning circle diameter at 60% MCR is 762metres being 4.77 times the ship's length between perpendiculars (L_{pp}) length and gives one indication that by derating the install power to 60%, the ship may still manoeuvre safely in calm weather. The minimum tactical diameter is seen to be 738m (4.21 Lpp) at the 100% MCR. Though the turning circle diameter is not the best indicator of the rudder performance, this plot gives an indication of how the rudder performance of a ship reduces with reduction in speed. Should the engine deration be as in condition '**b**' in chapter 4 (section 4.6), where a new ship of same ship form is to be built with the new reduced engine size, then the turning circle diameter could be improved by slightly increasing the capacity of the rudder and its machinery.

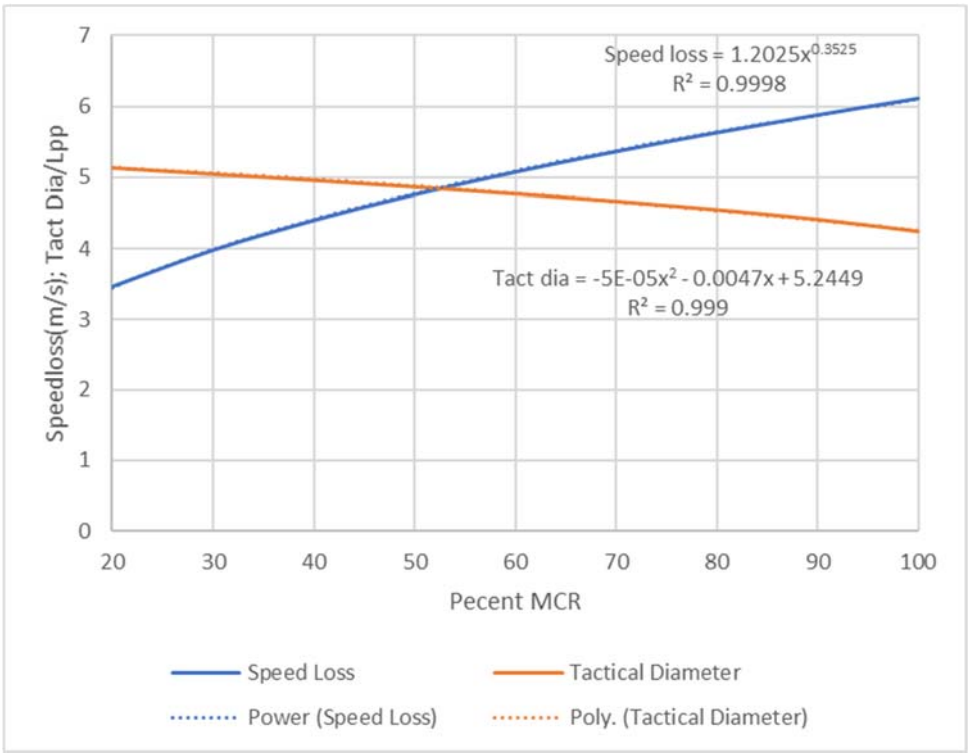

Figure 6-7 Speed Loss and Tactical diameter during turning circle manoeuvring in calm water at designated power percentages.

Figure 6-7, shows a relationship between percentage of MCR vs speed loss and tactical diameter, (in the equations shown in the plots, x-axis, represents the percentage of MCR) while the ship makes a turning circle motion, with the rudder turned to 35 degrees. Here, the tactical diameter, refers to the ratio of the actual tactical diameter to the length between perpendiculars of the ship. A high tactical diameter of the trajectory (of 5.2) occurred at the 20% power level which is above the

IMO recommended value of 5 times ship's length, thus as the power is reduced, the tactical diameter increases. Also on the other consideration, the speed loss does reduce as the MCR power is reduced.

Eshipman was used to demonstrate that increasing the rudder area by 9% of its value does reduce the turning circle diameter of this ship derated to 65% of its MCR to the turning circle diameter value when simulated at 100% MCR. There are other considerations that will put into perspective, however, this finding will give a lead towards making appropriate decisions at an early stage of the design.

6.1.1 Added Wind Effect Due to Roll

Majority of formulations that are meant to address wind loading on a floating ship or offshore structure, only applied the effects of a change in direction or angle of attack, but treats the windage area as constant, and does not take into consideration the fluctuating windage area as the ship rolls or pitches. The simulation of the vessel to perform a turning circle motion with the rudder at 35 degree angle showed a continuous roll angle of 10 degrees after some peaks. Now, for this roll angle, it implies an exposed additional lateral area of $391.8\ \mathrm{m}^2$ and the original calculated windage area on the assumption of a constant draft, was $738.5\ \mathrm{m}^2$. Thus there is a 53% increase in lateral windage area on one side of the ship, and if this happens to be the windward side, it will result in an overturning moment which may lead to a capsize in a combined wind and wave effect. Thus a correction formula was proposed in this research which take into consideration, this effect, when modelling the motion of a ship in adverse weather condition and results does show an increased roll angle and some drift motion. As was earlier mentioned in section 5.1, the effect of a change windage area due to roll motion as described in equations 5-8 and 5-9 were applied in the derivation of the instantaneous windage area in EShipman to test its influence when run in wind only. In one instance, the draft was assumed to be constant and in the other instance the modified equation (5-10) was applied. With a wind speed of 19m/s approaching at 270 degrees, a turning circle motion simulation was made and the roll and turning circle plots are shown in Figure 6-8 and Figure 6-9.

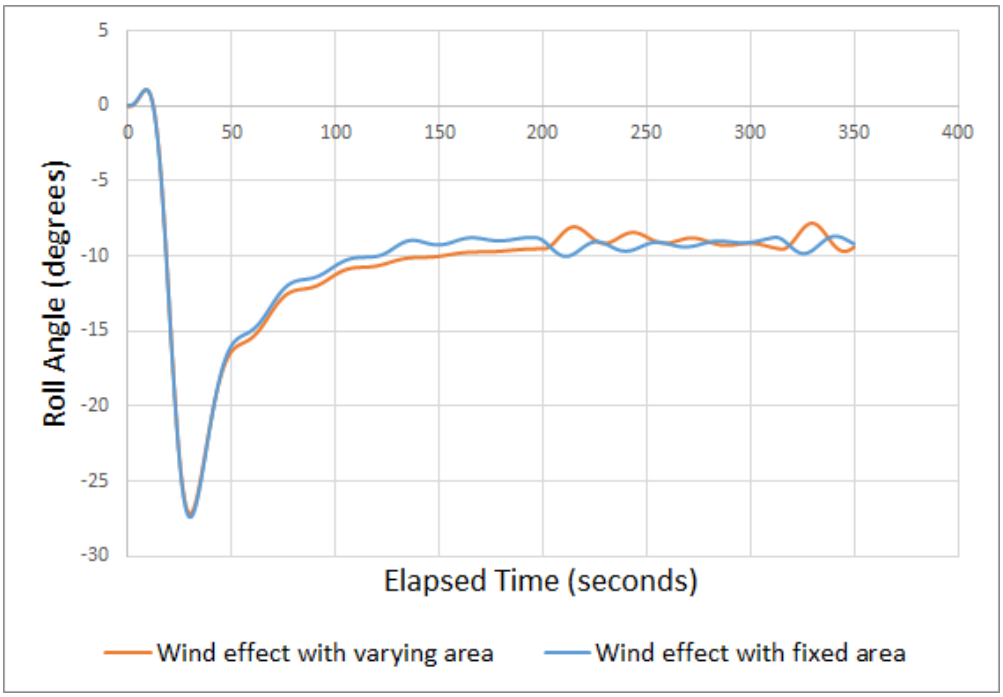

Figure 6-8 Roll Angle vs Time With, and Without the effect of changing windage area due to roll motion

From Figure 6-8, The peak roll angle increased by 1 degree and then started fluctuating, when the change in area is considered with a 35 degrees rudder turn at full load with the wind only action. The vessel was drifted inwards with a turning circle diameter difference of about 4.5meters, while making a turning circle test (Figure 6-9)), as seen, the turning circle diameter difference is small in relation to the length of the ship but this effect needs to be taken into consideration in a proper performance simulation.

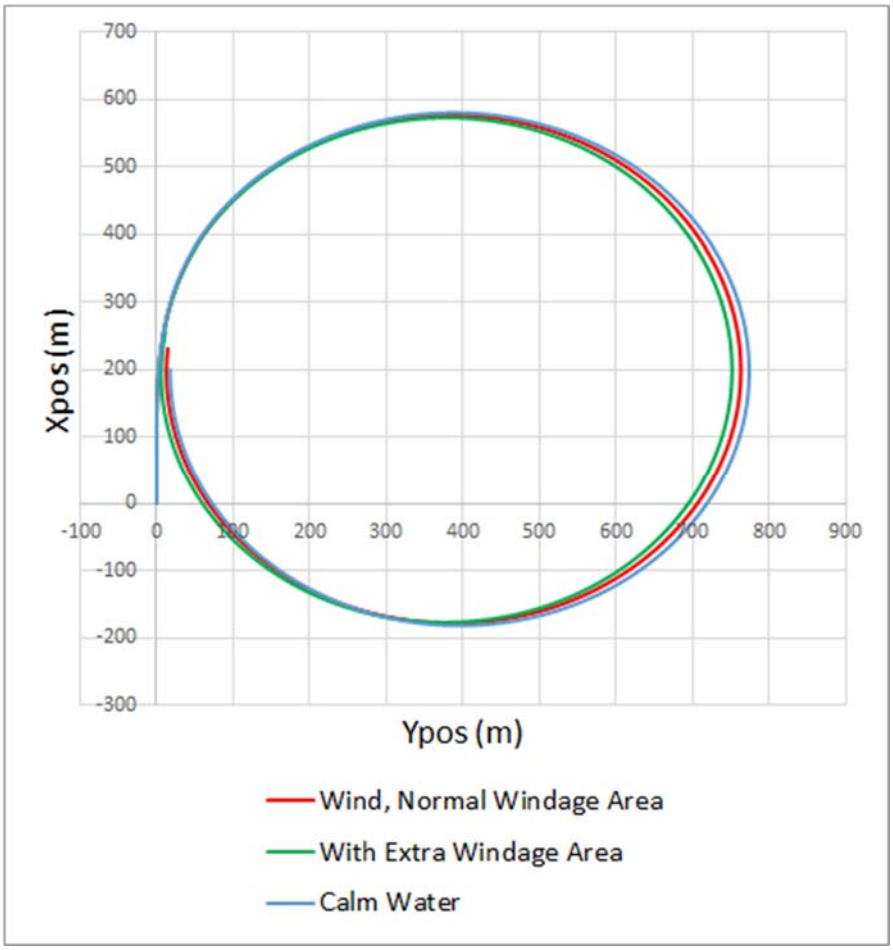

Figure 6-9 Wind-Only (@ 270degress) Effect with, and without varying Lateral Area due to Roll Motion

The increased windage area on the windward side would increase the overturning moment produced by the wind loading. This effect as seen from this simulation looks small, however it may make the vessel more susceptible to capsizing especially when combined with wave effects as mentioned in Paroka *et al.* (2006) and Taylan (2003).

6.1.2 Combined Wind, Wave and Current Effects.

The plots in Figure 6-10, does indicate the turning circle motion of the ship when the environmental forces and moments are combined.

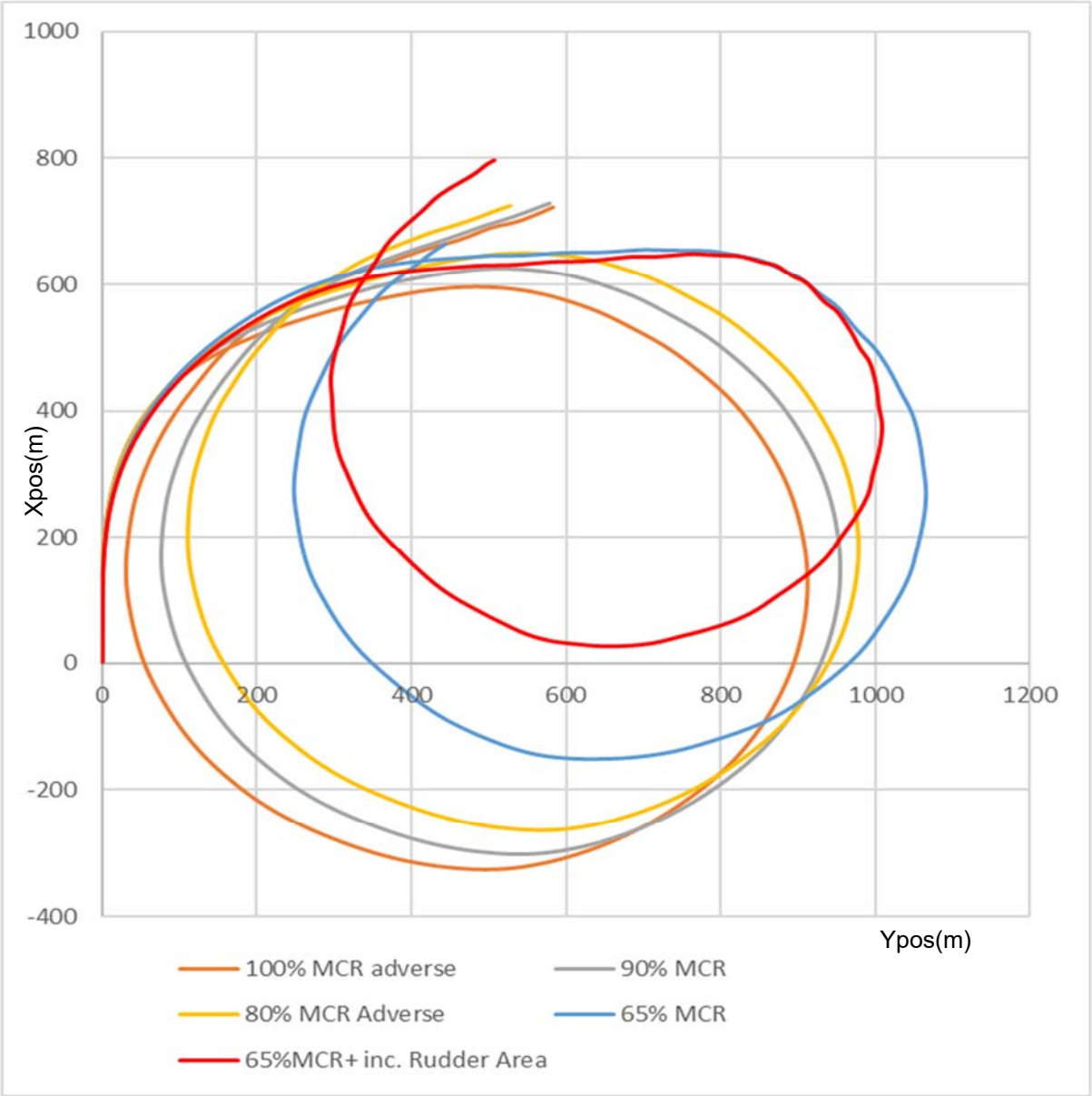

Figure 6-10 Vessel under the influence of wave wind and current, with wave approaching at an initial angle of 20 degrees (clockwise, following) and Engine MCR as indicated. (Significant wave height of 5.5m, wind velocity of 17m/s, current of 3m/s).

The above plots in Figure 6-10 is the trajectory of the ship as it executes a turning motion in adverse weather with a significant wave height of 5.5m, wind velocity of 17m/s, current of 3m/s. The tactical diameters with normal simulation in adverse weather are: 906m at 100% MCR, 948m at 90%MCR, 972 at 80% MCR and 1059 at 65%MCR. It demonstrates how the reduction in MCR of the engine to the indicated percentages, affects the turning circle manoeuvring characteristics of the ship. The influence of the ocean currents affects the shape of the curve as the ship eventually turns into a position that the current, starts adding to and increasing its speed thus the normal oval shape of the turning circle motion in calm weather is not achieved. It

could be seen that, the vessel drifted further as the engine power is reduced such that it will take much longer for a full circle to be executed. Also, drifting of the vessel due to the environmental loading was initially less due to the effectiveness of the rudder at higher speeds, the rudder was able to take control eventually. At reduced power, the rudder effectiveness is diminishing, thus response time is substantially reduced. This is not a desirable situation, especially in harbour environment, where such a response will lead to accidents as the ship could go on uncontrollably.

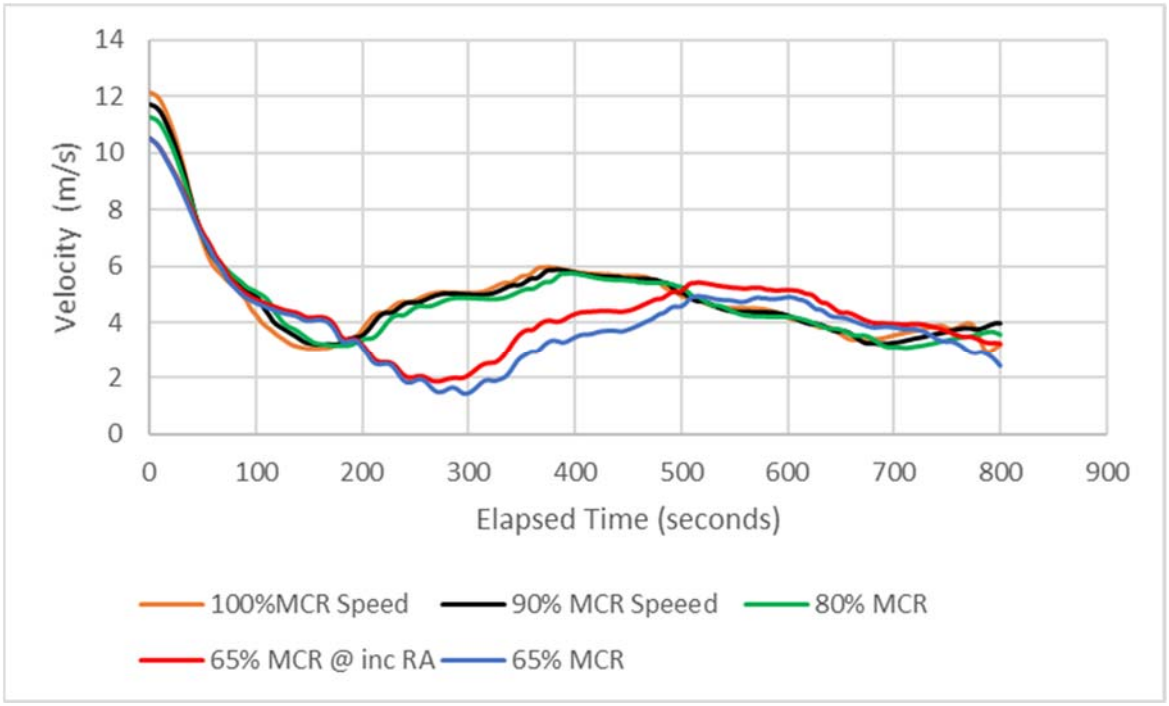

Figure 6-11 Velocity vs Time in Adverse Weather condition during the turning circle.

In Figure 6-11, the charts demonstrate the velocities of the ship at different power. It can be seen that at 65% of the Engine maximum continuous rating, the velocity drops slightly below 2m/s (3.89 knots) which is just below the safe manoeuvring speed of 4 knots mentioned above. By applying the 9% increase in rudder area, the turning circle diameter for the 65% MCR simulation reduces to 1003 from 1059 which is an improvement in the ship's control response. Also the minimum velocity increased from 1.46 for a normal simulation at 65%MCR to 1.9m/s with a 9% increased rudder area, which is an indication of improved performance which will result in reduced emissions. Though an increased rudder area does imply an increased mass of steering gear equipment, that increase will be more than compensated by the reduced size of the main engine and the auxiliary machinery, and there may be more room for cargo which will further improve the EEDI.

In carrying out an analysis of a new ship of same class, the builder who analyses this effect, will straight away, know that under the set environmental conditions (significant wave height of 5.5m, wind velocity of 30knots, current of 3m/s), taking a decision concerning reducing the engine power meant that it must not go down to 65% of its present capacity for it to be able to sustain safe manoeuvring. This does not mean that the vessel shall be designed with adverse weather conditions (with a consequence of an overpowered ship), thus the manoeuvring indices are not expected to meet the IMO standards in these conditions, thus in this research, conditions that are practically known to cause problems such as excessive reduction in speed which additionally reduces rudder efficiency, and excessive roll motion was used as criterion for safety.

It should be noted that the ship's speed increased slightly at some point. This is due to the strong current that increased the speed during the turning circle motion at some points when the direction of attack favours the forward motion of the ship. Also, as mentioned earlier, within an area with restriction for speed, the effect of ocean current and wind may predominate, at the manoeuvring speed of the ship (3.5 to 4.5 knots), the manoeuvrability of the rudder is insufficient due to reduced inflow velocity of the water arriving at the rudder. In that case, the rudder may not be able to restore the vessel to safe manoeuvring levels this is demonstrated below. In practice, an alarm sounds once the ship's speed drops below five knots and the auto-pilot system changes over to manual, or is manually changed over, and the ship is manually controlled. This mostly happens during manoeuvring in restricted waters, and in extremely poor weather conditions.

The plots in Figure 6-12 (Irimagha *et al.* (2019)), compares the roll angle obtained from the experimental work of Son and Nomoto for a ship making a turning circle motion with the rudder turned to an angle of 15 degrees in calm weather.

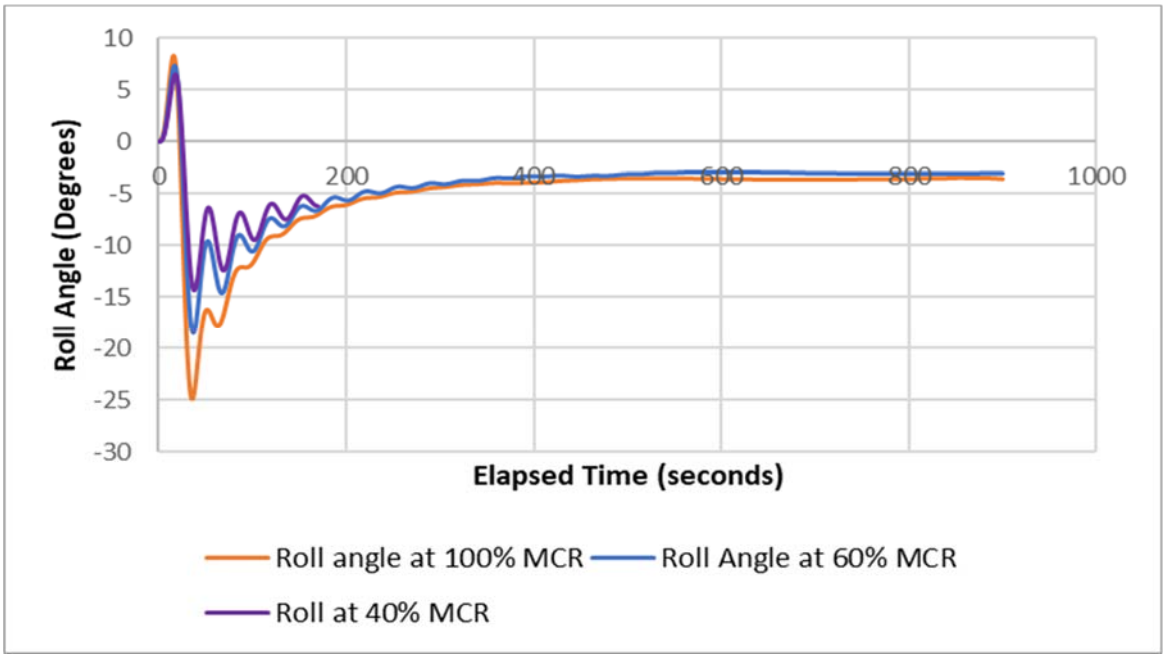

Figure 6-12 Roll Angle vs. Elapsed Time. GM=0.3m, $H_{\frac{1}{3}}$=3.0, wind velocity of 24knots, current of 2.0 m/s.

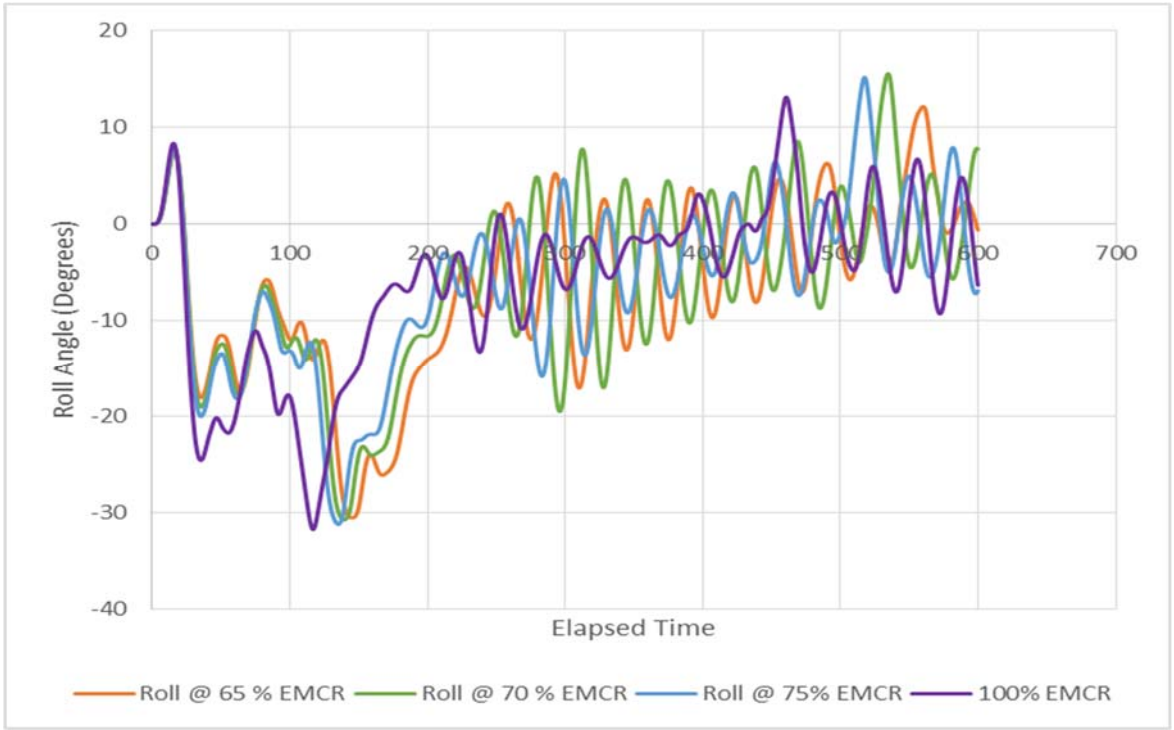

Figure 6-13 Roll Angle vs. Elapsed Time (Irimagha *et al.* (2019)).

Figure 6-13 are characteristics of the roll angle with time at stated percent of Engine MCR as the ship attempts to make a Turning circle motion in adverse weather

condition (significant wave height of 5.5m, wind velocity of 33knots, current of 3m/s, initial angle of wave approach is 20 degrees).

At some time as seen, the roll angle went dangerously large and possibly attain an angle of loll or capsize in the worst case scenario (this level of roll will mean a considerable change in wetted area and thus make the assumption of a constant draft invalid if more detailed investigation is required thus a method of computing large angle rolls need to be utilised). This is probably due to broaching as the Ship will be subjected to following seas (an initial angle of 20 degrees following), and the high ocean current being simulated. It can also be seen that at higher power, the peak rolling angles tend to be high.

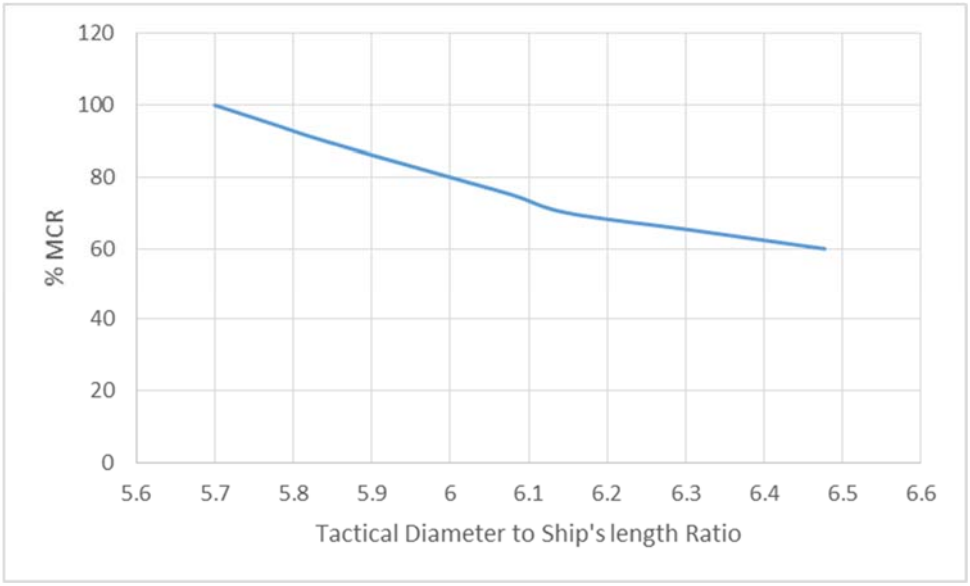

Figure 6-14 Plot of %Maximum Continuous Rating vs Tactical Diameter, 15 degrees rudder command in adverse weather.

The smaller the ‘advance’ and ‘tactical diameter’, the greater the chances of being able to steer away to avoid collision in an emergency at normal speed. IMO requirement is that the tactical diameter should be no more than 5 times the Ship’s Length. For this ship, the original tactical diameter in calm water is about 4.5 times the Ship’s length at 35 degrees rudder command which is within the recommended criterion, and 5.7 times with a 15 degrees rudder command. The plot above, Figure 6-14, demonstrates that the tactical diameter in adverse weather condition, and it gets much larger as the installed power is reduced. This will mean that the vessel may not be able to manoeuvre and avoid collision safely in an emergency.

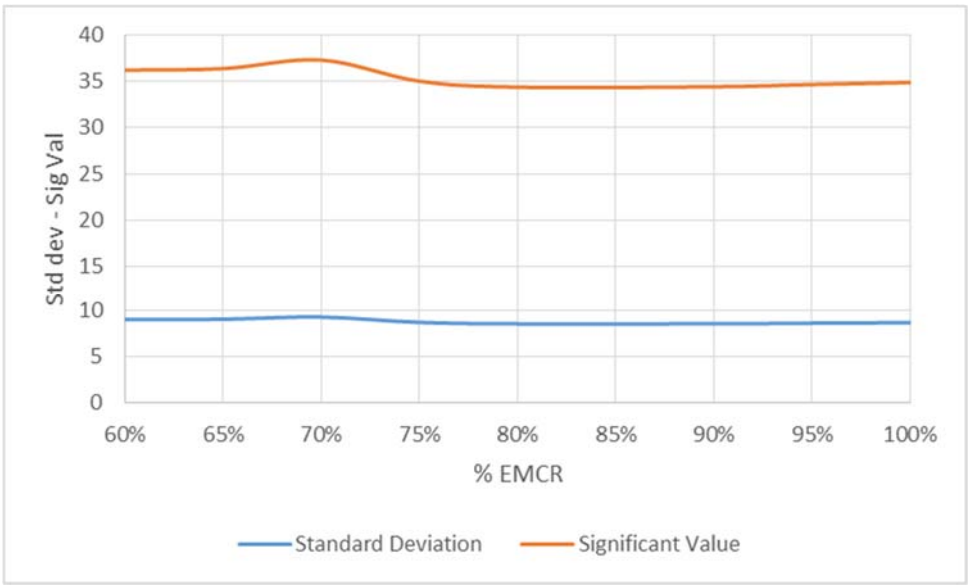

Figure 6-15 Standard Deviation (SD) and Significant Value (4*SD) for the Roll angles, at % Engine MCRs

Furthermore, the standard deviation for the roll angles recorded during the period for each percentage of the engine MCR were computed and each multiplied by 4 to give a significant figure. It can be seen that at 65% engine MCR, the significant value is at their maximum. The high roll angles has serious implications for passenger and crew comfort. In reality, these momentary peaks will not be experienced because, there is the assumption that the ship is a rigid body which may have led to such figures. In reality, the liquids in the ballast tanks, fuel oil tanks etc. will act as some passive roll control device which will dampen the rate of roll and also help in improving stability; there is also the fact that some of the parameters used in this study were assumed – a ship designer/builder, will have more accurate parameters. Also, Dong *et al.* (2015) mentioned that the roll result from the conventional 4-DOF manoeuvring model used in this work diverges as the roll angle exceeds 10 degrees thus given misleading higher figures thus the need for some improved model.

As a further step towards assessing the functionality of the study, the ship was run into head wind and irregular long crested waves (180 degrees).

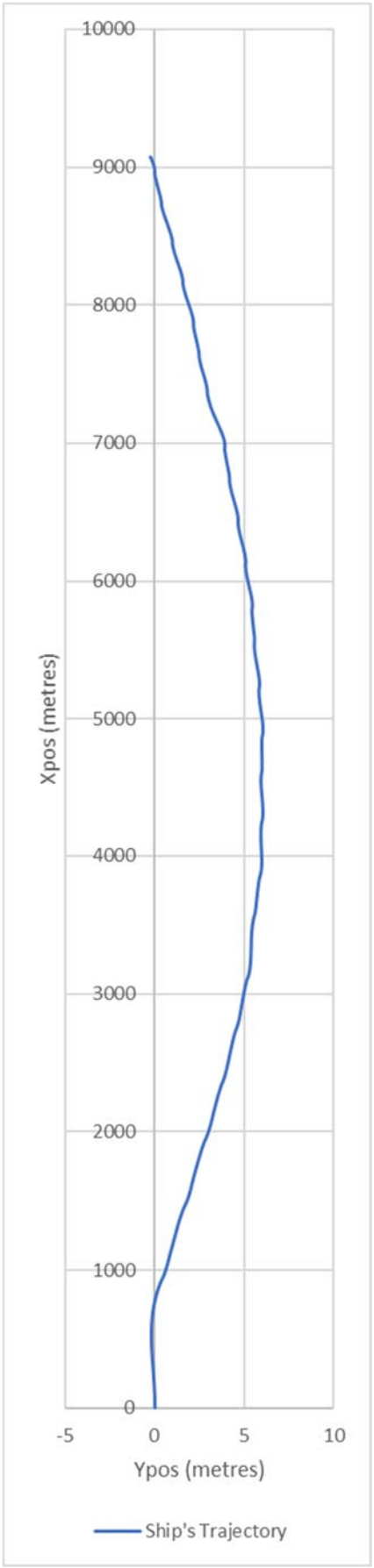

Figure 6-16 Ship's trajectory while heading into 10m/s wind and 2.5 waves.

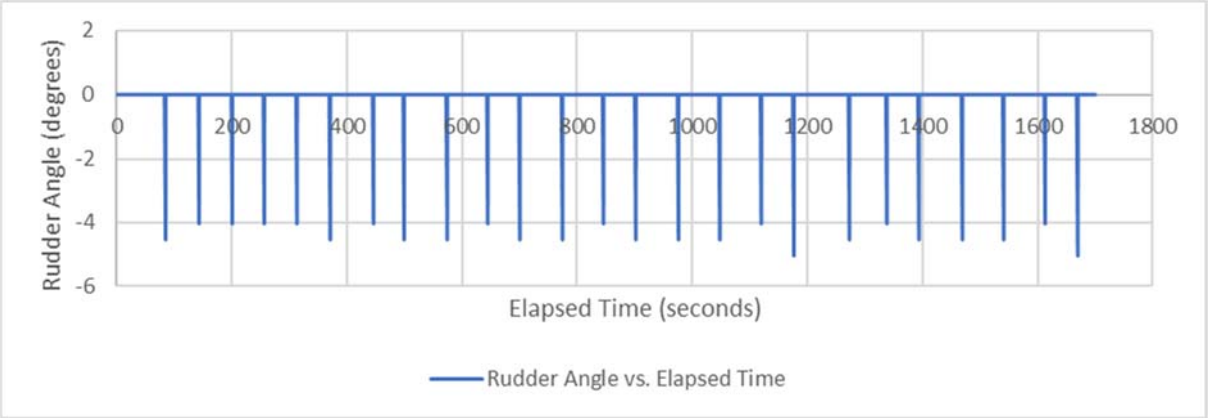

Figure 6-17 Rudder movement while heading into wind and waves

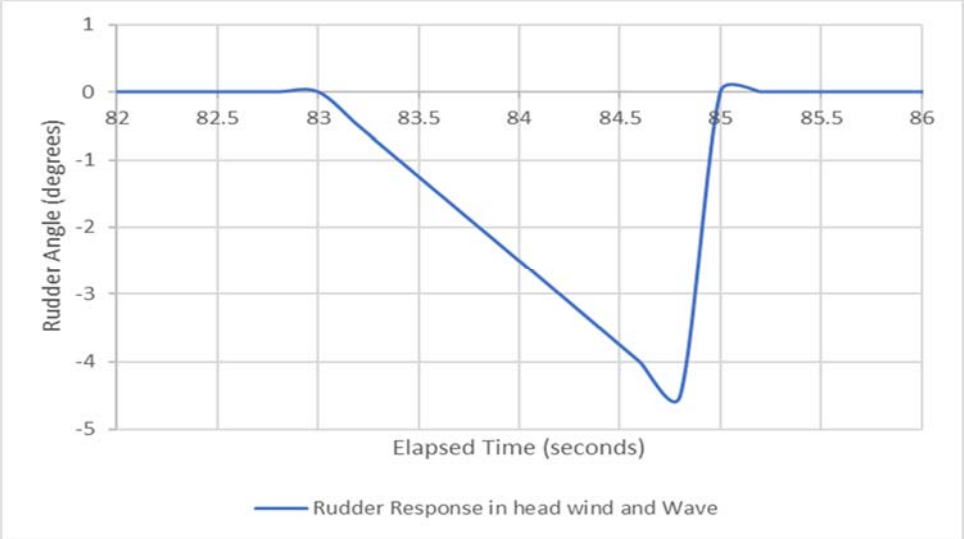

Figure 6-18 Exploded version of one motion in Figure 6-17 for clarity

The speed drop during the motion in wind and waves after a set span of time is subtracted from the still water figure over the same time to obtain the figures used in Figure 6-19.

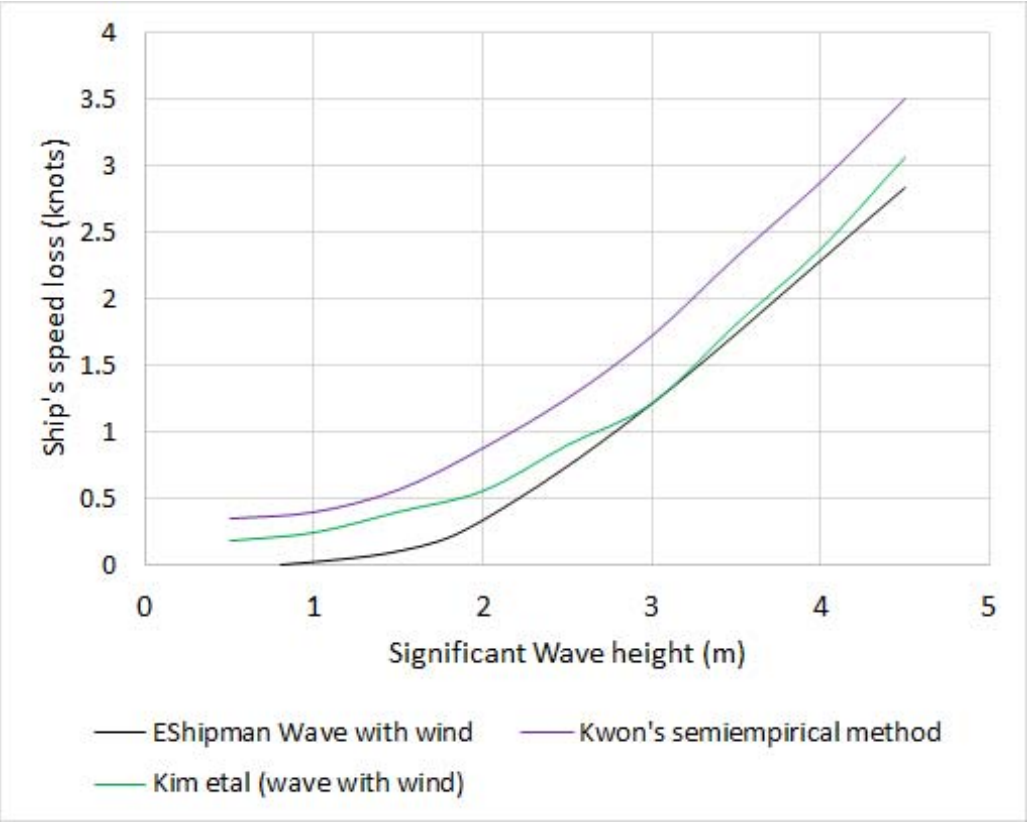

Figure 6-19 Speed loss under the influence of wind and waves (Irimagha *et al.* (2019)).

This plot tends to follow the trend but shows figures lower figures than those of Kwon (2008) and Kim *et al.* (2017), and presents a situation that depicts no very little or no loss of speed at significant wave height of less than 1.5meters. However the formulation can be improved upon to improve the accuracy of Eshipman, for instance, the rudder algorithm is very basic, a more comprehensive adaptive controller will make for improved ship motion response and reduce the speed loss.

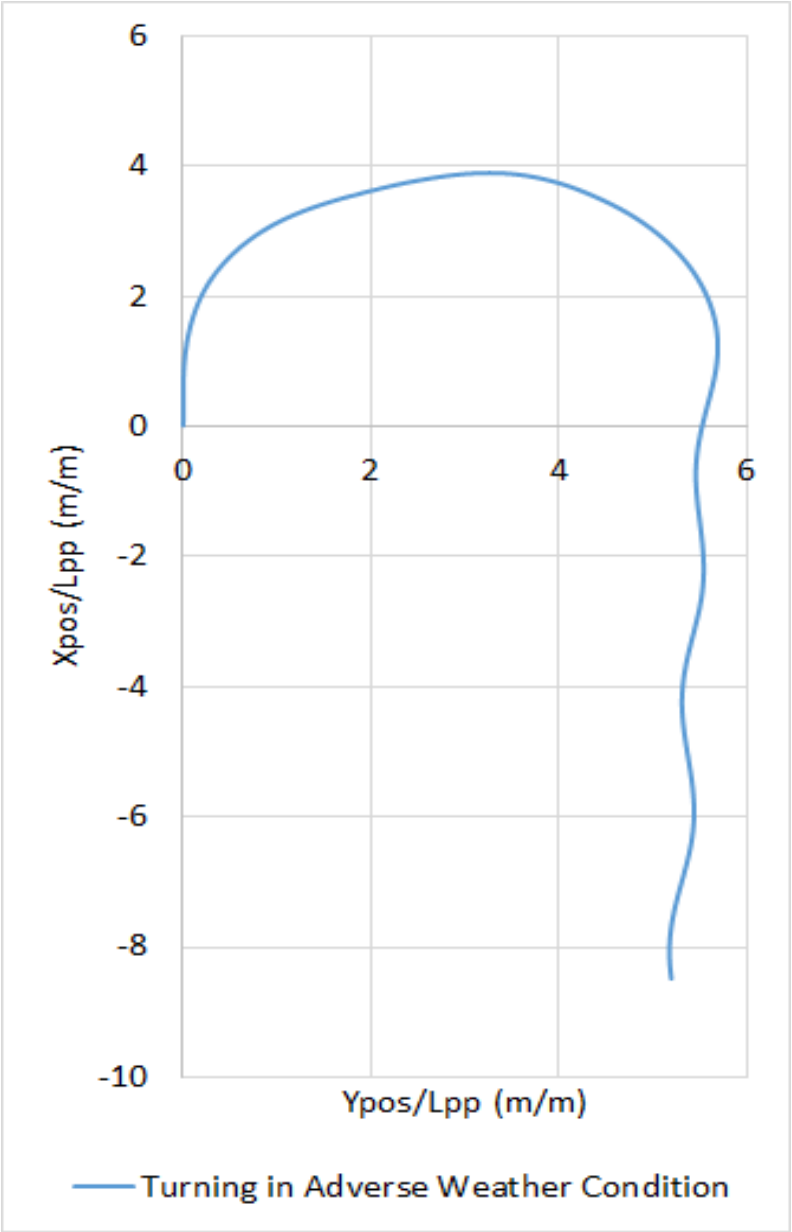

Figure 6-20 Trajectory of Ship Turning into head seas (200 degrees waves) in adverse weather condition

Figure 6-20, is a trajectory of the ship turning as in previous plot and in adverse weather condition. It can be seen that the rudder is trying to sustain the path of the ship as it is being influenced by the additional environmental loading with a wave height of 2.5m, wind speed of 30 knots and 2.5m/s current. Figure 6-20 was included here for the sake of demonstrating some of the capabilities of the self-built control system. Due to the environmental effects (the wind, and current being modelled to come in the same direction while the wave comes 30 degrees ahead of them), the fluctuation is much more as the ship tends to respond much slower to rudder action, the use of a better controlled or an adaptive autopilot will improve the responses.

Besides, the distance travelled before the ship is able to attain a 180 degrees turn is slightly lesser due to the effect of the reduction in speed of the ship owing to the weather condition. As was earlier pointed out, the efficiency of the rudder reduces as the speed reduces below some value and thus leads to poor controls, however on this occasion the speed was high enough to sustain efficient rudder output. Thus if the ship speed were reduced in way of reducing the installed power, it is likely to come to a situation where the rudder may not be able to cope, hence for a new build that will operate at a slightly reduced installed power, a new rudder may have to be designed and its parameters inputted accordingly in this method to see that that they are able to perform satisfactorily.

6.2 Regarding Improvement of EEDI by Engine Derating

This section is meant to discuss the results obtained from reducing the maximum continuous rating to some proportion of its original value to simulate a condition of a derated engine, and how this does affect the efficiency of the ship, any issues that could arise from such decisions and possible ways to get over identified challenges.

Firstly, it needs to be noted that just reducing the power alone will not always improve the efficiency due to the specific fuel oil consumption characteristics (Figure 4-10 which shows points ‘A’ and ‘B’) which will reduce to a given engine load and then start to rise again below this load, thus the ship’s engine cannot be derated to any point below the most efficient load for fuel consumption. Thus the engine at a higher load (point ‘B’) will consume the same amount of fuel as when running at a lower load (point ‘A’), while running at load ‘B’ will subject the ship to safer manoeuvring in adverse weather.

The Required EEDI computed for the specimen ship considering full load and applying the approved formulation is 35.74, and the attained EEDI at full load and 80% load considerations, applying the current formulation for attained EEDI, are 47.45 (28.77% more than the required value) and 39.25 (9.806% more than the required value), which means an 18.96% reduction of the EEDI is achieved by reducing the power alone. This is a very substantial reduction, however, the vessel’s attained EEDI is still not below the required value, this is because, this is an older ship which probably met the requirements based on the technological standard and expectations at the time of build. There are other issues that do influence the

efficiency of a ship that were not adequately addressed in the derivation of EEDI and are described as follows:

It is a known phenomenon that engines are normally more efficient when the lowest possible cooling water temperature are used to cool the air for increased mass flow, which in turn reduces the fuel oil consumption. However, Ship builders do prefer a constant temperature central cooling water system which uses treated fresh water that is maintained at temperatures of between 32°C and 36°C to the air coolers for both areas with warm and cold sea water, mostly for cost related purposes (reduced maintenance cost, greater use of relatively inexpensive materials, reduced wear, reduced electric power consumption of the cooling water pumps and improved reliability etc.). However the engine builder, MAN B&W (2014), mentioned that when operating at 36°C instead of 10°C of water to air coolers, specific fuel oil consumption will increase by approximately 2g/kWh. Thus for a ship operating within cold regions and still using the central cooling system, this means more emissions to the atmosphere in these circumstance.

The energy efficiency can be improved by using the right ships in a transport system, thus, efficiency will generally increase if cargo is transported in larger ships where possible. Hence, while using large ships tends to reduce energy consumption in the shipping leg itself, the total impact on overall door-to-door logistics performance may be negative unless such a move is complemented by smaller ships (which could be propelled by a less emitting power system) that can assist in the onward distribution of cargoes. The larger ships are not efficient if not enough cargo is available and they have to sail only partly loaded. Net energy efficiency may be better for a small ship with access to more ports and cargo types, being able to fill its cargo hold to capacity.

Another circumstance of concern is in the areas of effecting mitigating measures towards reducing the NOx emissions most of which do amount to reducing the efficiency of the engine or reducing the recoverable heat energy due to relatively reduced exhaust temperature. EEDI formulations do include weather factors that will increase the resistance of a ship as mentioned earlier, however, these two scenarios described, need to be properly researched and some more innovative method

developed that could replace these measures that reduces environmental pollution from one perspective and increases another environmental issue.

At 80% of engine power, EShipman was used to simulate a zigzag motion in calm weather condition, to check whether it is able to meet the recommended benchmark set by IMO.

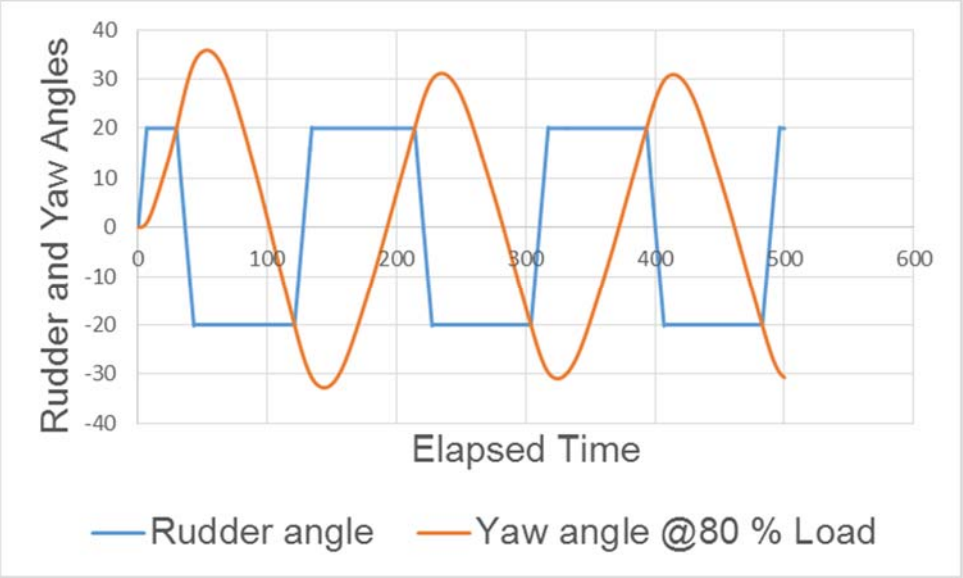

Figure 6-21 Zigzag Motion with the Engine Power Derated to 80%

From the zigzag motion plot in Figure 6-21, the first overshoot angle is 15.8 degrees which is still less than the IMO criteria of 20 degrees maximum.

Thus from this results and being that this vessel is able to manoeuvre safely with the ship velocity not reducing below 4 knots, in weather conditions consistent with that recommended by the IMO for defining adverse weather condition for determining minimum installed power (IMO (2017)), then installed power can be reduced safely by 80%.

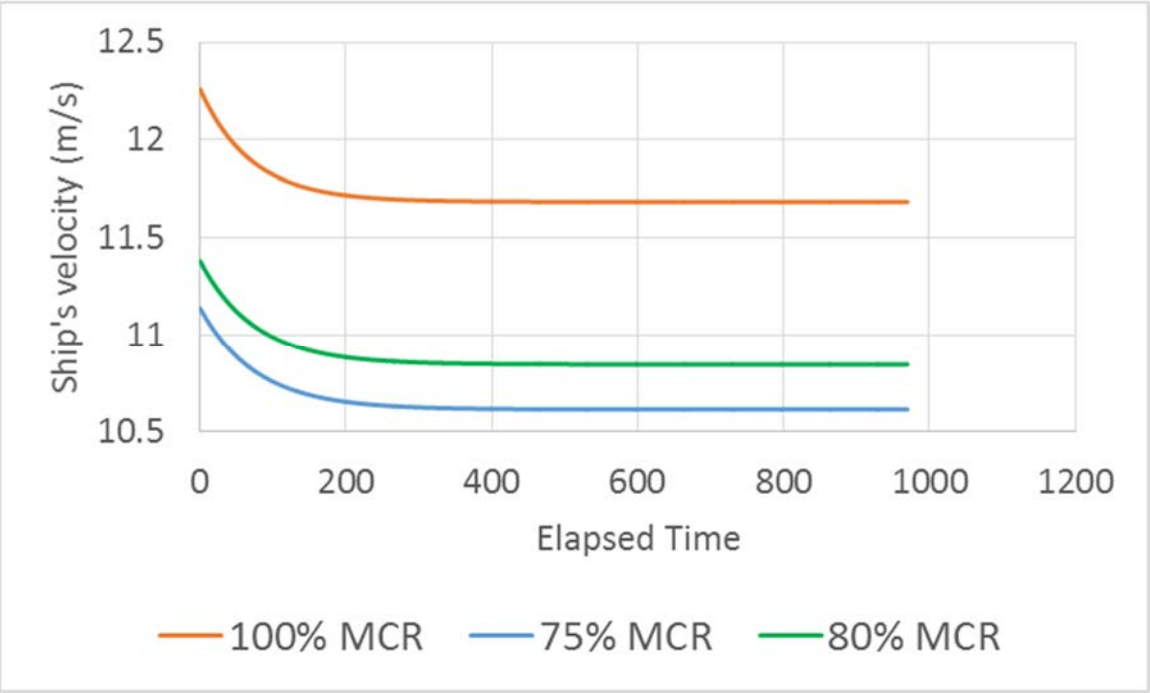

Figure 6-22 Velocity-Time profile of ship while making a straight line journey at 0.5m wave height

Thus if due to the need to improve its EEDI, the power is reduced to 80% of its MCR, then some assessment was carried out regarding fuel consumption and CO_2 emissions during a straight journey trip of about 2010 miles, firstly in calm water conditions for the 100% SMCR and then for the 80% SMCR.

For a 2010 nautical miles route, the journey was completed in 88.504 hours from Eshipman computation at full load thus the total amount of fuel consumed is 213588.47kg of HFO. And at 80% power, the trip was carried out in 95.8395 hours, thus the total fuel consumed is 179394.29kg of HFO. Thus a fuel saving of 35.137mT was made on a 2010miles trip, resulting in a carbon emissions saving of about 140.371 metric tonnes. A summary in the tabular form is shown in Table 6-3.

Table 6-3 Summary of Trip results

Power reduction	*2856 kW*
% Power reduction	*20%*
fuel Oil saved	*35137.24 kg*
% savings in Fuel Oil	*16.45129%*
time lost due to speed reduction	*6.830956hrs*
% Loss	*7.718426%*
CO_2 Emission saved	*109417kg*

From the other point of view, for a company that has say 4 of this class of ship and in tight schedule, and under a tight schedule contract, 7.7% loss of time is a significant amount of time and as such the option for improving its EEDI should be directed towards increasing its cargo carrying capacity as simply reducing its power might mean adding one more ship into the fleet to meet with the demand.

Thus considering the given curve in Figure 6-13, the engine will operate more efficiently if derated to 80% of its maximum continuous rating, and could safely manoeuvre, however, any circumstance that forces a reduction in power for any prolonged period (say fault that results in the control system, isolation of one cylinder/piston system) that could bring it to some value below the maximum efficiency point of 70% of the original engine MCR in which case the rate of fuel consumption would rapidly increase and result in an unfavourable Energy Efficiency Operational Indicator value. If it can be foreseen that the vessel will definitely pass through a region for a considerable length of its passage where there will be voluntary reduction of speed to reduce excessive motions and propeller racing, it will be great if the point of operation will fall within the range of speed where the specific fuel consumption is minimal while achieving optimal speed thus good EEOI. One way to get around this kind of problem, is to ensure that any modification done to derate the engine is easily reversible, i.e., It is probably done electro-mechanically, such that should conditions require, permission could be officially obtained and the modification reversed (say reinstatement of any cylinder(s) previously isolated in order to derate the engine) until appropriate remediation is achieved. In making a decision to derate the engine for EEDI improvements purposes, there is need to carry out extensive investigation on the known experience of operators that did derate their engines due to the need to improve engine efficiency in the past due to high fuel costs as some of these lessons are beneficial to reaching a final decision.

6.3 Coupled Heave and Pitch motion Case

Manoeuvring trials is normally considered to occur under calm water condition, with the influence of wind in some cases, and as such only 3 degrees of freedom are normally organised in a coupled motion and recently 4 degrees of freedom, when considering the effect on roll motion due to the forces and moments generated by the

steering of the rudder. Heave and pitch motions change the position and orientation of the ship hull in incident waves.

Due to the reasons that wave effects will increase heave and pitch motion to a level which they cannot be entirely neglected, these were included in the methodology, so results can straight away be analysed to deduce such important parameters such as the Response Amplitude Operator (RAO), bow immersion, and propeller emergence. However, due to insufficient data and present day technological limitations due to limited facilities able to model all coupled six degrees of freedom, the heave and pitch motion were decoupled from the rest of the motions and the computation was done in the frequency domain such that solution was derived once for each percentage of power. By this, one frequency is used for running the entire program. It is to be done according to the power reduction steps that a user wishes to apply and results extracted each time. One result is taken for each power reduction step, it was not made to run in the loops like the other four degrees of freedom. The results are then recorded in excel and plotted accordingly. The plot below demonstrate the effect of reducing the power in steps of 5% of the Engine Maximum Continuous Rating.

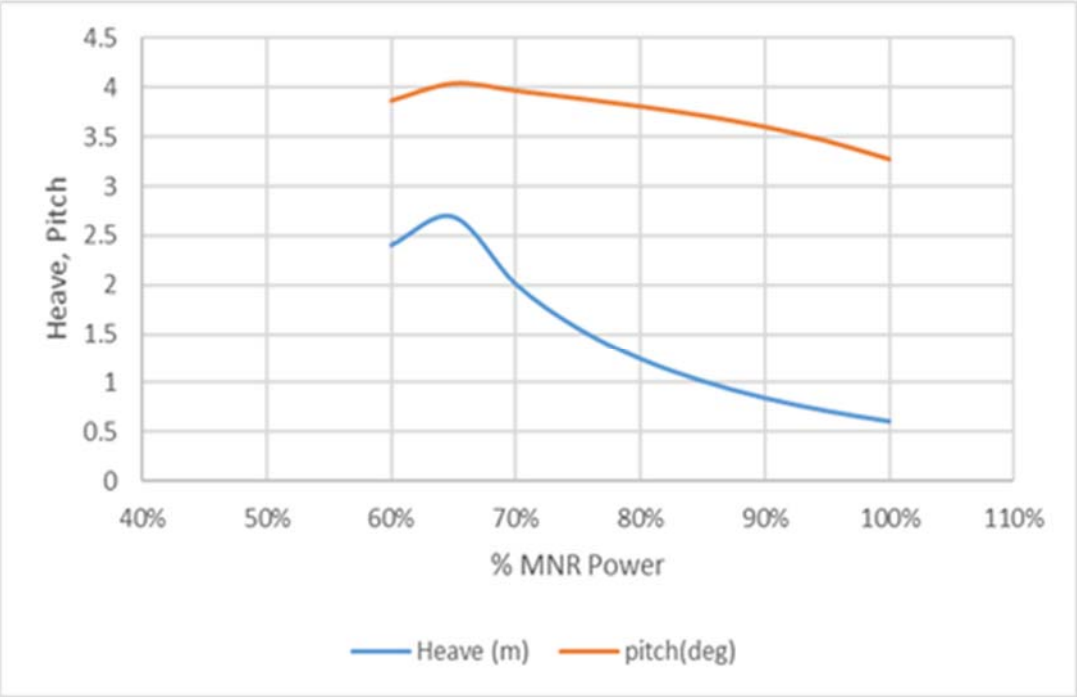

Figure 6-23 Heave and Pitch Motions Response with Reduction in Engine Power, Sig. Wave Height of 5.5m.

The above plot Figure 6-23 (Irimagha *et al.* (2019)), demonstrates how the heave and pitch amplitudes increase with a reduction in installed power. For this

circumstance where the significant wave height is 3.5 metres, wave period is 13s. The heave motion went as high as 2.6m at 65% power from 0.09m at full power, while the pitch angle increased from 3.2 degrees at full power to 4.04 degrees at 65% power. Though there was substantial change in motion with power reduction to 65 percent, because of the chosen wave height, these motions are still within practically safe limits. However, with reduced power, the vessel will get susceptible to unacceptably high motions with increased wave height. This tend to agree with the velocity – time characteristics Figure 6-11, where the unsafe speed drop was seen to begin from 65% downwards of Engine maximum continuous rating. Severe pitching can result in propeller racing due to its emergence, which could further lead to speed reductions, and other effects mentioned in previous chapters.

There is the trend towards reducing the weight of ship's hull and internal fittings by the use of high tensile steel and due to limited dynamic assessments there is increased incidence of excessive vibration and unusual fatigue cracks being witnessed in practice Oppen and Kvitrud (1995). Incidence like this could be minimised or avoided by proper initial assessments with proper preventive measures taken.

Chapter 7 Conclusion

The aim of this chapter is to give some concluding remarks on the key items discussed earlier in this thesis. The discussion so far does point out a novel method that can be included in predicting the future performance of a ship in weather conditions and as well define a safe minimum power. This thesis does propose a wholesome prediction of the ship motion in adverse weather condition when considering derating of a ship's engine for the purpose of improving EEDI using a fast, cheap approach with reduced hardware requirement and can run on any computer, for such prediction before carrying out any detailed experiment.

The simulation study showed that reducing the installed power will reduce the peak roll angle of the ship which is a good point and which probably supports why ship masters will slightly reduce engine loads during heavy rolling to make the passengers comfortable. However, the results from the coupled heave and pitch motion demonstrated a rise in the amplitudes which starts dropping off as the power is reduced lower than 65%. This will give reasonable information as to what level the vessel's power will have to be derated to, in order to achieve both the benefit of improved EEDI and as well have relatively safer motions in the defined adverse weather conditions.

The plots of turning circle motion in adverse weather condition was meant to demonstrate one way of easily predicting the influence of ocean current in addition to wind and waves when the power is reduced thus for a new build, Eshipman was used to predict a suitable size of rudder that will give say, the calm water manoeuvring indices at 65% power to be as close as practically possible to that at 100% power, so that in adverse weather condition, one mode of failure (steering effectiveness) has been reasonably mitigated. In this study, it was found that with 9% increase in rudder area, the 65%MCR simulated tactical diameter was reduced to the calm water tactical diameter of that obtained with 100% MCR turning circle simulation. Also, the effect of the heel observed when performing turning at high speed may expose the ship to greater overturn moment due to wind loading which may result in a critical condition when as the ship turns with this increased above waterline surface area being windward in the presence of strong wind for a prolonged time period.

The outcome, relevant equations of motion and method of application have been explained. For this research, a ship with known experimental model test data was used but there is a need for future work especially in the area of improving the empirical formulae for manoeuvring derivatives using ship's basic dimensions. The existing methods do have formulations which provides for only coupled 3 degrees of freedom. With future advancement in measuring techniques, a coupled 6 degrees of freedom measuring system may lead to derivations of hydrodynamic coefficients formulations that could give more accurate results for newer designs of ship hull, thereby increasing the dependency rate on analytical formulations and in turn reduced the cost of carrying out the required investigations.

The simulation of the vessel to perform a turning circle motion with the rudder at 35 degree angle showed a stable roll angle of 10 degrees after some peaks. This showed a 53% increase in area on one side of the ship, and if this happens to be the windward area, it will result in an overturning moment which may lead to a capsize, damage to internal complements (for instance, a turbo-alternator or could suffer loss of lubrication as the pump loses suction leading to extensive damage) or severe discomfort. Thus a correction formula was proposed which take into consideration, this effect, when modelling the motion of a ship in adverse weather condition and results does show an increased roll angle and some drift motion.

To demonstrate that Reduction in Power does actually improve the EEDI, calculations were made (see a sample in section 9.1 – Appendix B, for one sample calculation illustration) for a 100 percent MCR case and for 80% case on the assumption that the engine is to be derated to a point where its new MCR will be 80% of the existing power. Also, it was taken into account that the power used for the calculation of EEDI is the 75%MCR value with the equivalent reference speed for each case. The Required EEDI computed for the specimen ship considering full load and applying the approved formulation is 35.74. The attained EEDI at full load is 47.45 (28.77% more than the required value) and the attained EEDI at 80% MCR considerations 39.25 (9.806% more than the required value). This figure does not really meet the required EEDI probably because of the inefficient design of the ship at the time of build as it is an aged vessel (over 35 years). However, being that there is an 18.96% reduction of the EEDI achieved by reducing the power alone this ship could be derated to 80% of its rating and kept in service till such a time that future

regulation requires it to be put out of service. At this point, it could be further derated to say 70% and put to use in an area of relative calm weather for the rest of its life.

There is room for improving the functionality of EShipman by improving the empirical prediction method for deriving hydrodynamic derivatives which will reduce the dependence on physical experimental or CFD base results. Also, Dong *et al.* (2015) did propose a 4 degrees of freedom model which is more stable and does not give excessively high values at large heel angles this formulation can be used to improve the accuracy of the results, however it will require the user to conduct physical model experiments to obtain the data required to use the equations.

At the moment, there is no regulatory framework (such as permissible range of tactical diameter, overshoot, etc.) for the manoeuvring motion in adverse weather conditions, thus the manoeuvring motions simulated in adverse weather conditions were not expected to meet with the present IMO recommendations. However, there is a provision for weather factor which is included in the computation of EEDI of which method of obtaining it have been proposed and is still undergoing further improvements.

Most of the NOx mitigative measures do either lead to reduced overall efficiency due to increased weight or power consumption of the facility (e.g. the Selective Cathalytuic Reducer), or does reduce the recoverable energy (e.g. the Exhaust Gas Recirculation system). Hence there is need to include some NOx index to EEDI formulation to encourage solutions that employ innovative NOx mitigating measures that maximises engine efficiency.

This proposed methodology is mainly limited to ships that have been conceived as overpowered, such that reduction in speed will not in itself create the need for another ship in order to meet with supply schedule.

7.1 Summary

In this section, the work explained in the preceding chapters are summarised.

i. This research points out a method that can be included in predicting the future performance of a ship in adverse weather conditions, especially where there is an existing version of the ship that is being considered for a

reduction in engine capacity. The perspectives of a derated engine were clarified and some generic forms of possible modifications were explained.

ii. This work does propose a holistic prediction approach of the ship motion in adverse weather condition considering situations of a derated engine using a fast, cheap program with reduced hardware requirement for such prediction before carrying out any detailed experiment. Also, ship's continuous operating speeds are set taking account of avoidance of resonance zones which considers the vessel's natural frequency and engine operating frequency. With the heave and pitch motion results, this prediction method will help give more insights on the environmental effects and enable the structural designer to improve on the fatigue strength of members, and as well forecast situations that could lead to undesirable effects such as propeller emergence, bow emersion,etc.

iii. The results of the turning circle motion simulations at the different power levels showed that the ship in calm weather condition at 60% engine power will still have sufficient manoeuvring speed (above 4 knots) and the turning circle diameter only slightly increase but not above the regulation limit of 5 times ship's length. Also, in the defined adverse weather condition, the manoeuvring speed will reduce to less than 4 knots at 65% MCR and as such, the ship cannot be derated to this level. Furthermore, one method of improving the ship response at reduced power was demonstrated by showing that the tactical diameter at 65% MCR reduced to the value for 100% tactical diameter, by increasing the rudder area by 9%. Thus this new rudder area was used to simulate a turning circle motion at 65% MCR with a result showing some reduction in the tactical diameter and a higher minimum speed during the turning circle motion as in chapter 0.

iv. A coupled heave and pitch motion analysis was done with results showing that reducing the engine power does increase the heave and pitch motions in the defined adverse weather conditions and that the peak motion occurred at 65% of engine power below which the motion starts reducing. This is a key observation that definitely indicates that it will not be convenient to run the vessel on a continuous basis at this load in the

defined adverse weather condition and it is important to know this before any decision to derate the engine of a ship is implemented.

v. From the simulation result, the peak roll angle does reduce with a reduction in the MCR power. However, a key finding is that there is an instantaneous change in the windage area when the ship rolls and this is not normally reflected in most formulations for windage area in manoeuvring studies, thus a correction formula was added to an existing windage area formulation and some simulation did show that the occurrence of rolling can significantly increase the windage area and the roll angle will further increase if the increased area is on the windward side. This effect will be more pronounced if the ship has a low metacentric height and (or) in ballast condition.

vi. Information as to what power levels the vessel will have to be reduced to so as to obtain the benefits of improved EEDI and as well have relatively safer motions in adverse weather conditions of the defined type could be reasonably deduced as was shown in the specific fuel ol consumption curve in Figure 4-10 and the simulation plots explained in 0. It could also give an indication of the range of engine power that the vessel should avoid in a continuous operation at certain defined weather conditions.

vii. EShipman was also used to perform a trip simulation for a 2010 nautical mile distance was done in calm weather condition using the given engine parameters. The result showed that for a 20% reduction in power from the 100%MCR, there was 16.45% savings in fuel oil consumption and a 7.7% lost time, so the operational requirement of the ship will have to be considered before making the decision to derate the engine. From the specific fuel consumption plot, it can be seen that the minimum safe level of 65% is not at the most efficient point which is 70%, thus the vessel can as well have its power reduced to 80% which gives it an improved level of safety while fuel consumption is at the same magnitude as when running at 65%. This is a common characteristics with most engines.

It is very important to suggest that attempting to derate an existing ship’s engine in order to improve its EEDI should be given a very detailed consideration as a

reduction in scheduled speed (i.e. accepting longer voyage times) will increase efficiency but result in more ships being needed. Reductions in scheduled speed can be expensive, since they directly affect the amount of freight carried and hence the income of a small ship. However, there is a trade-off between freight rates and freight cost: when freight rates are low and fuel prices are high, it may be profitable to reduce speed.

Having an improved EEDI will reduce the carbon-dioxide emissions however there are ships that operate their main engine for days and even weeks while waiting to enter into the port for security or logistics reasons. This similarly applies to situation steam turbine propelled ships in which the process of restarting of boilers means that a minimum of five hours will be gone before at a warm boiler can come on line thus they are normally allowed to run almost continuously. Hence working towards improving security measures in such areas could encourage such ships to stop and go on light loading. Also improved metal properties, instrumentation and controls systems, and efficient training of personnel could enable shorter start-up and shut-down times. Thus in both cases, emissions during predictable long waiting times could be reduced significantly.

At present, there are regulatory provisions that defines acceptablle manoeuvring characteristics based on trials in relatively calm weather conditions (ITTC (2014) and IMO (2002)). There are no such guides for adverse weather condition. The proposed method when tested with various ship types could create a framework for defining some acceptable safe manoeuvring criteria in defined adverse weather conditions.

7.2 Recommendations for Future Works

A major setback for applying this method is that it will require some physical experiment to determine the hydrodynamic coefficients for better accuracy. The present state of CFD method of deriving these lacks much accuracy. For this research, a ship with known experimental data was used but there is need for future work to be done especially in the area of improving on the numerical method for manoeuvring derivatives using Ship’s basic dimensions, so that this program will be less dependent on physical model experiments as most of the existing methods still show some significant errors of up to 24% for some parameters as in Pan *et al.* (2012), when compared with physical model experimental results.

Some of the parameters were obtained using approximate empirical formulations. The four degrees of freedom (Surge, sway, yaw and roll) were treated as coupled motion due to available research data, and the pitch and heave treated separately. With improvements to research facilities that allows parameters for coupled six degrees of freedom to be obtained simultaneously, equation of motion could be updated to meet with the development. Also, some experimental research need to be carried out on different types of ships, and corrections made to the formulations to fit different types of ship, as the response pattern may slightly differ. However, for a given type of ship, a pattern could be noticed and this could pave the way to developing some acceptable safe manoeuvring indices in defined adverse weather condition. There are financial implications initially but there are be long-term benefits.

At the moment, the model used for this research is said to have better accuracy for roll motions less than 10 degrees, the modelling equations can be improved for better results by, for example, the model proposed by Dong *et al.* (2015) that is designed to give a better accuracy when studying the effects at large heel angles. However, the user will have to perform the required physical experiment so as to obtain the parameters required to apply the model. One of the advantages of the modular approach, coupled with the use of the high level programming language. When new knowledge, say of, a new numerical methods, model test results or new empirical formula, becomes available for certain components whose formulations were based on some assumptions, it can be directly used to replace the existing unit without any major modifications of the code. Again, based on requirements, suitable algorithms can be inputted for certain research purpose to enable the code to give more of the results in probabilistic format.

In conclusion, the work done thus far is an introduction to a methodology that can reveal scenarios not normally seen from the usual ship resistance modelling and if this methodology is improved on, it will lead to proper design of ships that will reduce incidents that result from unforeseen factors especially when it is being considered to derate a ship’s engine.

Chapter 8 References

1. ABS (2005) 'Commentary on the ABS Rules for Building and Classing Mobile Offshore Drilling Units 2001', *ABS Rules, Guides And Guidance Notes*, Part 3 - Hull Construction & Equipment.

2. ABS (2006) 'Guide for Vessel Maneuverability', *ABS Rules, Guides And Guidance Notes*.

3. ABS (2013) 'Ship Energy Efficiency Measures Advisory, Status and Guidace', *ABS Rules, Guides And Guidance Notes*.

4. Ančić, I., Šestan, A. and Vladimir, N. (2013) 'EEDI calculation for passenger and Ro-Ro passenger ships', *International Conference on Design & Operation of Passenger Ships*.

5. Andersen, I.M.V. (2013) 'Wind loads on post-panamax container ship', *Ocean Engineering*, 58, pp. 115-134.

6. Araki and Motoki. (2013) *Ship Maneuvering Mathematical Model Using System Identification Technique with Experimental and CFD Free Running Trials in Calm Water and Astern Waves*. Osaka University.

7. Araki, M., Sadat-Hosseini, H., Sanada, Y. and Umeda, N. (2013) *Proceedings of 13th International Ship Stability Workshop. Brest, France*.

8. Attah, E.E. and Bucknall, R. (2015) 'An analysis of the energy efficiency of LNG ships powering options using the EEDI', *Ocean Engineering*, 110, pp. 62-74.

9. Ayaz, Z. (2003) *Manoeuvring Behaviour of Ships in Extreme Astern Seas*. PhD thesis. Universities of Strathclyde, Glasgow.

10. Ayaz, Z., Vassalos, D. and Spyrou, K.J. (2006) 'Manoeuvring Behaviour of Ships In Extreme Astern Seas', *Ocean Engineering*, 33(17), pp. 2381-2434.

11. Azad, A.K., Alam, M.M. and Islam, M.R. (2010) 'Statistical analysis of wind gust at coastal sites of Bangladesh', *International Journal of Energy Machinery*, 3(1), pp. 9-17.

12. Badea, N., Epureanu, A., Badea, G.V. and Frumuşanu, G. (2015) *IOP Conference Series: Materials Science and Engineering*. IOP Publishing.

13. Bailey, P.A. (1997) 'A unified mathematical model describing the maneuvering of a ship travelling in a seaway', *Trans RINA*, 140, pp. 131-149.

14. Betancourt, M.K. (2003) *A comparison of ship maneuvering characteristics for rudders and podded propulsors*. Monterey, California. Naval Postgraduate School.

15. Bhattacharyya, R. (1978) *Dynamics of marine vehicles*. New York: John Wiley and Sons.

16. Blendermann, W. (1994) 'Parameter identification of wind loads on ships', *Journal of Wind Engineering and Industrial Aerodynamics*, 51(3), pp. 339-351.

17. Blendermann, W. (1995) 'Estimation of wind loads on ships in wind with a strong gradient'.

18. Boese, P. (1970) 'A Simple Method for Calculating the Increase in Resistance of a ship in Waves', *Shipbuilding Series* Designing of ships and ship safety M-6(258), p. 18.

19. Borkowski, T., Kasyk, L. and Kowalak, P. (2012) 'Energy efficiency design index of container vessel-operational approach', *Journal of KONES*, 19, pp. 93-100.

20. Brasel, M. and Dworak, P. (2014) 'Multivariable Adaptive Controller for the Nonlinear MIMO Model of a Container Ship', *TransNav: International Journal on Marine Navigation and Safety of Sea Transportation*, 8(1), pp. 41--47.

21. Brix, J. (1987) 'Manoeuvring technical manual', *Schiff und Hafen*, 36(5).

22. Calleya, J., Pawling, R. and Greig, A. (2014) *Royal Institution of Naval Architects* London. RINA.

23. Cariou, P. (2011) 'Is slow steaming a sustainable means of reducing CO2 emissions from container shipping?', *Transportation Research Part D: Transport and Environment*, 16(3), pp. 260-264.

24. Cepowski, T. (2017) 'Prediction of the Main Engine Power of a New Container Ship at the Preliminary Design Stage', *Management Systems in Production Engineering*, 25(2), pp. 97-99.

25. Clarke, D., Gedling, P. and Hine, G. (1983) 'Application of manoeuvring criteria in hull design using linear theory', *Naval Architect*, pp. 45-68.

26. Copela, S. (2013) 'Climate Change and the International Maritime Organization: Another Breakthrough at the Marine Environment Protection Committee', *American Society of International Law*, 17(24).

27. Dand, I. (1987) *International Conference on Ship Manoeuvrability--Prediction and Achievement*.

28. Devanney, J. (2011) 'Detailed Studies of the Impact of Energy Efficiency Design Index on Very Large Cruide Carriers Design and CO2 Emissions', *Journal of Ships and Offshore Structures*, 6(4), pp. 355-368.

29. Djamila, H., Ming, C.C. and Kumaresan, S. (2014) 'Exploring the dynamic aspect of natural air flow on occupants thermal perception and comfort', *Proceedings of 8th Windsor conference: Counting the cost of comfort in a changing world cumberland lodge, Windsor, London*, 8.

30. DNV-GL (2015) 'Rules for Classification: Ships', *DNVGL-RU-SHIP-Pt3Ch15 Stability - Rules and standards*, Part 3, Hull(Chapter 15 Stability).

31. Dong, J.Y., Yeon-Gyu, K. and Kunhang, Y. (2015) 'A Study On Captive Manoeuvring Model Test Of A Ship At Large Heel Condition', *International Conference on Ship Manoeuvrability and Maritime Simulation (MARSIM 2015)*, p. 296.

32. Dubbioso, G., Durante, D. and Broglia, R. (2013) *5th International Conference on Computational Methods in Marine Engineering, Hamburg, Germany, May*.

33. Duman, S. and Bal, S. (2017) 'Prediction of the turning and zig-zag maneuvering performance of a surface combatant with URANS', *Ocean Systems Engineering-An International Journal*, 7(4), pp. 435-460.

34. Faltinsen, O. (1993) *Sea loads on ships and offshore structures*. Cambridge University Press.

35. Faltinsen, O.M., Minsaas, K., Liapis, N. and Skjørda}, S. (1980) *Proceedings of the 13th symposium on naval hydrodynamics, Tokyo, 1980*.

36. Fossen, T.I. (1994) *Guidance and Control of Ocean Vehicles*. Chichester, West Sussex, England.: John Wiley & Sons Ltd.

37. Fossen, T.I. (2011) *Handbook of marine craft hydrodynamics and motion control*. John Wiley & Sons.

38. Fossen, T.I. and Paulsen, M.J. (1992) *Control Applications, 1992., First IEEE Conference on*. IEEE.

39. Fujiwara, T., Ueno, M. and Nimura, T. (1998) 'Estimation of wind forces and moments acting on ships', *Journal of the Society of Naval Architects of Japan*, 1998(183), pp. 77-90.

40. Germanischer Lloyd (2013) 'Rules for Classification and Construction ', *Additional Rules and Guidelines for Determination of the Energy Efficiency Design Index*, VI.

41. Gerritsma, J. (1957) *Experimental Determination of Damping, Added Mass and Added Mass Moment of Inertia of a Shipmodel*. Studiecentrum TNO voor Scheepsbouw en Navigatie.

42. Gerritsma, J. and Beukelman, W. (1972) 'Analysis of the resistance increase in waves of a fast cargo ship', *International shipbuilding progress*, 19(217), pp. 285-293.

43. Gillmer, T.C. (1982) *Introduction to naval architecture*. London: London : E. & F. Spon.

44. Hasan, S.M. (2011) *Impact of EEDI on Ship Design and Hydrodynamics A Study of the Energy Efficiency Design Index and Other Related Emission Control Indexes*. Chalmers University Of Technology, Gothenburg, Sweden.

45. Havelock, T.H. (1937) 'The resistance of a ship among waves', *Proceedings of the Royal Society of London. Series A-Mathematical and Physical Sciences*, 161(906), pp. 299-308.

46. He, S., Kellett, P., Yuan, Z., Incecik, A., Turan, O. and Boulougouris, E. (2016) 'Manoeuvring prediction based on CFD generated derivatives', *Journal of Hydrodynamics*, 28(2), pp. 284-292.

47. Holtrop, J. and Mennen, G.G.J. (1982) 'An approximate power prediction method', *International Shipbuilding Progress*, 29(335), pp. 166 - 170.

48. Hooft, J.P., Nienhuis, U., Hutchison, B.L., Daidola, J.C., Jakobsen, B.K. and Ankudinov, V. (1994) 'The prediction of the ship's maneuverability in the design stage. Discussion. Authors' closure', *Transactions-Society of Naval Architects and Marine Engineers*, 102, pp. 419-445.

49. IACS (2013) 'Procedure for calculation and verification of the Energy Efficiency Design Index (EEDI)', *International Association of Classificarion Societies*, No. 38(First Industry Guidelines For Calculation And Verification Of The Energy Efficiency Design Index (EEDI)).

50. IMO (2002) 'Standards For Ship Manoeuvrability', *Resolution MSC.137(76)*, Agenda Item 5, 70th Session(MSC 76/23/Add.1).

51. IMO (2010) 'The Energy Efficiency Design Index (EEDI) and Underpowered Ships Submitted by Greece', *Prevention Of Air Pollution From Ships*

52. IMO (2011) 'Main events in IMO's work on limitation and reduction of greenhouse gas emissions from international shipping ', *International Maritime Organisartion*

53. IMO (2016) 'Progress report of SHOPERA and Japan's projects and outline of draft revised Guidelines for determining minimum propulsion power to maintain the manoeuvrability of ships in adverse conditions', *Air Pollution and Energy Efficiency*, Agenda Item 5, 70th Session(MEPC 70/5/20).

54. IMO (2017) '2013 Interim Guidelines For Determing Minimum Propulsion Power To Maintain The Manoeuvrability of Ships In Adverse Conditions as Amended ', *Marine Environment Protection Committee*, (MEPC.1/Circ.850/Rev.2 (Resolution MEPC.232(65), as Amended by Resolutions MEPC.255(67) AND MEPC.262(68))).

55. Irimagha, E., Zhiqiang, H., Birmingham, R. and Woodward, M. (2019) *5th International Conference on Ship Manoeuvring in Shallow and Confined Water*. Ostend, Belgium, 19th - 23rd May 2019.

56. Isherwood, R.M. (1973) 'Wind resistance of merchant ships', *RINA Supplementary Papers*, 115, pp. 327 – 338.

57. ITTC (2002) 'Recommended Procedures - Full Scale Measurements, Full Scale Manoeuvring Trials Procedures', *International Toiwing Tank Conference*, (7.7 - 04; 02 - 01), p. 18.

58. ITTC (2014) 'ITTC - Recommended Procedures and Guidelines', *International Towing Tank Conference*, (7.5-02 07-02.1), pp. 1 - 22.

59. ITTC (2017) 'Full Scale Manoeuvring Trials', *International Towing Tank Conference*, (7.7-04-02-01), pp. 1 - 18.

60. Jensen, J. and Dogliani, M. (1996) 'Wave-induced ship hull vibrations in stochastic seaways', *Marine Structures*, 9(3-4), pp. 353-387.

61. Journee, J.M.J. (2001) 'User manual of SEAWAY', *Technology University of Delft*, Release 4.19 (12-02-2001)(Report 1212a).

62. Kempf, G. (1944) 'Maneuvering Standards of Ships', *Deutsche Schiffahrts-Zeitschrifft*, (00323804), p. 27/28.

63. Khattab, O. and Pourzanjani, M. (1997) 'Safety Assessment of Handling of a VLCC by Tugs in Confined Waters and Variable Environment', *IFAC Proceedings Volumes*, 30(22), pp. 1-14.

64. Kijima, K., Katsuno, T., Nakiri, Y. and Furukawa, Y. (1990) 'On the manoeuvring performance of a ship with theparameter of loading condition', *Journal of the society of naval architects of Japan*, 1990(168), pp. 141-148.

65. Kijima, K. and Tanaka, S. (1993) 'On a prediction method of ship manoeuvring characteristics', *International Conference on Marine Simulation & Ship Manoeuvrability*. St. John's, Newfoundland, 26 Sept - 2 Oct. 1993. Canada: Marine Institute & NRC-IMD, Canada.

66. Kim, M., Hizir, O., Turan, O., Day, S. and Incecik, A. (2017) 'Estimation of added resistance and ship speed loss in a seaway', *Ocean Engineering*, 141, pp. 465-476.

67. Korvin-Kroukovsky, B.V. and Jacobs, W.R. (1957) *Pitching and heaving motions of a ship in regular waves*. Stevens Inst of Tech Hoboken NJ Experimental Towing TANK.

68. Kristensen, H.O. and Lützen, M. (2013) 'Prediction of resistance and propulsion power of ships', *Clean Shipping Currents*, 1(6).

69. Kwon, Y.J. (2008) 'Speed Loss Due to Added Resistance in Wind and Waves', *Naval Architect, Royal Institute of Naval Architecture, UK.*, (3), pp. 14-16.

70. L., D.G. (2015) 'Navigation, Manoeuvring and Position Keeping', *DVV GL AS Rules For Classification: Ships*, Part 6.

71. Lee, H.Y. and Shin, S.-S. (1998) *Proceedings of the PRADS practical design of ships and other floating bodies conference, Maritime Research Institute Netherlands, The Hague*.

72. Letki, L. and Hudson, D.A. (2005) *Simulation of ship manoeuvring performance in calm water and waves*. University of Southampton

73. Lewis, E.V. (1989) *Principles of naval architecture. Vol. 3, Motions in waves and controllability*. 2nd rev. ed.. edn. Jersey City, N.J.: Jersey City, N.J. : Society of Naval Architects and Marine Engineers.

74. Longva, T., Eide, M.S. and Skjong, R. (2010) 'Determining a required energy efficiency design index level for new ships based on a cost-effectiveness criterion', *Maritime Policy & Management*, 37(2), pp. 129-143.

75. Ma, Z., Chen, H. and Zhang, Y. (2017) 'Impact of waste heat recovery systems on energy efficiency improvement of a heavy-duty diesel engine', *Archives of Thermodynamics*, 38(3), pp. 63-75.

76. MAN (2011) 'Basic Principles of Ship Propulsion', *Basic Principles of Ship Propulsion," MAN Diesel &Turbo, Copenhagen*.

77. MAN (2014) 'Project Guide Electronically Controlled Two-stroke Engines.', *MAN B&W S60ME-C8.2-TII*, (Edition 0.5), pp. 1–377.

78. Martins, P.T. and Lobo, V. (2007) 'Estimating Maneuvering and Seakeeping Characteristics with Neural Networks', *IEEE Conference Oceans 07*. Abardeen. eeexplore, pp. 1-5.

79. Matsumoto, K. and Suemitsu, K. (1980) 'The prediction of manoeuvring performances by captive model tests', *J Kansai Soc Naval Archit Jpn*, 176, pp. 11-22.

80. McCreight, W.R. (1991) *A Mathematical Model for Surface Ship Maneuvering*. David Taylor Research Center Bethesda and Ship Hydromechanics Dept.

81. MEPC (2012) 'Interim Guidelines For The Calculation Of The Coefficient fw for Decrease in Ship Speed in a Representative Sea Condition for Trial use', *International Maritime Organization. London*, IMO MEPC.1/Circ.796, pp. 1 - 22.

82. MEPC (2013) '2013 Guidelines For Calculation Of Reference Lines For Use With The Energy Efficiency Design Index (EEDI)', *International Maritime Organisation*, I. M. O. Resolution MEPC.231(65), ANNEX 14, pp. 1 - 12.

83. MEPC (2017) '2014 Guidelines On The Method Of Calculation Of The Attained Energy Efficiency Design Index (Eedi) For New Ships, As Amended (Resolution MEPC.245(66), as Amended by resolutionsMEPC.263(68) AND

MEPC.281(70))', *International Maritime Organisartion*, I. M. O. MEPC.1/Circ.866, pp. 1 - 33.

84. Mitchell, J.H. (1898) 'XI. The wave-resistance of a ship', *The London, Edinburgh, and Dublin Philosophical Magazine and Journal of Science*, 45(272), pp. 106-123.

85. Mohammadafzali, S. (2016) *A mathematical model for the maneuvering simulation of a propelled SPAR vessel*. Memorial University of Newfoundland.

86. Molland, A.F. (2011) *The maritime engineering reference book: a guide to ship design, construction and operation*. Elsevier.

87. Muckle, W. and Taylor, D.A. (2013) *Muckle's naval architecture*. Butterworth-Heinemann.

88. Notteboom, T.E. and Vernimmen, B. (2009) 'The effect of high fuel costs on liner service configuration in container shipping', *Journal of Transport Geography*, 17(5), pp. 325-337.

89. OCIMF (2008) *Mooring Equipment Guidelines (MEG3)*. Witherby Publishing Group Ltd Livingston, UK.

90. OCIMF (2010) 'Estimating the Environmental Loads On Anchoring Systems ', *Oil Companies International Marine Forum, Bermuda*.

91. Ogawa, A. and Kasai, H. (1978) 'On the mathematical model of manoeuvring motion of ships', *International Shipbuilding Progress*, 25(292).

92. Oppen, A.N. and Kvitrud, A. (1995) *Wind induced resonant cross flow vibrations on Norwegian offshore flare booms*. American Society of Mechanical Engineers, New York, NY (United States).

93. Ozaki, Y., Larkin, J., Tikka, K. and Michel, K. (2011) 'An Evaluation of The Energy Efficiency Design Index Baseline for Tankers, Containerships, and LNG carriers', *Society of Naval Architects and Marine Engineers*, (Climate Change and Ships: Increasing Energy Eficiency), p. 8.

94. Pan, Y.-c., Zhang, H.-x. and Zhou, Q.-d. (2012) 'Numerical prediction of submarine hydrodynamic coefficients using CFD simulation', *Journal of Hydrodynamics, Ser. B*, 24(6), pp. 840-847.

95. Papanikolaou, A., Zaraphonitis, G., Bitner-Gregersen, E., Shigunov, V., El Moctar, O., Soares, C.G., Reddy, D.N. and Sprenger, F. (2016) 'Energy efficient safe ship operation (SHOPERA)', *Transportation Research Procedia*, 14, pp. 820-829.

96. Paroka, D., Ohkura, Y. and Umeda, N. (2006) 'Analytical prediction of capsizing probability of a ship in beam wind and waves', *Journal of Ship Research*, 50(2), pp. 187-195.

97. Patel, M.H. (2013) *Dynamics of offshore structures*. Butterworth-Heinemann.

98. Pearson, D.R. (2014) 'The use of flettner rotors in efficient ship design', *Proceedings of the Influence of EEDI on Ship Design Conference*.

99. Psaraftis, H.N. and Kontovas, C.A. (2009) 'CO2 emission statistics for the world commercial fleet', *WMU Journal of Maritime Affairs*, 8(1), pp. 1-25.

100. Rahman, M. (2017) *Development of energy efficiency design index for inland vessels of Bangladesh*. Bangladesh University of Engineering and Technology.

101. Sandaruwan, D., Kodikara, N., Rosa, R. and Keppitiyagama, C. (2009) 'Modeling and simulation of environmental disturbances for six degrees of freedom ocean surface vehicle', *Sri Lankan Journal of Physics*, 10.

102. Schröder, C., Reimer, N. and Jochmann, P. (2017) 'Environmental impact of exhaust emissions by Arctic shipping', *Ambio*, 46(3), pp. 400-409.

103. Shenoi, R.R., Krishnankutty, P. and Selvam, R.P. (2016) 'Study of maneuverability of container ship with nonlinear and roll-coupled effects by numerical simulations using RANSE-based solver', *Journal of Offshore Mechanics and Arctic Engineering*, 138(4), p. 041801.

104. Shigunov, V. (2012a) 'Background information to Marine Environment Protection Committee document', *Marine Environment Protection Committee*. International Maritime Organisation.

105. Shigunov, V. (2012b) 'Consideration of the Energy Efficiency Design Index for new ships – Minimum propulsion power to maintain the manoeuvrability in adverse conditions', *Marine Environment Protection Committee* 29 June 2012 International Maritime Organisation.

106. Shigunov, V. (2015) 'Manoeuvrability in Adverse Conditions', *ASME 2015 34th International Conference on Ocean, Offshore and Arctic Engineering*, 11(OMAE2015-41628 - Prof. Robert F. Beck Honoring Symposium on Marine Hydrodynamics), p. 12.

107. Shigunov, V. (2018) 'Manoeuvrability in adverse conditions: rational criteria and standards', *Journal of Marine Science and Technology*, pp. 1-19.

108. Son, K.-H. and Nomoto, K. (1981) '5. On the Coupled Motion of Steering and Rolling of a High-speed Container Ship', *Naval Architecture and Ocean Engineering*, 20, pp. 73-83.

109. Strasser, G., Takagi, K., Werner, S., Hollenbach, U., Tanaka, T., Yamamoto, K. and Hirota, K. (2015) 'A verification of the ITTC/ISO speed/power trials analysis', *Journal of Marine Science and Technology*, 20(1), pp. 2-13.

110. Stroud, K.A. (2011) *Advanced engineering mathematics*. 5th edn. Basingstoke: Basingstoke : Palgrave Macmillan.

111. Takashina, M.H.a.J. (1980) 'A calculation of ship turning motion taking coupling effect due to heel into consideration', *The Japan Society of Naval Architects and Ocean Engineers*, (59), pp. 71-81.

112. Tasai, F. (1961) 'Damping force and added mass of ships heaving and pitching', *Transaction of the West Japan Society of Naval Architecture.*, 1959(105), pp. 47-56.

113. Taylan, M. (2003) 'Static and dynamic aspects of a capsize phenomenon', *Ocean engineering*, 30(3), pp. 331-350.

114. Tello Ruiz, M., Candries, M., Vantorre, M., Delefortrie, G., Peeters, P. and Mostaert, F. (2012) 'Ship manoeuvring in waves: a literature review', *WL Rapporten*.

115. Trodden, D.G. (2014) *Optimal propeller selection when accounting for a ship's manoeuvring response due to environmental loading*. Newcastle University, Newcastle Upon-Tyne.

116. Tsujimoto, M., Shibata, K., Kuroda, M. and Takagi, K. (2008) 'A practical correction method for added resistance in waves', *Journal of the Japan Society of Naval Architects and Ocean Engineers*, 8, pp. 177-184.

117. Ueno, M., Kitamura, F., Sogihara, N. and Fujiwara, T. (2012) *Proceedings of the international conference on advances in wind and structures*.

118. Vladimir, N., Ančić, I. and Šestan, A. (2017) 'Effect of ship size on EEDI requirements for large container ships', *Journal of Marine Science and Technology*, pp. 1-10.

119. Woodward, M.D. (2009) *Control and response of pod driven ships*. PhD thesis. Newcastle University, Newcastle Upon Tyne, UK.

120. Yang Xingyan, a.C.M. (2013) 'Discussion on Calculation Method of windage Area of Ships', *Port Engineering Technology*, 50(1), p. 210.

121. Yasukawa, H. and Nakayama, Y. (2009) *Proceedings of the International Conference on Marine Simulation and Ship Manoeuvrability*.

122. Yasukawa, H. and Yoshimura, Y. (2015) 'Introduction of MMG standard method for ship maneuvering predictions', *Journal of Marine Science and Technology*, 20(1), pp. 37-52.

123. Ăgan, R., Chiţu, M.-G. and Manea, E. (2015) 'New Approach In Ship Manoeuvrability Prediction', *International Journal of Modern Manufacturing Technologies*, Vol. VII(No. 2 / 2015).

124. Żelazny, K. (2014) 'Approximate method of calculation of the wind action on a bulk carrier', *Zeszyty Naukowe/Akademia Morska w Szczecinie*.

125. Zhang, H., Xu, Y.-r. and Cai, H.-p. (2010) 'Using CFD software to calculate hydrodynamic coefficients', *Journal of Marine Science and Application*, 9(2), pp. 149-155.

126. Zheng, J., Hu, H. and Dai, L. (2013) 'How would EEDI influence Chinese shipbuilding industry?', *Maritime Policy & Management*, 40(5), pp. 495-510.

Chapter 9 Appendix A: Data from Son and Nomoto

On the Coupled Motion of Steering and Rolling of a High-speed Container Ship (J.S,N,A ,Japan,Vol. 150, Dec. 1981)

Non-dimensioned Coefficients	Value	Dimensioning expression
X_{uu}	-0.0004226	$0.5 \times \rho \times L^2$
X_{vr}	-0.00311	$0.5 \times \rho \times L^3$
X_{rr}	0.00020	$0.5 \times \rho \times L^4$
$X_{\phi\phi}$	-0.0002	$0.5 \times \rho \times V_s^2 \times L^2$
X_{vv}	-0.00386	$0.5 \times \rho \times L^2$
K_v	0.0003026	$0.5 \times \rho \times V_s \times L^3$
K_r	-0.000063	$0.5 \times \rho \times V_s \times L^4$
K_p	-0.0000075	$0.5 \times \rho \times V_s \times L^4$
K_ϕ	-0.000021	$0.5 \times \rho \times V_s^2 \times L^3$
K_{vvv}	0.002843	$0.5 \times \rho \times L^3/V_s$
K_{rrr}	-0.0000462	$0.5 \times \rho \times L^6/V_s$
K_{vvr}	-0.000588	$0.5 \times \rho \times L^4/V_s$
K_{vrr}	0.0010565	$0.5 \times \rho \times L^5/V_s$
$K_{vv\phi}$	-0.0012012	$0.5 \times \rho \times L^3$
$K_{v\phi\phi}$	-0.0000793	$0.5 \times \rho \times V_s \times L^3$
$K_{rr\phi}$	-0.000243	$0.5 \times \rho \times L^5$
$K_{r\phi\phi}$	0.00003569	$0.5 \times \rho \times V_s \times L^4$
Y_v	-0.0116	$0.5 \times \rho \times V_s \times L^2$
Y_r	0.00242	$0.5 \times \rho \times V_s \times L^3$
Y_ϕ	-0.000063	$0.5 \times \rho \times V_s^2 \times L^2$
Y_{vvv}	-0.109	$0.5 \times \rho \times L^2/V_s$
Y_{rrr}	0.00177	$0.5 \times \rho \times V_s \times L^5$
Y_{vvr}	0.0214	$0.5 \times \rho \times L^3/V_s$
Y_{vrr}	-0.0405	$0.5 \times \rho \times L^4/V_s$
$Y_{vv\phi}$	0.04605	$0.5 \times \rho \times L^2$
$Y_{v\phi\phi}$	0.00304	$0.5 \times \rho \times V_s \times L^2$
$Y_{rr\phi}$	0.009325	$0.5 \times \rho \times L^4$
$Y_{r\phi\phi}$	-0.001368	$0.5 \times \rho \times V_s \times L^3$
N_v	-0.0038545	$0.5 \times \rho \times V_s \times L^3$
N_r	-0.00222	$0.5 \times \rho \times V_s \times L^4$
N_p	0.000213	$0.5 \times \rho \times V_s \times L^4$
N_ϕ	-0.0001424	$0.5 \times \rho \times V_s^2 \times L^3$
N_{vvv}	0.001492	$0.5 \times \rho \times L^3/V_s$
N_{rrr}	-0.00229	$0.5 \times \rho \times L^6/V_s$
N_{vvr}	-0.0424	$0.5 \times \rho \times L^4/V_s$
N_{vrr}	0.00156	$0.5 \times \rho \times L^5/V_s$
$N_{vv\phi}$	-0.019058	$0.5 \times \rho \times L^3$
$N_{v\phi\phi}$	-0.0053766	$0.5 \times \rho \times V_s \times L^3$
$N_{rr\phi}$	-0.0038592	$0.5 \times \rho \times L^5$
$N_{r\phi\phi}$	0.0024195	$0.5 \times \rho \times L^4 \times V_s$
c_{Rr}	-0.156	-

Non-dimensioned Coefficients	Value	Dimensioning expression
$c\delta_{rrr}$	-0.275	-
$c\delta_{rrv}$	1.96	-
$c\delta_x$	0.71	-
x_R	-0.5	-
x_p	-0.526	-
a_H	0.235	-
τ	1.09	-
γ	0.088	-
w_p	0.184	-
c_{pv}	0.0	-
c_{pr}	0.0	-
k	0.631	-
ε	0.921	-
m	0.00792	$0.5 \times \rho \times L^3$
m_x	0.000238	$0.5 \times \rho \times L^3$
m_y	0.000238	$0.5 \times \rho \times L^3$
$m + m_x$	0.079438	$0.5 \times \rho \times L^3$
$m + m_y$	0.01497	$0.5 \times \rho \times L^3$
$-m_y l_y$	-0.000205	$0.5 \times \rho \times L^4$
$m_y \alpha_y$	0.0003525	$0.5 \times \rho \times L^4$
I_x	0.0000176	$0.5 \times \rho \times L^5$
I_z	0.000456	$0.5 \times \rho \times L^5$
J_x	0.0000034	$0.5 \times \rho \times L^5$
J_x	0.000419	$0.5 \times \rho \times L^5$

9.1 Appendix B Sample Calculation of EEDI

Full MCR Power is 14280 kW and the power from Energy recovery devices is 1180kW.

From equations 4-57 to 4-60:

$$\text{Attained EEDI} = \frac{0.75 \times \sum \text{P} \times \text{sfc} \times \text{C}_\text{F}}{\text{f}_\text{cf} \times \text{capacity} \times \text{V}_\text{ref} \times \text{f}_\text{w}} \quad \textit{9-1}$$

$$\text{required EEDI} = \text{a} \times \text{b}^{-\text{c}} \quad \textit{9-2}$$

$$f_i = \frac{0.0377 \times L_{pp}^{2.329}}{capacity} \quad \textit{9-3}$$

$$\text{f}_\text{w} = \text{a}_\text{w} \times \ln(\text{capacity}) + \text{b}_\text{w} \quad \textit{9-4}$$

$\text{Capacity} = \text{deadweight} = 2628.884$

$\text{required EEDI} = 174 \times 2628.884^{-0.201} = 35.7417$

$\text{a}_\text{w} = 0.0208$
$\text{b}_\text{w} = 0.633$
$\therefore \text{f}_\text{w} = 0.0208 \times \ln(2628.884) + 0.633 = 0.7968$

$\text{f}_\text{i} = \frac{0.0377 \times 175^{2.329}}{2628.884} = 2.40218$

$\text{pmcr} = \%\text{MCR} = 1$ for full load condition

Going by equation 4-50, the reference equivalent rpm for determining EEDI at 75% power is given by:

$$n_{mref} = C \times \sqrt[3]{\frac{0.75 \times P_M \times pmcr}{(D_{prop})^5}} \quad \textit{9-5}$$

Thus

$$n_{mref} = 104 \times \sqrt[3]{\frac{0.75 \times P_M \times 1.0}{(6.533)^5}} = 100.4096 rpm$$

$\text{pitch} = \text{D}_\text{p} \times \text{pitch ratio} = 6.533 \times 1.009 = 6.591797$

Specific fuel consumption at 75% MCR

= *167.35g/KW.hr*

$\therefore V_{ref} = 100.4096104 \times pitch/(60 * 0.4144) = rpm$

$V_{ref} = 100.4096104 \times \frac{6.591797}{60 \times 0.4144} = 21.44505\ knots$

Specific fuel oil consumption was derived from the expression formulated from the manufacturer's unsymmetrical plot as was shown in equations 4-52 and 4-53:

.

$$\text{sfoc} = 26.57 \times \ \%\text{smcr}^2 - 47.466 \times \%\text{smcr} + 183.56 \ ; 0.35 \geq \%\text{smcr} \leq 0.7 \qquad 9\text{-}6$$

$$\text{sfoc} = 38.677 \times \ \%\text{smcr}^2 - 52.407 \times \%\text{smcr} + 181.08 \ ; \ \%\text{smcr} > 0.7 \qquad 9\text{-}7$$

$$\text{Attained EEDI} = \frac{0.75 \times (14280 - 1180) \times 167.35 \times 3.114}{2.40218 \times 2628.884 \times 21.44505 \times 0.7968} = 47.45$$

Where f_w is the weather correction factor with a_w and given as 0.0208 and 0.633 for container ship, $\sum P$ is the sum of the engine power at 75% SMCR (for instance, for the full power consideration, $\sum P$ is 75% f the full MCR power, and for the 80% derated power consideration, $\sum P$, is 60% of the original full power), C_f is the fuel to CO_2 conversion factor V_{ref} is the reference speed determined at 75% of the SMCR, (calculated this to be equal to 11.2m/s for the full MCR consideration and 8.825 for the 80% MCR power consideration). f_{cf} is the product of all the capacity factors (for this research, others are considered as 1.0 except the ice class correction factor f_i

For calculating the required EEDI, a is given as 174.22, b is the deadweight and c was given as 0.201 for container ships.